Department of Electrical and Computer Engineering

Protection Considerations of Future Distribution Networks with Large

Penetration of Single Phase Residential Rooftop Photovoltaic Systems

Hadi Hosseinian Yengejeh

This thesis is presented for the Degree of

Doctor of Philosophy

of

Curtin University

November 2016

Declaration

To the best of my knowledge and belief this thesis contains no material previously published by any other person except where due acknowledgment has been made.

This thesis contains no material which has been accepted for the award of any other degree or diploma in any university.

Signature: *H. Hosseinian. Yengejeh*

Date: 13.11.2016

Acknowledgements

I am deeply grateful to my supervisor, Prof. Syed Islam for his incomparable guidance, continuous patience and encouragement throughout my doctoral study. Without your endless support, this thesis could not have been accomplished.

I am much obliged to the staff members of the Department of Electrical and Computer Engineering, Curtin University, for their support rendered in various ways during this work.

Finally, I need to acknowledge the financial support received from Curtin University through Curtin Strategic International Research Scholarship (CSIRS) to complete my studies with peace of mind.

Dedication

To my beloved wife, Parisa, for her love, understanding and commitment.

And to my beloved father and mother, for their unconditional love, encouragement and

support in my entire life and to my dear Aidin, hope he reads this himself one day.

Abstract

Single phase rooftop photovoltaic (PV) systems are the most common type of distributed generation units in most of the world especially Australia. During the last decade, a vast effort has been made towards the expansion and increase in the penetration level of distributed generation units within the electric distribution networks. However, some reasons deter the utilities from increasing the penetration level of PVs on their network. Arising problems for power quality, voltage profile and protection of the network and some unknown impacts are the most referred reasons to stop the increasing trend of installations of PVs in some areas.

Discussion about the limitation of PV penetration level has started from several years ago, and many papers have paid attention on it in medium voltage (MV) distribution networks. However, there are not many publications for the PV penetration impact analysis in the low voltage (LV) distribution systems independent from MV network.

In this thesis, a comprehensive analysis has been carried out to precisely determine the impact of installation of single phase rooftop PVs and high penetration level of them on the performance of protective devices in LV network. To this end, Sensitivity and stochastic analysis are carried out to cover all possible scenarios. Also, the impact of factors such as PV rating, fault location, fault impedance and fault type on the operation of protective devices has been taken into account. In the end, a new criterion based on successful operation rate of protective devices and successful disconnection rate of PVs during each type of faults is proposed. The study covers all main three types of fault (Line to ground, Line to Line and Line to Line to Ground). The new statistic based method is introduced to evaluate the consequences of increasing PV penetration level on successful operation of protective devices in LV network and accordingly the best penetration level selection criterion from protective system point of view is introduced.

Detail analysis of disconnection sequence of PVs is performed and effects of some critical parameters such as PV rating, location, fault impedance and location on disconnection time and sequence of PVs has been illustrated. Also, in situations where existing protection system are not sufficient is introduced. Results show, these

situations are more probable in none effectively grounded (NEG) systems or when the fault impedance is high in multiple earthed network (MEN) systems. Thus, only utilizing the under/over voltage protection function will not guarantee the successful disconnection of PVs. In such situations, Redesigning of the system is required.

Another point which is clarified in this thesis is the impact of penetration level of PVs on normal load current of residential MV feeders and its impact on the setting of pick up current of relays in overcurrent protection. In addition, the effect of load demand and PV penetration level on the pickup current of the relays is investigated. To achieve more precise results, the dynamic impedance fault is utilized instead of bolted fault and the outcome of results for both is presented to see that the discrepancy in relays operation time will not be considerable despite the small difference between them. The reduction of high impedance fault threshold as a result of high PV penetration level in network, and consequently being unable to detect the more faults is another finding of this thesis. To solve this issue the installation of high set relays in highly PV penetrated feeders is proposed, or the modification in their settings is suggested.

Table of Contents

List of Figures

xiv

List of Tables

List of Abbreviations

BOF	Beginning of feeder
EAV	Expected average voltage
EOF	End of feeder
FCD	Fault current difference
IOF	Impedance of fault
LG	Line-to-ground fault
LL	Line-to-line fault
LLG	Two-line to ground fault
LVF	Low voltage feeder
MCA	Monte Carlo analysis
MOF	Middle of feeder
MVF	Medium voltage feeder
PDF	Probability density function
PDP	Photovoltaic disconnection probability
PPL	Photovoltaic penetration level
PV	Photovoltaic unit
SCF	Short-circuit fault
SOP	Switch-Fuse Operation Probability
STD	Standard deviation
TCD	Transformer current difference
VD	Voltage difference

Chapter 1. Introduction

1.1 Literature review

Nowadays the renewable energy resources have become popular all around the world. Many countries try to increase the share of renewables in their energy mix. Australia is one of the countries that from many years ago have aimed to increase the renewable energy in its power network. Hence different forms of these types of energy resources such as wind energy and solar power are taken into account to reach this goal. The solar rooftop photovoltaic systems are very popular and cost effective in Australia as the country is very well positioned to install these units and get benefit from the clean and free energy resource. These energy resources can make a big difference for utilities and consumers at the same time. It means that they can reduce the greenhouse gas emission, reduce the air pollution, reduce the losses in transmission and distribution networks and enhance the voltage profile. Also, they can be attractive to consumers from an economic point of view.

Single phase rooftop photovoltaic systems is the most common type of distributed generation units in many parts of the world especially Australia. During the last decade, a vast effort has been made toward the expansion and increase in the penetration level of distributed generation units within the electric distribution networks. There are over 1.5 Million houses in Australia with rooftop PVs because of various local and federal government incentives [1-2].

1.1.1 DG and protection issue

The advent of DGs brought some new concepts and phenomenon to the power network. Among different issues that these devices impacted on the power systems, the protection issue is one of the most significant side effects. Distribution networks are usually radial in their nature and adding distributed energy resources (DER)

1

changes its structure and varies its unidirectional power flow. This variation of current flow during the faults changes the all previous consideration, and it may lead to different protective issues in the system. Some papers investigate problems in existing feeder protections in the presence of DGs, and aims to increase the operational dependability and security of distribution feeder protections. These papers present findings of detailed investigations on DG-imposed protection issues, typically sympathetic tripping, failure of fuse saving practice, misprotection due to feeder-network reconfiguration, reduction of reach in protection, unintentional islanding operation, and mis-coordination [3-5]

The majority of these works were carried out for three phase DGs and in MV distribution networks. A mathematical formulation is introduced to model protection trip problems in radial distribution networks, and a procedure to monitor failures of the protection systems based on Petri Nets and simple matrix manipulation is presented in [6]. Such procedures permit to have a central control and monitoring system for protection system of distribution networks. In [5] a new directional current protection by the positive- sequence fault component is proposed. The scheme using fault component principle analyzed the phase angle difference of the positive- sequence current before and after the fault, and thereby realized the fault location.

Reference [7] has paid attention to the location of DGs and their effect on the severity of protection problems arising from the installation of these units. This paper proposes a new method to optimize the connection point of DGs in the network to have a minimum impact on coordination and operation of protective devices. Interestingly the reference [8] focuses on solve the problems from DGs rating and size control method and tries to minimize the protection problems and miscoordinations in distribution networks.

However, the application of different types of DGs in power networks such as wind turbine, solar panels and their increasing applications in distribution network, can bring some side effects on network. These effects include impacts on voltage fluctuation, power quality and protection issues. Among the publications that have paid attention to these issues, some of them have focused on protection issues arising from PV installation in the distribution network. The following section is dedicated to review these research findings.

1.1.2 PV penetration consideration

The ever increasing trend of PV installations in buildings leads to different problems such as power quality and protection problems in residential distribution networks. However, there have been a number of publications which has tried to address some of these issues and solve them. One of the main points that Mokhtari et al [9] paid attention is the balance between generation and load in distribution feeders. They emphasized on the importance of this balance to relive the impact of high PV penetration level. They proposed using DC link connection in residential buildings to increase the maximum allowed penetration level in residential feeders and let the customers inject their extra power that otherwise would be limited because of AC power quality violation. The surplus generated power can easily be transferred to other phases and feeders through common DC link to maintain the balance between generated power and load demand [9].

Reference [10] has carried out research to evaluate the impact of high penetration of PV originated technical issues such as power fluctuation and voltage flicker in power distribution feeders (at different conditions of PV outputs due to variation of weather, e.g. cloudy weather). They have monitored the PV-induced voltage quality issues including the dynamic reaction of voltage control devices and they eventually come out with results that PV penetration up to 50% is tolerable. In reference [11] microgrid protection, adaptive control and fault location identification in presence of high penetration of PVs are discussed. This reference proposes differential current protection to overcome protection issues including the low fault current nature of conventional inverters. Reference [12] to solve the limitation on PV penetration level due to load transfer operation of the distribution system, has proposed the advanced distribution automation system (ADAS) to perform the control of PV inverter for generation curtailment during the load transfer for service restoration. Making overvoltage problem controlled through control of PV generation, PV installation capacity of distribution feeders may be increased to improve the penetration level PV system take full advantage of PV systems and solar energy.

1.1.3 Single phase PV and protection issues

Single-phase rooftop photovoltaic systems (PVs) are the most commonly utilized type of distributed generation that are installed in distribution networks of many countries. As an example, in the last 6 years, over one million rooftop PVs have been installed in Australia of which over 90% are single-phase PVs in the residential premises [13]. During last decade this increasing penetration level of the solar PVs has brought new concerns to utilities about the impact of this growing trend. The advent of the PVs especially in the form of rooftop units, which generates single phase power for houses and meets the residential power needs, has made some issues to distribution networks. These problems may be categorized into different groups. One of the most important impacts of this increasing trend of PV installation is on the system protection. As protection of the network has vital role in the stability of network and saving the assets of network including consumers and utilities, proper attention must be given to the adequacy of protection.

Some research has paid attention to analyzing the effect of high penetration of PVs on voltage and power quality of distribution systems [14-17]. Their research shows that high penetration of PV can change the direction of fault current and may have an impact on unidirectional power flow. In Australia to avoid the issues arising from the high penetration of PVs in distribution networks such as harmonic saturation, voltage rise, reverse power flow and protection issues, utilities have limited the percentage of penetration of PVs to 25-30% [18]. Another reason for putting this limitation is the unknown impacts of high penetration of PVs on distribution network during the faults. Some papers have paid attention to effects of PV plants on distribution networks in MV level and revealed their location and size and generation capacity effects on network protective factors. [19]

According to [20-22] findings, it is highly likely that in presence of three phase PVs in MV distribution system some protection issues will occur. For example protection blinding, mis-coordination between protective devices and unwanted tripping are some of them. References [19, 23-25] indicate that proper protection in networks with increasing penetration level of three phase DERs, requires using bidirectional relays, pilot signal relaying, communication-based transfer trip and impedance protection schemes

The increasing penetration level of these units in low voltage (LV) distribution networks has imposed several technical problems such voltage rise issues [26, 27] and power quality problems [28-29]. The technical and economic impacts of over-voltages by rooftop PVs in PV dominated distribution feeders are assessed in [28-29] and several improvement techniques are proposed in [30] to mitigate or minimize these problems. Furthermore, the sudden variations of voltage in PV dominated feeders, as the result of clouding, has been studied in [31] where some improvement methods are proposed to overcome rapid voltage fluctuations.

In addition to voltage rise, fluctuation and power quality problems, the utilities worldwide are concerned with the influence of high penetration of rooftop PVs on the mis-coordination among the protective devices in those networks [19], [32-35]. As an example, reference [36] has discussed the protection problems related to the high penetration of rooftop PVs in distribution networks. For medium voltage (MV) networks with high penetration of rooftop PVs in their LV feeders, reference [37] proposes a new technique to define and update the settings of the protective network devices to maintain a proper coordination among them. Also, reference [18] proposes a new technique based on current phase comparison at different points along MV feeders to detect the contribution of rooftop PVs on the short circuit faults. There are few papers they have considered the single phase residential connected PVs impact upstream on protection of MV network. However they have made some basic inappropriate assumption in their procedure and these wrong assumptions have led to inappropriate conclusions. For example, reference [36] considered the fault impedances in their study much bigger than what their real values are and hence the results have been affected significantly.

Although there are many studies which have taken the effects of three phase PV plants on fault condition in distribution network into account, however, there is not such a comprehensive and vigorous study for single phase rooftop PV cases in presence of vast number of PVs which may be unequally distributed (from location and rating viewpoints) among various phases of system. Also, they have not examined the distribution of PVs along the LV feeder neither the different nominal ratings of the PVs. These points need to be considered in protection-related studies of networks with high penetration of PVs.

In [25] the impact of single phase rooftop PVs during the fault on distribution network has been analyzed but the research has focused on distribution boxes as most likely points of fault which they are not. The paper has missed that in many cases overhead lines are the most frequently occurring fault points.

Reference [33] has investigated impacts of single phase PVs on the coordination of overcurrent relays of MV networks. The results of the mentioned research show that PVs position may have the reverse effect on operation time of relays. However, there are not any considerable research which pays attention to the effect of single phase rooftop PVs on distribution network protective factors such as short circuit current and also on voltage profile of feeder during the fault which is critical for PVs disconnection sequence as PVs are equipped with voltage based protection functions.

This limit prevents newer householders to install rooftop PVs. From protection side, the utilities are worried that due to high penetration of rooftop PVs, there is a possibility that the rooftop PVs will not allow the voltage along the feeder drop during short-circuit faults. This will results in the continuous supply of the fault through the rooftop PVs, even if the upstream circuit breakers have operated. It is stated in [26] that one important issue to be investigated about the networks with rooftop PVs is that whether it is possible for some PVs to continue to supply power to the feeder when the upstream network is lost, particularly in a situation where there are many PV systems on the feeder. The report states that such an issue should not occur due to design requirements of PV systems, but it is still a problem to be discussed and investigated. This is another research gap that this thesis focuses on.

Another factor which is going to be critical in the near future if not now is answering to the question of what is the maximum allowed PV penetration level? Moreover, determination of criteria to avoid the side effects of this new technology is another important concept. Currently, in Australia there is a concern among utilities that increasing the PV penetration level beyond the 30% level will lead to some unknown problems in distribution networks and therefore they are reluctant to permit consumers to install PVs when the penetration level rises above that percentage [18]. However, there is not a specific reference to their concern, and it has not been addressed anywhere. One of the points that have been addressed in this thesis is investigation on this concern and this limitation on consumers.

Moreover, using the vast numbers of PVs in the residential networks encounters utilities with some protection issues in case of short circuit faults. Some of these

problems are linked to the disconnection time and sequence of PVs in low voltage feeders. So it seems that investigation on how the connected rooftops PVs are going to be isolated in case of different faults is another point which will be focused more.

As distribution networks are not limited to LV systems and it is connected to MV network, hence the effect of PV installation in LV residential area will be transferred to MV network as well. So considering the consequences of single phase rooftop PVs on MV distribution networks are the next step in this research. To have valid and accurate results in this thesis, the dynamic fault impedance is utilized to understand the behavior of protective devices in the presence of vast numbers of PVs. The results for dynamic impedance applied fault and bolted fault will be compared in this thesis. On the other hand, the impact of penetration level on high impedance fault threshold will be investigated.

1.2 Aim and objective of the thesis

The effects of high penetration level of PVs on distribution networks behavior during the short circuit faults and the disconnection order of the PVs and impact of the disconnection order of PVs on protective devices operation time is scrutinized in this thesis. This was one of the significant research gaps in this field. Also, the definition of a new criterion to evaluate the suitability of installation of high penetration level of PVs in distribution networks has been done in this research. Analysis of impacts of high penetration level of PVs on MV networks is the last step in this study. To achieve these goals, the following measures have been carried out in this study.

First, the effect of one single PV on protective parameters in residential feeder has been determined using sensitivity analysis. Later, the impact of installing numerous PVs on the important protective factors of distribution networks (including voltage along the feeder and current of the transformer and fault current) has been analysed through stochastic Monte Carlo analysis. Then, the impact of various fault arameters including impedance, location, PV rating, and penetration level on disconnection of PVs and their consequences are analysed. On the next part of research a new criterion has been defined to assess the penetration level and of PVs such that the successful operation of protective devices is guaranteed. Also, investigating the

effect of PV penetration on MV distribution networks while considering dynamic characteristics of the fault impedance is another aim of this research. To have better understanding from further impacts of PV penetration on network protection, the variation of high impedance fault threshold in the presence of different penetration level of PVs is investigated. Finally, suggestions are made to improve the operation of high impedance relays in MV networks.

1.3 Significance of the research

It is expected that future distribution networks include large percentage of distributed energy resources (DER) such as PVs and the concerns about the effects of these DERs have been challenged and scrutinized in this thesis. This study focuses on accurate identification and analysis of single phase PVs impact on protective factors in distribution systems. As a result of this research, we will be able to mitigate the protection problems in highly penetrated PV networks with consideration of recommended penetration level and will be able to avoid the unpredicted aftermath of mass installation of various rating of rooftop PVs in the distribution network.

This research has carried out a statistic evaluation based on stochastic analysis of Monte Carlo to prove the findings of the allowed penetration level.

1.4 Original contribution to the research

The main objective of this investigation was to accurate analysis of the impact of single phase rooftop PVs on protective devices performance in the distribution network. The main contributions of this research can be listed as follows:

- Sensitivity analysis of the impact of the single residential unit connected PV on important protective factors of the distribution network.
- Stochastic analysis to identify the effect of penetration level and PV ratings on protective devices in low voltage residential feeders.
- Analysis of PVs disconnection sequence during different types of short circuit faults and effective parameters on it.

8

- Proposing a new criterion to assess the opertaion of protection system in distribution network. Moreover, evaluate the security level of different penetration levels in the presence of different faults.

- Investigation on the impact of high penetration level of single phase PVs on MV distribution network and to highlight the main influences of it.

1.5 Structure of the Thesis

This thesis is organized into seven chapters. The research aims and objectives along with the need and the justification through a literature review for the research topic are outlined in **chapter 1. Chapter 2** discusses the basics of Protection in distribution networks along with concepts of highly PV penetrated distribution networks. The sensitivity analysis and study on effects of one single PV unit on key parameters of protective devices is presented in **chapter 3**. The stochastic analysis on penetration level and rating of PVs has been carried out by Monte Carlo analysis in **chapter 4**. Also in this analysis, the impact of fault impedance and fault location has been taken into account. The investigation on how the PVs are disconnected from the network and their disconnection sequence in the case of different types of faults are studied in **chapter 5.** This chapter also pays attention to the impacts of network grounding type and fault impedance magnitude on disconnection of PVs during the fault. As the MV distribution systems are a vital part of the network and are necessary to be investigated from PV penetration level impact point of view, **chapter 6** is dedicated to this topic and to have accurate and real results the dynamic model of fault impedance is recruited. Conclusions drawn from this research and recommendations for future research are presented in **chapter 7**.

Chapter 2. Protection of Distribution Networks

2.1 Introduction

This chapter tries to illustrate the fundamentals of protection systems for distribution networks and evaluate the criteria of best and reliable protection for residential feeders. The main aspects of an electric power system are generation, transmission and finally delivery of electric energy to consumers. The electric power system should be designed in such a way that by correct management, generation, transmission, and distribution, consumers can be provided with electric power at a minimum cost and highest reliability. The important point from consumer's viewpoint is that the supply of energy continues without interrupt at an affordable cost. On the other hand, the power network operators are regularly challenged by different type of faults and failures. Consequently, these failures have a negative impact on normal operation of the network.

These faults include phase to phase faults, phase to ground faults, phase breaks and insulator partial or full failures. So, it is an essential to have a monitoring and protection subsystem to detect and isolate the faulty section of the power system in a shortest possible time without fail. Because, as long as the fault has not been cleared, the network is subject to negative impacts of this fault. This monitoring system is considered as protection system and consists of relays and circuit breakers. This chapter addresses the important factors in distribution system protection consideration using basic concepts of protection.

2.2 Assessment criteria for protection systems

It is possible to define and propose different protection plan and sketches for a power system. Moreover, there is a need to a criterion to assess and compare these possible plans and choose the most suitable one. As an example the relevant factors to choose the best protection system can be listed as; the speed, reliability, selectivity, sensitivity and economic.

The protection systems should be fast enough to prevent failure in other devices. At the same time, they should show proper action against transient faults. In fact, the speed of protection system has grave impact on the stability of power system. The faster the fault removal, the more the chances are that the network stays synchronized.

Reliability of protection system means that the system operates properly during the fault and do not show any unnecessary action. The system which shows more numbers of correct operation against the faults has higher reliability. A successful protection system has to act just for faults which are in its zone and for faults beyond its zone, should not operate to achieve the goal of maximum service continuity. This characteristic of the system is known as the selectivity and coordination of the system.

Different faults may have different impacts on the power system. The proper protection system should possess the ability to distinguish all types of faults to detect the faults, which happen in various conditions. In other words, it should show sensitivity to all kinds of fault. Last but not the least, system must be affordable. It is worth to mention that increase of reliability adversely changes the system cost. However, it is possible to have a compromise between these two parameters.

2.3 Coordination rules for protective devices in distribution networks

Coordination of protective devices is choosing the overcurrent protective devices and setting their time-current settings along the distribution feeder considering their

preset operation sequence in order to detect the line faults. When two protective devices have the specific operation sequence in order to detect the particular fault, and at the same time they do not have any conflicts on their operation, these two devices are called coordinated. The main protective device, which is designed to operate first, is known as primary protective device, and the other one which operates later is known as backup protective device. The backup protection operates just when the primary protection does not work. The proper coordination has benefits of listed below.

a) Minimize the number of consumers who may be affected from power loss.
b) Prevents having power interrupt due to transient faults
c) Locating the fault location using protective device
d) Clear the fault in a shortest possible time

As coordination is related to human judgment, experience and characteristic of devices, there are different attitudes among producers of protective devices and protection experts towards the setting and coordination of protective device. Some manufacturers present tables for setting and coordination of protective devices, which give recommended nominal values and settings. Also, introduce methods by comparison of time-current curves of protective equipment. Manual methods are used for coordination frequently in utility companies, which serve for small distribution networks include limited numbers of protective equipment. Some of the companies use standard methods and tables which help design engineers and other technicians to coordinate protective devices. However, some other utilities use semi-automatic methods or computer aided programs, which are provided by manufacturers. To coordinate all protective devices following information are required, since coordination of devices includes, selection of protective devices and their settings, choosing the protective zones for transient faults and minimization of power supply disruption to minimum possible number:

a) Configuration of network
b) Determination of location of protective devices
c) Time-current characteristic curves of protective devices
d) Load current (normal and emergency)

e) Short circuit current (under minimum and maximum generation) in all points that protective device may be connected

Usually, this information is not accessible altogether, so they should be provided from different sources. For example, time-current characteristics should be provided from manufacturers and short circuit currents can be achieved from simulation in load flow and short circuit analysis software.

Also, there are some other important factors in protective devices coordination which are listed below.

a) Difference in time-current characteristics
b) Variation in loads condition
c) Temperature of atmosphere
d) Impact of reconnection cycles

In this chapter an attempt is made to investigate different theories of coordination and finally a comprehensive coordination algorithm will be presented. To achieve this aim, the coordination of each pair of protective devices should be investigated to get to constraints and rules of coordination. Depending on the type of protective equipment, specific constraints will be applied to their coordination. Below the rules of coordination in distribution networks are briefly explained. [38]

2.3.1 Relay – Relay coordination

To avoid having interruption between the operation of main and backup relays, a discrimination time should be in existence between operation time of main and backup relays. The operation time of relays should be long enough to give enough opportunity to closest circuit breaker to fault point to operate during fault. Also, it should not be too long that operation of backup relay in the case of failure in main relay leads into damage of system. This time, interval depends on below parameters. [39]

a) Required time to disconnect the fault current by circuit breaker; as long as the fault current is not disconnected by circuit breaker, this current flows from circuit breaker. For this reason, this time, should be added to main relay

operation time. This time, depends on the type of circuit breaker and its operation speed and in average it is about 100 ms.

b) Time for extra distance passed in backup relay; after disconnection of fault current, the passing current from backup relay is reduced up to load current which is less than relay disc rotating current. However, in this condition, if the backup relay is an electromagnetic relay, its rotating part will not stop and takes a bit more distance toward the rotating direction. The time that relay rotating disc can take mentioned extra distance during fault current passing period must be considered in the coordination of relays. In static relays the capacitors and inductors have stored energy and have the same responsibility. It is worth to mention that design alleviates this effect. However, to compensate this effect 50 ms is considered in relays coordination.

c) Errors: the errors include relays, current transformers, and short circuit current calculations errors. Main and backup relays can operate faster or slower than setting time, and from operation time viewpoint it can have positive or adverse effects on error. This type of errors depends on relay current. Relay error gradually decreases for currents higher than four times of setting current.

Considering relay class some part of relay operation time is considered as relay error time. This error is different in relays depending on their type, and in each case, we should refer to relevant standard to determine the error. The time error is considered about 7.5% in overcurrent relays, and as the relays error for main and backup relays are considered adversely, the total error comes to 15%. In addition to this, 10% is taken into account to cover the effect of all current transformers. As a result of all these errors, the total time error for relays comes to 25% or $0.25t$ where t is the operation time of closest relay to fault point.

d) The time interval to make sure that backup relay will not operate; to keep the selectivity of protection system 100ms is added to previously mentioned values. To obtain the coordination time interval (CTI) above four values should be accumulated. So CTI of overcurrent relays is as (2.1).

$$C.T.I = 0.25t + 0.1 + 0.05 + 0.1 = 0.25t + 0.25 \tag{2.1}$$

where:

t is relay operation time (s)

In the early days, the relays have been coordinated just by considering a constant time delay for their operation. This constant time was 0.5s, and later it has been changed to 0.4s because of faster circuit breaker and reduction in relays. This time interval should not be less than 0.3s in any case. Some references propose 0.15 to a total of all errors [40]. In this case the coordination time interval is achieved by (2.2).

$$C.T.I = 0.1 + 0.05 + 0.15 + 0.1 = 0.4 \qquad\qquad (2.2)$$

2.4 Over current protection

Overcurrent protection is a most common method to protect lines because of cost and simplicity of it. Depending on the structure of the network (radial or loop) and its voltage, the right type for overcurrent protection is chosen. The overcurrent relay includes different kinds characteristics, such as constant time overcurrent relay, constant current overcurrent relay, inverse time-current characteristic overcurrent relay, directional overcurrent relay, earth fault overcurrent relay or a combination of them.

For distribution lines usually overcurrent relays are used as main protection in distribution systems, and in sub-transmission this relay sometimes is used as main protection and in some cases is used as backup protection. In transmission lines where distance relay is used as main protection, because of its higher sensitivity, the earth fault relay is used as well because it is likely that earth faults with high impedance arc to occur and distance relay fails to detect it.

2.4.1 Brief about overcurrent relays setting

An overcurrent relay consists of two main sections. Section one is related to fast operating element and second section is related to delay operation unit [41]. To set the instantaneous unit, the threshold current, which relay operates for currents higher than that, should be determined. The relay should be set for the protection of faults which occur in relay installed line. To avoid unnecessary trips of the relay for other

16

lines a safety coefficient should be defined. So to set the relays instantaneous unit, the maximum fault current on furthest busbar from relay connected point is obtained and then multiplies by COI which it is value is 1.3. COI is applied to prevent the relay from the triping for faults on adjacent busbars in furthest bus line. This unit is used either for cases that fast disconnection of fault is required or for cases that extreme variation in line impedance exists. Delay unit of overcurrent relay has two settings.

a) Plug Setting (PS)
b) Time Setting Multiplier (TSM)

Using plug setting, it is possible to set relay to trip for currents higher than specific value. Moreover, TSM is used to make coordination and to trip the relay for different short circuit currents at the minimum possible time. The current setting of delay unit should be set so that firstly, the relays do not trip for maximum load current and secondly, it can trip for minimum fault current. So this setting will include two limits. One lower limit and upper limit and the minimum value of this setting is the greater value of below two values.

a) The minimum available current setting on delay unit of overcurrent relay.
b) Maximum load current passing from relay multiply by COI (insurance factor). The COI is 1.3 for phase relays and earth fault relays is between 0.1 and 0.3.

The maximum value of the current setting is achieved from least value of below two parameters.

a) Short circuit current of furthest busbar from relay in normal operation mode
b) Minimum short circuit current of furthest busbar from relay

The maximum of current setting lets relay to trip during minimum fault current and minimum current setting assures that relay do not operate for maximum load current.

With adjusting relay current setting, relay operation is guaranteed for cleaning the power system faults. However, it is likely that systems relays are not coordinated fully. Hence, time setting multiplier is used for coordination of protective system relays. This coordination is carried out such that the faults are removed by main

relays quickly and secondly, main and backup relays are coordinated with each other. Relays time setting is done based on following rules.

The operation time of backup relay always should be at least CTI(s) higher than its according main relay. The normal range of CTI is 0.3 or 0.4. The value of this coefficient should assisst relay to trip for faults in the zone of the main relay as quick as possible. The difference in trip time between the main and backup relays should always be valid. It means that operation time difference between main and backup relay must always become greater than coordination time difference in the network for all type of short circuit faults. This needs to find the critical points in the network which for those points operation time difference for main and back up relays is minimum. However, there is no guarantee that application of this constraint is feasible for all conditions and sometimes there is no choice but to neglect this option. In this states, inverse time relays with great slope are used. The time interval between main and backup relay operation depends on below parameters.

a) Trip time of circuit breaker
b) Time for extra rotation of relay disk
c) Errors of measurement devices
d) Assurance time interval

2.4.2 Methods of overcurrent relay coordination

To coordinate relays, there are different methods which briefly are reviewed here.

2.4.2.1 Time coordination

In this method, an appropriate delay is applied for all relays in the system to let the closest relay to fault point trip earlier than others. In this method the furthest relay delay is set on maximum and as relays approach to source, the operation time of relays increases. The drawback of this approach is the longest trip time of most upstream relay which is close to the source which short circuit current is highest at this point. Using this method of coordination raises another issue for protection system. i.e. relays for higher fault currents trip in longer time and this can damage equipment of the network.

18

2.4.2.2 Current coordination

In this approach relays which are far from the source set to lower pick up current and relays on upstream of feeder set to higher current. In this way when a fault occurs the closest relay to fault point trips. The drawback of this method is the inability to distinguish and disconnection proper relay. Actually, in this method, the short circuit current of points in few meters distance of each other and around the busbars are very close in value. Because of the errors of measurement devices, it is probable that the relays cannot accurately discern the fault point and trip the relevant relay and disconnect the minimum possible part of the network. This type of protection is used in the networks which the fault current in specific sections are significantly different, and consequently, selectivity application for the protective system is easy.

2.4.2.3 Time - Current coordination

To escape from encounter to mentioned problems in last two sections for time coordination and current coordination, mixed method of time-current coordination is used to coordination of overcurrent relays. In this relays, the operation time is reduced as fault current increases. The characteristic of these relays is adjustable in current axis and also in time axis. So coordinating of these relays from current or time viewpoint is possible. Using these types of relays solves the problem of previous mentioned relays drawbacks. Because, as the fault point become closer to source, the short circuit current is higher, and in these relays the higher the fault current the shorter the trip time of relay. On the other hand, with correct adjustment of current and time settings the issue of appropriate fault allocation and minimum faulty section isolation (selectivity issue) is solved.

2.4.3 Models of relays characteristic curves

To coordinate overcurrent relays of a network, it is necessary to have that time-current characteristic curves of all relays. As these characteristics must be used in computers for calculations and coordination, so it needed that they get inserted into computer. The simplest method of doing this is the save of points of curves in the computer. To increase accuracy, more points should be inserted in characteristic curve. As each relay has several characteristic curves for different TSM and different

current setting, several characteristics should be given to the computer. If this is done for many relays not only it occupies large memory in computer, but also process speed is reduced. So in practice, this method is not used.

In other methods, characteristic curve of the relay is modeled in the form of mathematical equation regarding setting parameters. Several models have been introduced in the past. A good mathematic equation should have acceptable accuracy in an approximation of characteristic curve and also should not have many numbers of coefficients. The high numbers of coefficients increase the process time and occupy more space of memory. Selection of a model can be based on the type of calculation or their application.

Considering this topic, after discussion on different kinds of models and their comparison a suitable model is chosen below.

In mathematic equations, trip time (t) is shown in terms of passing current (I) and parameters involve in that. Passing current is shown regarding PSM (plug setting multiplier) which is the ratio of short circuit current to relay pick up current. Time setting multiplier is used as TSM or TDS in equations. For overcurrent relays some models have been introduced which are described below.

2.4.3.1 Warrington model

In this model, the operation time of relay is presented by parameters such as TSM and I_b.

$$t = c + \frac{k}{(\frac{I}{I_b})^n - 1} * TSM \tag{2.3}$$

Where;

TSM   Time setting multiplier

I   Short circuit current passing from relay

I_b Relay pickup current

K   Coefficient depends on relay type

20

C   Coefficient to represent the effect of fraction and hysteresis

Using this equation, it is possible to simulate different types of descending relays. These equations have been listed for several types of relays in Table 2.1. The advantage of this model is its less number of coefficients and simplicity of its calculation. To calculate coefficients of k and c in fix TSM, limited numbers on time- current curve can be chosen to cover the relay current zone. Then using approximation techniques the values for K and C can be achieved. Approximation technique is carried out by minimum square error method. This model is linear regarding TSM and descending regarding current. The drawback of this approach is its weakness of accurate estimation of overcurrent relays characteristic.

2.4.3.2 Polynomial models

Bajaj and Esmolk use These models. In Bajaj model, the current is stated in terms of time and the form of degree n polynomial. [38]

$$I = a_0 + a_1 t + a_2 t^2 + ... + a_n t^n \tag{2.4}$$

Whereas, in Esmolk model the time is stated regarding current and in the form of degree n polynomial.

Also in these models using the method of minimum square error try to estimate curve in several points and to find coefficients from a_0 to a_n. Usually, this method ends in solving the set of equations which a_0 to a_n are its unknowns. The matrix of coefficients for this set of equations is usually difficult, and its determinant mostly becomes very close to zero. So in computational calculations, it is probable to have an error and not accurate enough final results. To cope with this issue, firstly the variables with high accuracy can be used and secondly, to increase precision more numbers of points must be used to the estimation of the curve.

In these equations usually, the aim is finding the trip time of relay while the current is in our hand. Looking at two above equations, it is evident that Esmolk model is easier to do this rather than Bajaj model. Moreover, from curve estimation accuracy point of view, the Esmolk model is preferred. In this model selected points

should be in between of minimum to a maximum current of relay points to cover all of this area.

Table 2.1. Warrington equations for different type of relays

$t = \dfrac{0.14}{(\dfrac{I}{I_b})^{0.02} - 1} * TSM$	Inverse relay
$t = \dfrac{13.5}{(\dfrac{I}{I_b})^{1} - 1} * TSM$	Very inverse relay
$t = \dfrac{80}{(\dfrac{I}{I_b})^{2} - 1} * TSM$	Extremely inverse relay
$t = \dfrac{35}{(\dfrac{I}{I_b})^{2} - 1} * TSM$	Thermal relay
$t = \dfrac{120}{(\dfrac{I}{I_b})^{1} - 1} * TSM$	Earth fault relay with delay

$$t = a_0 + a_1 I + a_2 I^2 + ... + a_n I^n \tag{2.5}$$

2.4.3.3 Radke model

In this model, the time-current curve of the relay is modeled in logarithmic scale. It means that $Log(I)$ and $Log(t)$ appear in logarithmic characteristic.

$$Log(\frac{t}{TSM}) = K + A_1(LogI) + A_2(LogI)^2 + A_3(LogI)^3 + A_4(LogI)^4 \tag{2.6}$$

In this model having short circuit current, easily can obtain the relay trip time. As it is seen in this equation the trip time has a linear relationship with TSM. The accuracy of this model for shorter trip times is not good, but for longer trip times its accuracy is acceptable. Having linear relationship between t and TSMM is the advantage of this model which makes is desired in the optimal coordination of

overcurrent relays but having different accuracy for short and long operation times is the drawback of this model.

2.4.3.4 Sachdev model

There are two basic drawbacks in previously discussed models.

a) Considering PSM definition, for PSM=1 the time of operation should become infinite while in discussed equations this occurs for PSM=0.

b) The acquired curve for PSMs greater than applied ones in curve estimation brings huge deviation from the real curve.

So, the appropriate model for relays should satisfy the following criteria.

a) The estimated curve should not have a big difference and error compared to real curve.

b) Achieved curve should give infinite for PSM=1.

c) The estimated curve should be similar to the real curve for minimum relay operation current (pickup current) and big values of PSM and other current values between these two.

d) The mathematical equation should have a simple form, and its calculations can be done easily.

e) Sachdev proposed the following model after many investigations.

$$\frac{t}{TSM} = a_0 + \frac{a_1}{Log(I)} + \frac{a_2}{(Log(I))^2} + ... \tag{2.7}$$

Logarithmic and anti-logarithmic equations are time-consuming for computers to be solved compared to normal division and multiplication functions. So for making it simpler, the above relationship can be converted to this form.

$$\frac{t}{TSM} = a_0 + \frac{a_1}{(I-1)} + \frac{a_2}{(I-1)^2} + ... \tag{2.8}$$

The relationship between operation time (t) and TSM is assumed linear in ((2.8). This affair is done for regular TSM considering the fitness of characteristic curve, or curve fitness is done for an average of all TSMs.

Another model that Sachdev has presented is nonlinear as well regarding TSM. This equation is in the form of a polynomial regarding TSM for constant currents.

$$t = C_1 + C_2 TSM + C_3 \frac{TSM}{(I-1)^2} + C_4 \frac{TSM^2}{I-1} + C_5 \frac{TSM^2}{(I-1)^2} + C_6 \frac{TSM}{(I-1)^3} + C_7 \frac{TSM^2}{(I-1)^4}$$ (2.9)

2.4.3.5 *Sachdev multiplied two polynomials of current and time model*

In this model, the operation time of relay is stated in terms of time and current by multiplication of two polynomials.

$$t = Poly(TSM) * Poly(I)$$ (2.10)

where

$PolyTSM$ is a polynomial in terms of TSM

$PolyI$ is a polynomial in terms of I

And are defined as below

$$Poly(TSM) = b_0 + b_1 TSM + b_2 (TSM)^2 + b_3 (TSM)^3 + \dots$$ (2.11)

$$Poly(I) = a_0 + \frac{a_1}{I-1} + \frac{a_2}{(I-1)^2} + \frac{a_3}{(I-1)^3} + \dots$$ (2.12)

In this model the operation time will be a polynomial regarding TSM for specific current value and for constant TSM it will be a polynomial regarding I, with inverse powers of current. This model has better accuracy than other models, but it has a nonlinear format. Its nonlinearity is so that it can be used for optimal coordination of overcurrent relays. Hence this model is the best one among all discussed models to make better coordination from accuracy and simplicity point of view. And its precision about both current and TSM is acceptable.

2.5 Brief about coordination methods

From 1964 lots of methods have been proposed to coordination of overcurrent relays in different papers. Initially, the calculation of protective systems was charging out manually by engineers. For this reason, it was not applicable to big networks, and it was very time-consuming. The advent of computers helped to calculate the coordination problem faster. The method of computer solving included two groups of optimized coordination and ordinary coordination. The optimized methods recruited because ordinary methods were not able to discern the best solution among all solutions.

2.5.1 Overcurrent relays coordination algorithm in interconnected networks

Coordination of overcurrent relays in radial distribution systems is simple and does not have any specific difficulty. Also, there is the solution for bidirectional supplied radial systems and ring networks and parallel lines by using bidirectional relays. However for interconnected networks, making coordination among all relays is very difficult because of structure complexity of the network and mutual interference of relays in fault clearance. This cannot be done without computer assistance. In radial and ring networks the relays just have communication with one or two adjacent relays, and therefore the interference between them is easy to handle. However, in interconnected networks as many lines can be connected to one busbar, more numbers of relays can be considered as neighbors and coordination must be carried out for all pairs of main and backup relays which is so difficult and time-consuming in this condition.

On the other hand, as these networks are supplied from several directions, fault currents can flow from both sides of lines, and this can bring some issues in relays coordination. Therefore it is a must to use directional relays for interconnected networks. Using this, relays trip just for fault currents flow in a specific direction, and this makes the coordination much easier. Despite this, sometimes the complexity of network is so high that does not let complete coordination be made. So it is likely that many of coordination methods could not achieve coordination fully among all

relays. However, this issue can be relatively solved by chasing suitable relay characteristics and appropriate relay coordination method.

There are specific numbers of current in specific points of the network which must be checked to set the Setting of relays and make coordination among overcurrent relays of an interconnected network [42]. Some of this information are used to obtain current setting of overcurrent relays, and some others which usually are in pairs are used to do coordination.

2.5.1.1 Required currents to get current setting of overcurrent relays

To make coordination among all relays critical information such as maximum load current, maximum, and minimum short circuit current, etc should be obtained and then using these data current setting of overcurrent relays can be adjusted. This setting should be such that for worst load condition must not pick up and even for minimum fault currents pick up. This information includes following data.

a) Maximum fault current of the relay for fault in front of the relay.

This current is used for setting of the instantaneous element of the relay. If the setting of the instantaneous unit is higher than this value, there is no point to use it. This current is calculated for different conditions of the network. For example, it is calculated for normal state and a different configuration of the network after disconnection of various lines. So the maximum amount of that can be found.

b) Maximum fault current for relays furthest busbar.

This current also is used for calculation of setting of an instantaneous unit of over current relay. To obtain this current, the fault is applied in different conditions of network and the maximum current is chosen out of all of them. If the line has other branches, first maximum short circuit current of the relay for a fault on around busbars is calculated and then a maximum of them is chosen.

c) Minimum fault current in relay location for a fault on the furthest busbar.

If the information about the maximum current of relays at the end of backup protection zone or at the end of next line were not sufficient, the current setting could be carried out considering short circuit current of the relay for a fault on the furthest busbar.

d) Minimum relay current for short circuit of the line when the circuit breaker of the end of the line is open.

This current is similar to previously mentioned current and is obtained by short circuit program.

e) Minimum short circuit current of the relay.

This current is used to determine maximum current of overcurrent relays. In phase overcurrent relays this current is considered %50 to 60% of relay passing current during three-phase fault at the far end of backup relay's protection zone. If this current is less than maximum load current in relay location and its operation direction, the maximum load current is substituted. In earth fault relays this current is considered a quarter of minimum relay passing current for single phase fault at the far end of a protection zone of the backup relay. Here again if this current become less than zero sequence component of load current in relay operation direction, it is replaced by this zero sequence component current.

f) Maximum load current in relay operation direction.

This current is used for calculation of relays current setting. Relays should never trip for load currents. Hence correct calculation of this current is vital for current setting of the relay. This current usually is obtained from load flow program running in different conditions. If the relay is not directional, maximum load current regardless of its direction is the target. As it mentioned before, setting of instantaneous and delay units done taking this fact into account that delay unit should not trip for load currents and also should trip for minimum fault current and the instantaneous unit is set considering that relay should operate just for its protective zone. To do the setting of relays, these currents calculations is necessary. Also these currents help us to decide whether the directional relay is required or not.

The next chapter will pay attention on sensitivity analysis in presence of one single PV in the feeder. Important factors such as fault current, voltage of different nodes along the feeder have been analysed. Also a comparison has been made between these factors in NOPV mode with those in PV included network.

2.6 Summary

This chapter paid attention to protection rules of the distribution network and described the criteria for proper selection of protection system in the network. Also in this chapter, the different characteristic modeling of overcurrent relays was discussed, and the advantage and disadvantage of them were revealed. The rules of coordination for relay-relay were presented in the chapter to pave the way of utilizing them in next chapters which will focus on protection of distribution in the presence of huge number of PVs.

Chapter 3. Sensitivity Analysis in the
Presence of One Unit of Rooftop
PV in Distribution Feeder

3.1 Introduction:

As it was mentioned in the literature review in chapter one of this thesis, there are not much considerable research which pays attention to the effect of single phase rooftop PVs on distribution network protective factors such as short circuit current and also on voltage profile of feeder during the fault. This is due to newly raised concern which was not focused by the researchers previously. These parameters are very important for PVs disconnection sequence as PVs are equipped with voltage based protection functions. The voltage of PV connecting point to the network is a key factor in disconnection of PVs after a fault in LV distribution network. Also the current on the secondary side of a distribution transformer is an important parameter in operation of the fuse for the protection of the system against short circuit faults in the LV feeders. So this chapter concentrates on these two mentioned parameters in the presence of a single phase PV in the distribution feeder.

This chapter focuses on the impact of single phase PV on voltage profile and short circuit current sensed by protective devices in case of different types of faults occurrence. The fault types include a line to ground (LG), line to line (LL), and line to line to ground (LLG) types which are the most frequent types of faults in LV feeders particularly where overhead distribution exists [43]

The rest of the chapter is organized as follows: Section 3.1 presents the network under consideration and the impact of a PV on the system voltages and currents

during a short-circuit fault. The modeling of the considered system for short-circuit studies is introduced in detail in Section 3.3 this section also discuss the developed sensitivity analysis model. Section 3.4 illustrates the sensitivity analysis results for the voltage profile along the LV feeder as well as the current sensed at the secondary side of the distribution transformer during different types of short-circuit faults. Section 3.5 pays attention to discussion on results, and last part is a summary, which describes general findings of this chapter.

3.2 Network under consideration

Let us consider the residential supply network of Figure 3.1 which represents a typical Australian urban residential network. In Australia, residential LV feeders are mostly three-phase 4-wire multiple earthed neutral (MEN) systems and are supplied by three-phase Dyn distribution transformers [44]. The distribution transformer is supplied by a three-phase MV feeder. Most of houses are single-phase loads. The LV feeders are protected by LV switch-fuses at the secondary side of the distribution transformer to protect the system in case of short-circuit faults in the LV feeder. In Australia, the distribution transformers are usually in the range of 25 to 630 Kva and the LV feeders are usually 400 meters long. It is to be noted that although this system is common in Europe, Asia and Africa, it is different from the structure and topology aspects compared to the LV residential network of the North American countries.

The residential rooftop PVs in Australia are also single-phase units (composed of PV cells, inverters and disconnectors). Depending on financial status of the householder and their needs, PV ratings in Australia varies between 1 to 5 kW. There is no specific regulation to make a balance among the different phases for connecting PVs and PVs are connected randomly to phases.

All PVs available in Australian market are equipped with an islanding protection function (e.g. under/over voltage protection function) based on Australian Standard on grid connection of energy systems via inverters [45] and are required to disconnect after a short-circuit fault in the LV feeders. The output current of the PV systems are equipped with a current limiting technology and protection fuses which limit their output current to 1.5 times of their nominal current [46].
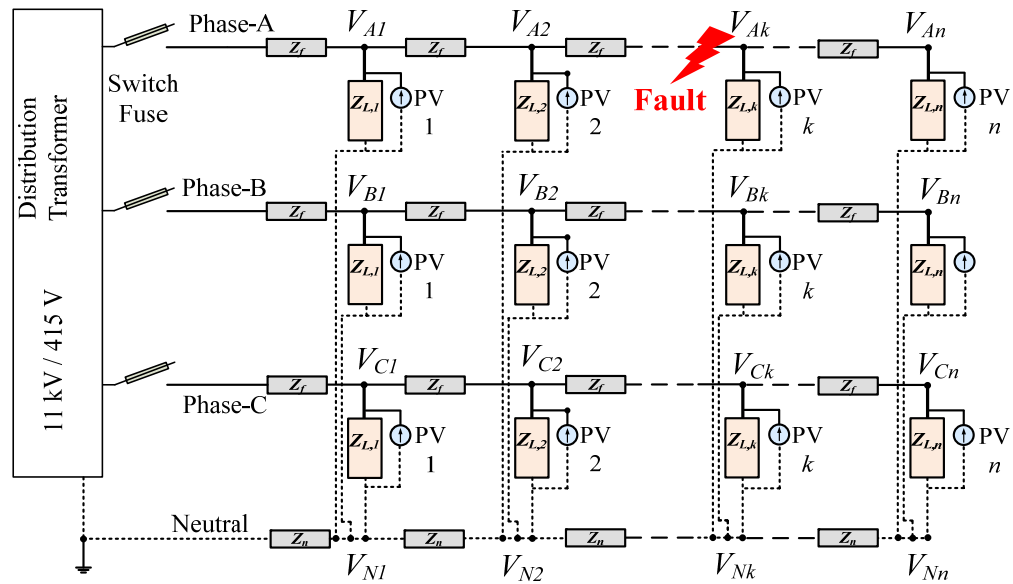
Figure 3.1. Low voltage residential network under consideration

Now, let us assume that a single-phase PV system is connected to one of the
phases of the LV feeder (see Figure 3.2a). The aim of this section is to analyze the
impact of PV on important factors of protection of network, including the fault
current (I_{Fault}), current supplied from the distribution transformer towards the fault
(I_{DT}) and the voltages of different nodes along the feeder (V_n). There are two types of
combination for fault location and PV connecting point. The short circuit fault can
occur either in upstream of PV (see Figure 3.2b) or at its downstream (see
Figure 3.2c). In both cases, the fault current is composed of two components: the
current supplied by PV and current which is injected from transformer side. Thus,
the short-circuit current increases in the systems of Figure 3.2b and Figure 3.2c
compared to the system of Figure 3.2a. The higher the PV rating, the higher the
increase of fault current.

For a fault at the upstream of the PV location (Figure 3.2b) as the PV is located
closer to the end nodes of the LV feeder, the node in which the PV is installed
experiences a greater voltage. This is because as the PV is located closer to the end
of feeder (EOF), its output current passes through a larger portion of the LV feeder
and thus, a greater voltage appears for every node between the fault and the PV
location. The voltage reduces from the node in which the PV is located towards the
fault point. For a bolted fault (in which the fault impedance is zero), the PV presence
does not have any impact on the voltages of the nodes between the distribution

31

transformer and the fault location. Also, it does not affect the current supplied by the distribution transformer. It is to be reminded that for a realistic fault (in which the fault impedance is small but not zero), the current supplied by the PV system will cause an increase in the voltage of the node in which the fault has occurred. This slightly increased voltage will reduce the current supplied by the distribution transformer to reduce slightly. It is to be noted that the impact is stronger if the PV has a higher rating.

For a fault at the downstream of the PV location (Figure 3.2c), the voltage at the node in which the PV is located is increased compared to the system of Figure 3.2a, and thus, the current supplied by the distribution transformer reduces. As the PV is located closer to the beginning nodes of the LV feeder, the impact becomes stronger. Thus, the fault current reduces slightly (however, it is still larger than the fault current of Figure 3.2a .This impact is enhanced as the PV has a higher rating.

3.3 System modeling and analysis

If installed PVs are ignored in the Figure 3.1, it will be completely a traditional distribution network. However, a different number of PVs can be connected to each phase and this lead to the creation of distribution network with unequal numbers of DERs in phases and system will be unbalanced. Also, PVs connected to different points of the system may have different rating and output power. So, the network of Figure 3.1 should be considered as an unbalance network which can be solved using Fortesque's sequence component method. [47]. This fact is true even in the case that impedances of each phase of the system are identical.

The analysis of the network of Figure 3.1 using sequence components are given in this section and it worth to mention that main difference of the considered unbalanced system with traditional feeder initiated unbalanced system is that negative and zero sequence components of voltage appears in addition to positive sequence. Assuming an equivalent distance between two adjacent poles (nodes) in the LV feeder, the LV feeder impedance matrix can be represented for phase-A, B and C as;

$$TCD = I^*_{DT} - I_{DT} \qquad VD = V^*_n - V_n \qquad FCD = I^*_{Fault} - I_{Fault}$$
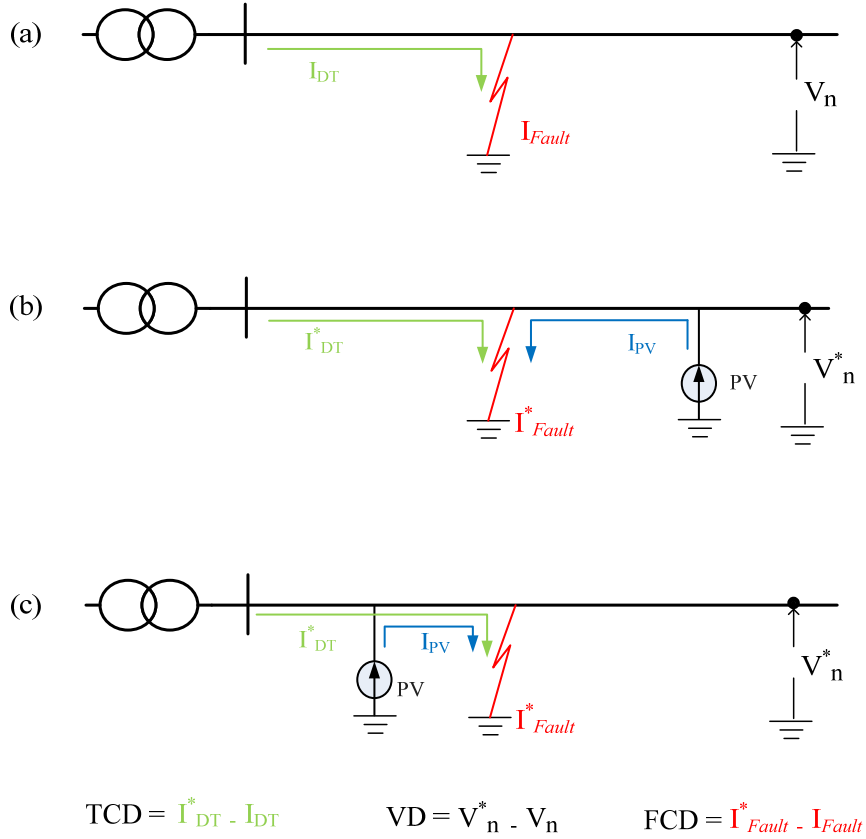
Figure 3.2. Schematic diagram of different states of PV and fault location situations. (a) No-PV mode (b) Fault at upstream of PV location (c) Fault at downstream of PV location.

$$[\mathbf{Z}^{LV}_f]_{ABC} = z_f . \mathbf{I}_{(3)} \tag{3.1}$$

where z_f is equal to the per-phase impedance between two adjacent nodes and $\mathbf{I}_{(3)}$ is the identity matrix of order 3. Similarly, the MV feeder impedance and distribution transformer impedance can be represented as

$$[\mathbf{Z}^{MV}_f]_{ABC} = z'_f . \mathbf{I}_{(3)} \tag{3.2}$$

$$[\mathbf{Z}^{trans}]_{ABC} = z_{trans} . \mathbf{I}_{(3)} \tag{3.3}$$

where z'_f is equal to the per-phase impedance of the MV feeder between two adjacent nodes and z_{trans} is the equivalent per-phase impedance of the distribution transformer. From (3-1), the LV feeder impedance in sequence components can be expressed as

$$[\mathbf{Z}^{LV}_f]_{012} = [\mathbf{A}]^{-1}[\mathbf{Z}^{LV}_f]_{ABC}[\mathbf{A}] \tag{3.4}$$

where

33

$$[\mathbf{A}] = \begin{bmatrix} 1 & 1 & 1 \\ 1 & a^2 & a \\ 1 & a & a^2 \end{bmatrix}$$

and a = $1\angle 120°$. In a similar way, the sequence components for the impedance of the MV feeder and the transformer can be calculated.

It worth mentioning that the dynamic characteristic of PV current and fault impedance are ignored in this research in spite of their dynamic characteristic in reality [48]. Hence, in the rest of this research, Z_{Fault} shows the steady-state value of the fault impedance and I^{PV} represents the steady-state output current of a PV. With this assumption, each PV can be considered as a current source during the fault period [49]; hence the matrix of the output current of PVs connected to phase-A, B and C at node i ($1 \leq i \leq n$) can be expressed as

$$[\mathbf{I}_i^{PV}]_{ABC} = [I_A^{PV} \quad I_B^{PV} \quad I_C^{PV}]_i^T \tag{3.5}$$

where T is the transpose operator. From (3.5), the output current of the PVs in each node, in sequence components, is

$$[\mathbf{I}_i^{PV}]_{012} = [\mathbf{A}]^{-1}[\mathbf{I}_i^{PV}]_{ABC} \tag{3.6}$$

From (3.4) and (3.6), for an asymmetrical fault at node k of the network of Figure 3.1, the equivalent sequence networks are modeled as shown in Figure 3.3a. The network is later simplified using the Thevenin-Norton equivalent circuit from the fault point of view. This simplification is carried out separately for the PVs located at the downstream and upstream of fault.
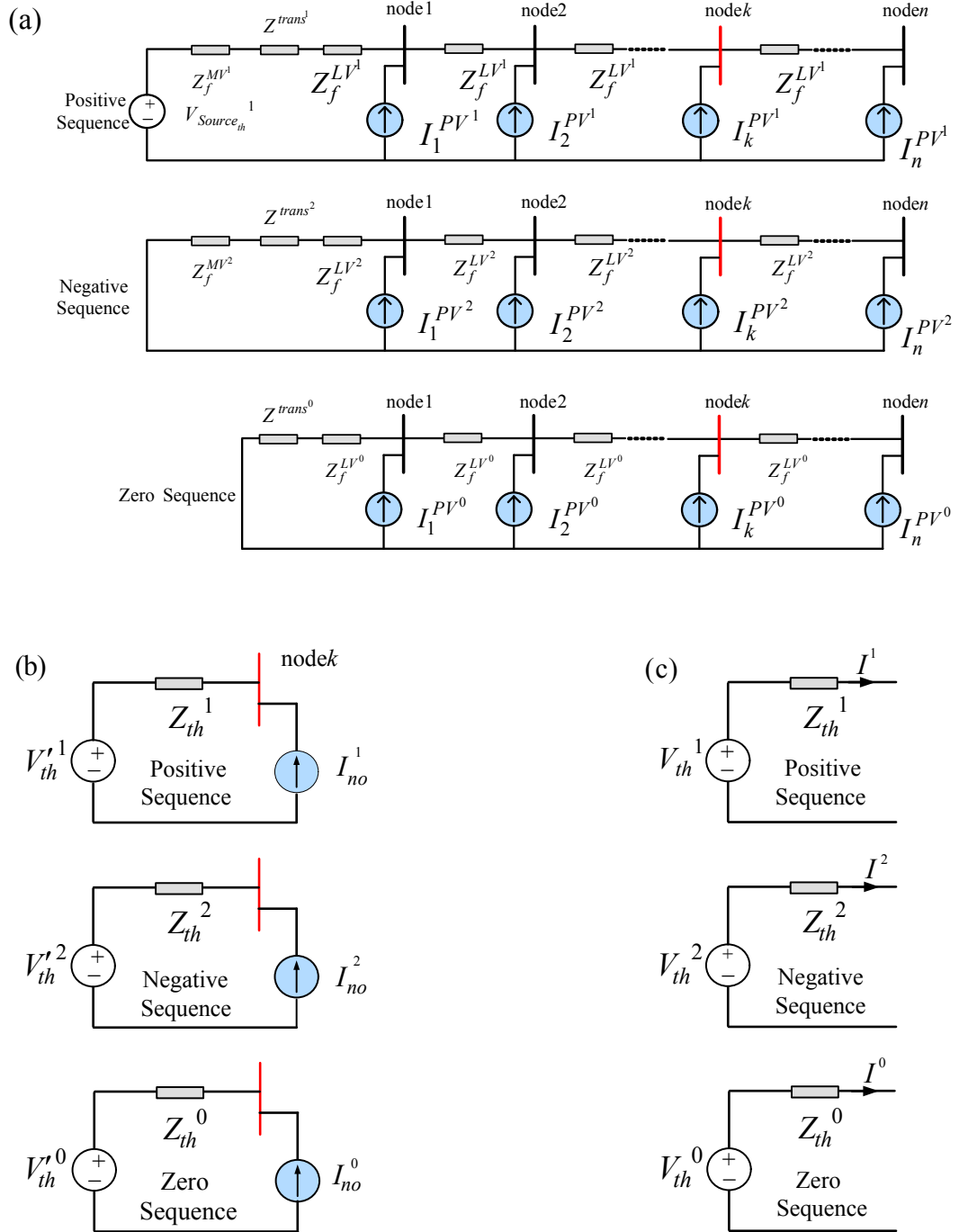
Figure 3.3. (a) Sequence networks of the system of Figure 3.1 for a short-circuit fault at node k. (b) Equivalent sequence networks, (c) Simplified Thevenin equivalent of sequence networks.

where the suffix *no* denotes Norton equivalent.

For the PVs at the downstream of fault, their output currents are summed, based on Norton equivalent circuit, as illustrated in Figure 3.3b and can be expressed as

The thevenin equivalent of the system at the upstream of fault, including the PVs, can be illustrated as shown in Figure 3.3b and can be expressed as

$$
\begin{cases}
I_{no}^1 = \sum_{i=k}^{n} I_i^{PV^1} \\[2mm]
I_{no}^2 = \sum_{i=k}^{n} I_i^{PV^2} \\[2mm]
I_{no}^0 = \sum_{i=k}^{n} I_i^{PV^0}
\end{cases}
\tag{3.7}
$$

$$
\begin{cases}
V_{th}'^1 = V_{Source_{th}}{}^1 + \sum_{i=1}^{k-1} I_i^{PV^1}\left(Z_f^{MV^1} + Z^{trans^1} + i.Z_f^{LV^1}\right) \\[2mm]
V_{th}'^2 = \sum_{i=1}^{k-1} I_i^{PV^2}\left(Z_f^{MV^2} + Z^{trans^2} + i.Z_f^{LV^2}\right) \\[2mm]
V_{th}'^0 = \sum_{i=1}^{k-1} I_i^{PV^0}\left(Z^{trans^0} + i.Z_f^{LV^0}\right) \\[2mm]
Z_{th}{}^1 = Z_f^{MV^1} + Z^{trans^1} + kZ_f^{LV^1} \\[2mm]
Z_{th}{}^2 = Z_{th}{}^1 \\[2mm]
Z_{th}{}^0 = Z^{trans^0} + kZ_f^{LV^0}
\end{cases}
\tag{3.8}
$$

where th denotes Thevenin equivalent.

The Thevenin equivalent of the system upstream of (3.8) and the Norton equivalent of the system downstream of (3.7) can be further simplified as Figure 3.3c where

$$
\begin{cases}
V_{th}^1 = V_{th}'^1 + I_{no}^1 Z_{th}^1 \\[2mm]
V_{th}^2 = V_{th}'^2 + I_{no}^2 Z_{th}^2 \\[2mm]
V_{th}^0 = V_{th}'^0 + I_{no}^0 Z_{th}^0
\end{cases}
\tag{3.9}
$$

which can be represented as

$$
[\mathbf{V}_{th}]_{012} = [\mathbf{V}_{th}']_{012} + [\mathbf{I}_{no}]_{012}\,[\mathbf{Z}_{th}]_{012}
\tag{3.10}
$$

Equation (3.10) demonstrates that, in addition to the expected negative and zero sequence impedance and positive sequence of voltage, a negative and zero sequence of voltage also appear due to the presence of single-phase PVs that are distributed unequally among the three phases of the network [34].

36

3.3.1 Faults in the network

LG, LL and LLG are considered in this research as they have been reported as the most frequent types of LV feeders [43]. It is to be noted that three-phase-to ground and open conductor faults are beyond the scope of this research. It should be noticed that all faults have been considered between different phases. For example for LL fault, three different types of phases have been chosen. First, phase A to B, second, phase A to C and third, phase B to C. and for the line to ground one all three different phases have been used (i.e., AG, BG, CG). This is true for line to line to ground fault as well. Which ABG, ACG and BCG are three different combinations that can be made for the line to line to ground fault. Figure 3.4 illustrate schematic diagram of all applied faults in this study.
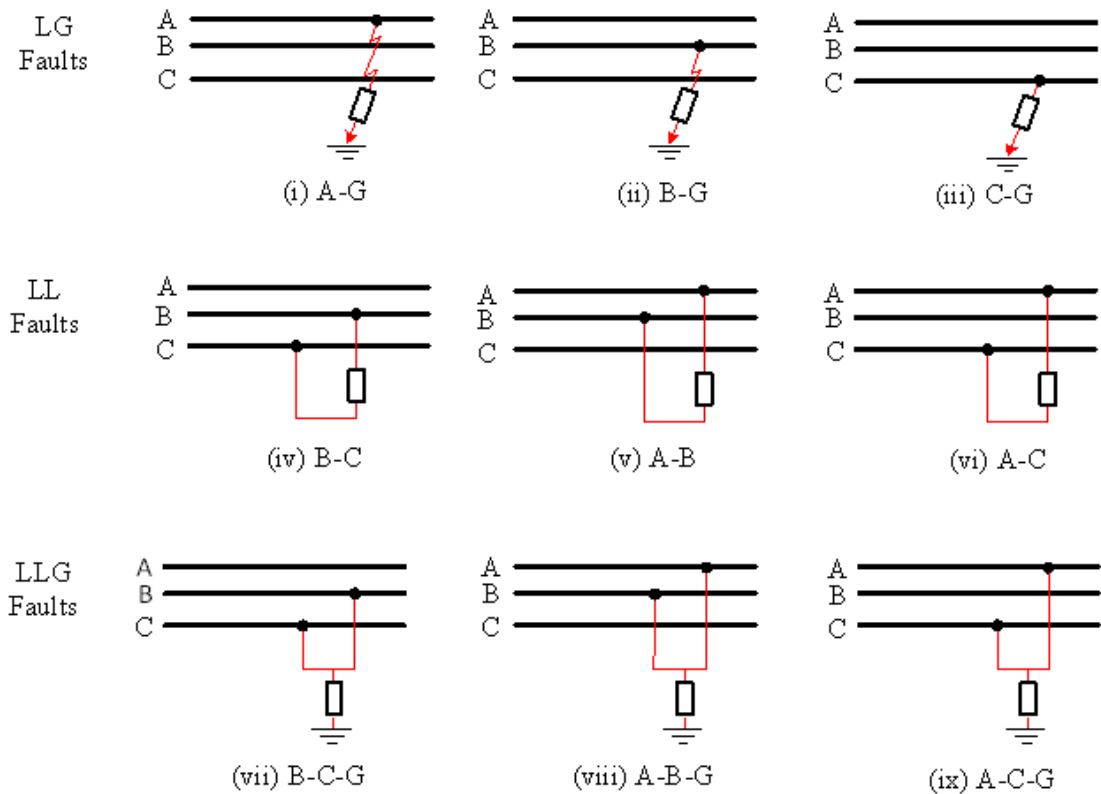
Figure 3.4. Different types of faults considered in this study.

3.3.1.1 LG faults

For an LG fault (see Figure 3.4i), the fault current is calculated from the current sequence components. Depending on the faulted phase, (i.e. Phase-A, B or C), the fault current is calculated as

$$[\mathbf{I}^{Fault}]_{ABC} = 3I\,[\lambda_A \quad \lambda_B a^2 \quad \lambda_C a]^T \tag{3.11}$$

where

$$I = \frac{V_{th}{}^1 + V_{th}{}^2 + V_{th}{}^0}{Z_{th}{}^1 + Z_{th}{}^2 + Z_{th}{}^0 + 3Z_{Fault}}$$

while $\lambda_j = 1$ if the LG fault is in phase j (j = A, B or C); otherwise it is zero.

After fault current calculation, the voltage at the fault location is calculated using Kirchhoff's voltage law (KVL) in sequence components as

$$[\mathbf{V}_{Fault}]_{012} = [\mathbf{V}_{th}]_{012} - [\mathbf{I}]_{012}[\mathbf{Z}_{th}]_{012} \tag{3.12}$$

and is then transferred to ABC frame by

$$[V_{Fault}]_{ABC} = [A]_{012}[V_{Fault}]_{012} \tag{3.13}$$

Finally, the voltage of each node along the feeder of Figure 3.2a is calculated.

3.3.1.2 LL faults

For an LL fault (see Figure 3.4 iv), the fault current is calculated from current sequence components based on the faulty phases as

$$[\mathbf{I}^{Fault}]_{ABC} = [\mathbf{A}]_{012}[\mathbf{I}_{Fault}]_{012} \tag{3.14}$$

where

$$I^1 = \frac{V_{th}{}^1 - V_{th}{}^2}{Z_{th}{}^1 + Z_{th}{}^2 + Z_{Fault}}$$

and

$I^2 = -I^1$ and $I^0 = 0$ if the fault is in phases B and C. (see Figure 3.4iv)

$I^2 = -I^1 \angle + 60$ and $I^0 = 0$ if the fault is in phases A and B. (see Figure 3.4v)

$I^2 = -I^1 \angle - 60$ and $I^0 = 0$ if the fault is in phases A and C. (see Figure 3.4vi)

From the current sequence components, the fault current and voltage profile along the feeder are calculated.

3.3.1.3 LLG Faults

For an LLG fault, if the LLG fault is between phases B and C (see Figure 3.4vii), the current sequence components are

$$\begin{cases} I^1 = \dfrac{(1+a)\,V_{th}^{\ 1} + V_{th}^{\ 2} - Z_{th}^{\ 2} I^2}{(1+a)\,Z_{th}^{\ 1}} \\[2mm] I^2 = \dfrac{\beta_1 - \beta_3\beta_4}{\beta_2 - \beta_3\beta_5} \\[2mm] I^0 = -aI^1 - a^2 I^2 \end{cases}$$

(3.15)

where

$$\begin{cases} \beta_1 = V_{th}^{\ 0} + a^2 V_{th}^{\ 1} + a V_{th}^{\ 2} \\[1mm] \beta_2 = (1+a-2a^2)\,Z_{Fault} + a Z_{th}^{\ 2} - a^2 Z_{th}^{\ 0} \\[1mm] \beta_3 = (1+a^2-2a)\,Z_{Fault} + a^2 Z_{th}^{\ 1} - a Z_{th}^{\ 0} \\[1mm] \beta_4 = \dfrac{(1+a)\,V_{th}^{\ 1} + V_{th}^{\ 2}}{(1+a)\,Z_{th}^{\ 1}} \\[2mm] \beta_5 = \dfrac{Z_{th}^{\ 2}}{(1+a)\,Z_{th}^{\ 1}} \end{cases}$$

Similarly, for an LLG fault between phase A and C (see Figure 3.4viii), the current sequence components are

$$\begin{cases} I^1 = \dfrac{V_{th}^{\ 1} + (1+a)V_{th}^{\ 2} - Z_{th}^{\ 2}(1+a)I^2}{Z_{th}^{\ 1}} \\[2mm] I^2 = \dfrac{\gamma_1 - \gamma_3\gamma_4}{\gamma_2 - \gamma_3\gamma_5} \\[2mm] I^0 = -a^2 I^1 - a I^2 \end{cases}$$

(3.16)

where

$$\begin{cases} \gamma_1 = V_{th}^{\ 0} + a V_{th}^{\ 1} + a^2 V_{th}^{\ 2} \\[1mm] \gamma_2 = (1+a^2-2a)\,Z_{Fault} + a^2 Z_{th}^{\ 2} - a Z_{th}^{\ 0} \\[1mm] \gamma_3 = (1+a-2a^2)\,Z_{Fault} + a Z_{th}^{\ 1} - a^2 Z_{th}^{\ 0} \\[1mm] \gamma_4 = \dfrac{V_{th}^{\ 1} + (1+a)\,V_{th}^{\ 2}}{Z_{th}^{\ 1}} \\[2mm] \gamma_5 = \dfrac{Z_{th}^{\ 2}(1+a)}{Z_{th}^{\ 1}} \end{cases}$$

From the current sequence components, the fault current and voltage profile along the feeder can be calculated.

3.3.2 Sensitivity analysis

The impact of one single-phase rooftop PV on the short-circuit current of the feeder as well as the voltage profile along the feeder is investigated by the sensitivity analysis. PV output power and location in addition to the fault location are considered as the variables of the sensitivity analysis. In this study, a discrete sensitivity analysis is carried out as the PV output power is assumed to be varied from 0.7 to 3.5 kW in steps of 0.7 kW. The fault and PV locations are also varied from node 1 to node n =10. The outputs of this analysis are the fault current; the current sensed at the transformer secondary and the voltage at each node along the LV feeder. It is to be noted that only bolted fault conditions are focused in the sensitivity study analysis. The results of this analysis are presented and discussed in Section 3.3.

A few of the sensitivity analysis results carried out in MATLAB, were compared with PSCAD/EMTDC results. This comparison revealed a maximum of 0.02% error, which validates the accuracy of the system modeling in MATLAB.

3.4 Sensitivity analysis results

The sensitivity analysis evaluates the effect of one unit of single-phase PV on the fault current, the current sensed in the transformer secondary and the voltage profile along the feeder, during an LG fault on phase-A as well as an LL and LLG fault on phase A and B, all assuming Z_{Fault} = 0. The sensitivity analysis is carried out in MATLAB while a few of the case studies in this section are remodeled in PSCAD/EMTDC and the results are compared to validate the accuracy of MATLAB modeling.

3.4.1 Voltage profile along the feeder

One of the parameters which play an important role in the disconnection of PVs following short-circuit faults in the network is the voltage profile along the feeder. In

this section, the deviation of the voltage along a feeder in the presence of a PV is investigated during short-circuit faults.

3.4.1.1 LG faults

Let us consider the network of Figure 3.1 without any PVs. This is referred to as 'No-PV' case in the rest of the chapter. Now let us consider a single-phase PV with a rating of 2 kW (i.e. approximately 8.3 A at 240 V with a unity power factor). The output current of the PV is limited to 150% of its nominal rating (i.e. 12.5 A) during the short-circuit fault. The network in the presence of this PV is referred to as 'PV-available' case in the rest of the paper. Let us assume an LG fault on phase-A at the beginning of the feeder (BOF), i.e. node 1, while the PV is located at different nodes along the feeder (node 1 to 10). The voltage of the nodes along the feeder in the PV-available case is more than the No-PV case. Let us define the voltage difference (VD) as the voltage of the PV-available case minus the voltage of the No-PV case during the short-circuit fault. The VD is shown in Figure 3.5 and illustrates that the feeder end nodes experience a greater VD compared to the beginning nodes. The reason for this increase is that as the PV is located closer to the EOF, its output current passes through a larger portion of the feeder and a greater voltage appears for every node between the fault and the PV location. Also, it can be seen from Figure 3.5 that VD increases from feeder beginning towards PV location. However, it is not affected for the nodes at the downstream of PV. In addition, greatest VD is observed when the PV is located at feeder far end nodes.

Now, let us assume the fault is at the EOF, i.e. node 10. In this case, VD is much smaller compared to the case in which the fault is at node 1 (Figure 3.6). VD increases from the feeder beginning towards the PV location and then decreases towards the fault location. This is due to the fact that only the current supplied from the distribution transformer flows between the distribution transformer and the PV location while both of the output current of PV and the current supplied from the distribution transformer flow between the PV and fault locations. Thus, a larger voltage appears on the downstream nodes of PV location. The greatest VD is observed when the PV is at the middle of feeder (MOF).
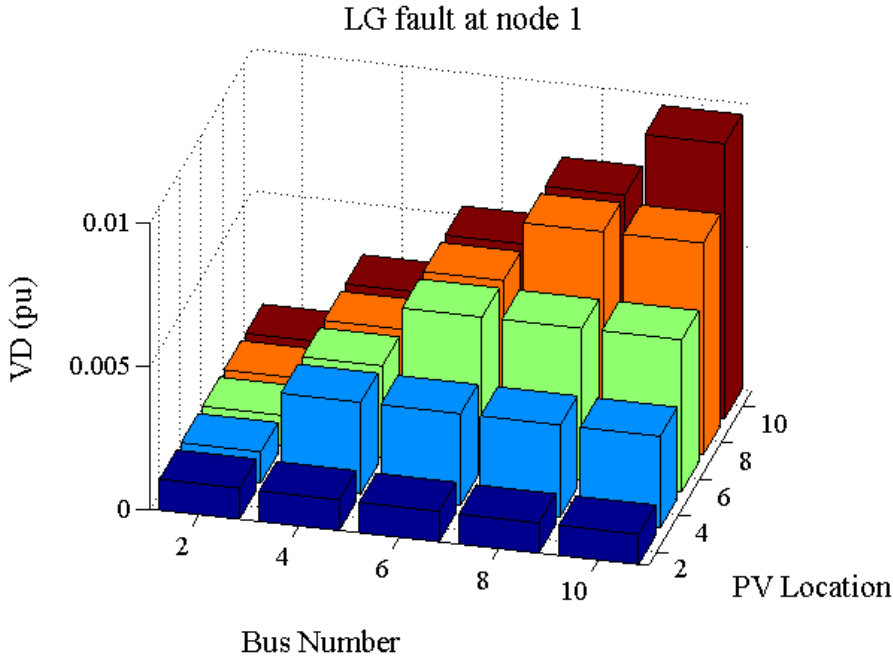
Figure 3.5. Sensitivity analysis results for voltage profile along the feeder during an LG fault at the beginning of feeder (node 1).
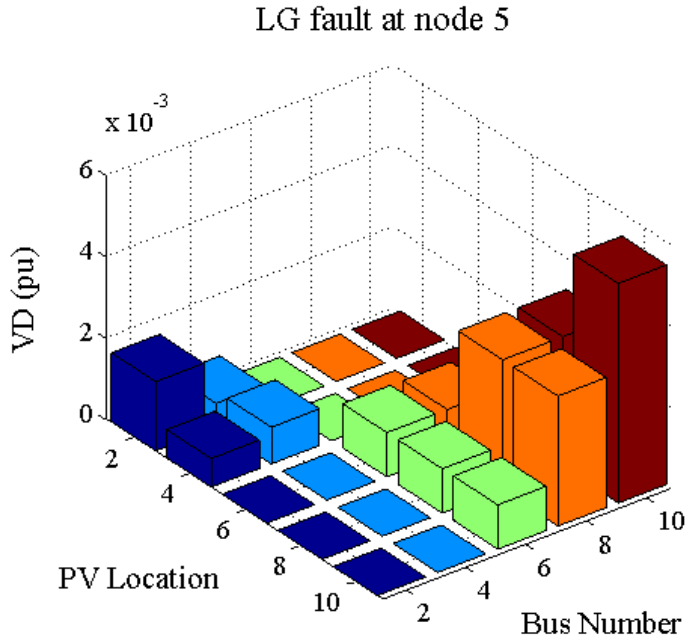
Figure 3.6. Sensitivity analysis results for voltage profile along the feeder during an LG fault at middle of feeder (node 5).

42
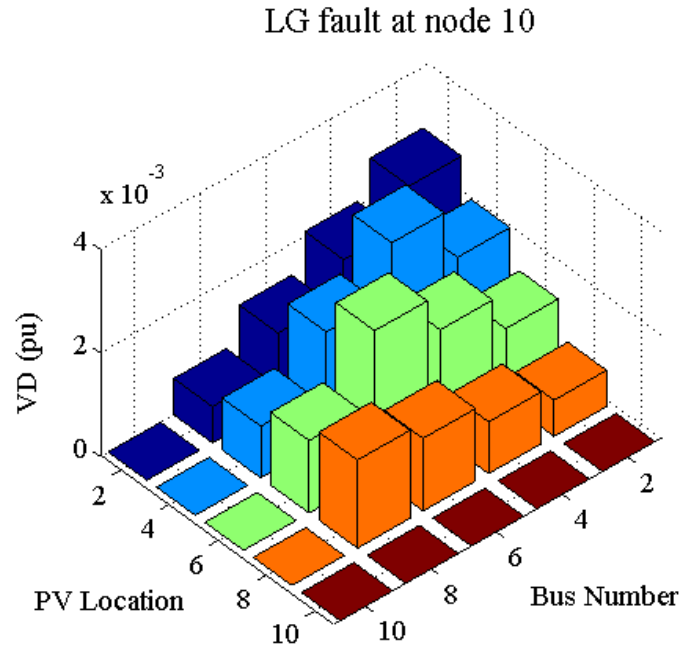
Figure 3.7. Sensitivity analysis results for voltage profile along the feeder during an LG fault at the end of feeder (node 10).
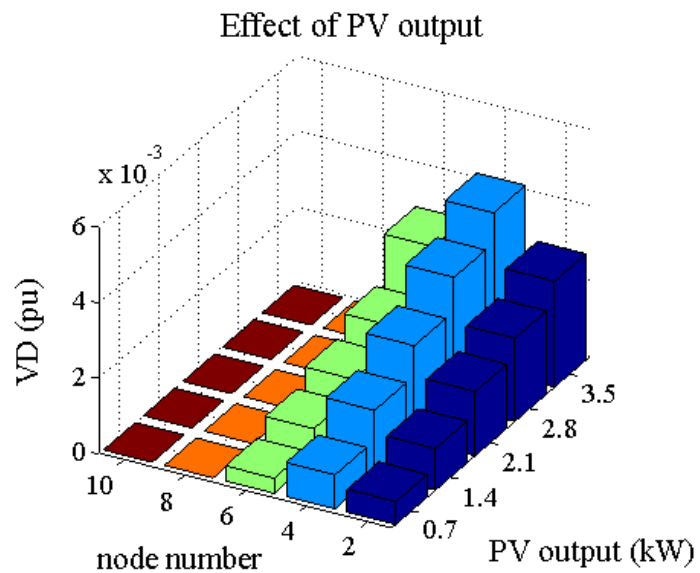
Figure 3.8. Sensitivity analysis results for voltage profile along the feeder during an LG fault.

43

Let us now assume the fault is at the MOF, i.e. node 5. When the PV is at the upstream of fault, VD has a similar trend to the one shown in Figure 3.7 while a similar trend to the one shown in Figure 3.5 is observed, when the PV is at the downstream of fault (Figure 3.7). This observation can be justified based on the above-mentioned facts. To investigate the effect of PV rating, let us assume an LG fault at node 8 where a PV, located at node 4, is assumed to have a rating of 0.7 to 3.5 kW. In this case, as the PV output power is increased, a greater VD is observed (Figure 3.8). This is because for a PV with a higher rating, the output current will be higher and consequently a larger voltage appears.

3.4.1.2 LL faults

Another analysis is carried out for LL faults. Let us consider a fault at the BOF. In this case, VD trend is similar to the LG fault results but almost half of that (Figure 3.9). Assuming the fault location at the EOF, VD variation is greater at PV upstream side and lower at PV downstream side (Figure 3.10). Also VD is greater as the PV is closer to the EOF.

Now let us assume an LL fault at the MOF. In this case, two trends are observed for VD. In the cases that the PV is at the downstream of fault, VD increases towards the EOF. For the cases in which the PV is at the upstream of fault, VD is high for the nodes at the upstream of PV and low for the nodes at the downstream of PV (Figure 3.11).

Let us now assume a PV with a rating of 0.7-3.5 kW. The PV is installed at node 4 and the fault occurs at node 8. In this case, VD on the nodes at fault downstream is not affected by the PV rating. However, it is increased on the nodes at fault upstream for higher PV ratings (Figure 3.12).
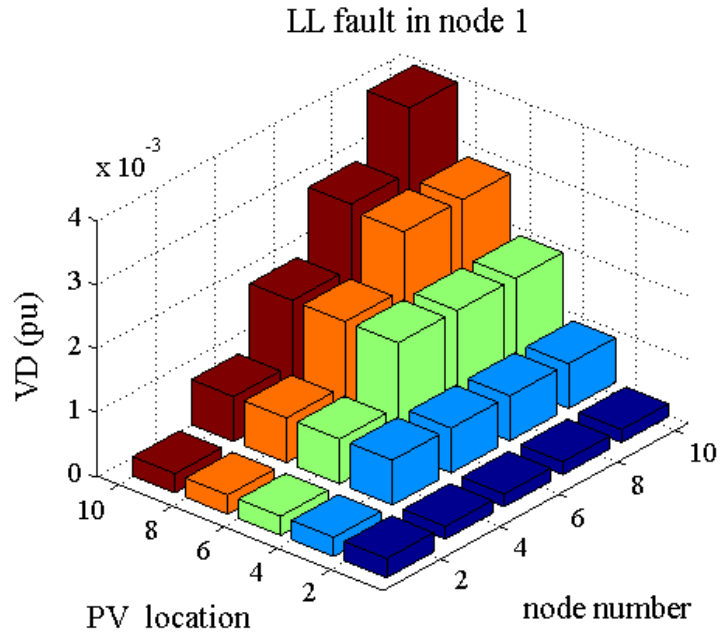
Figure 3.9. Sensitivity analysis results for voltage profile along the feeder during an LL fault at the beginning of feeder (node 1).
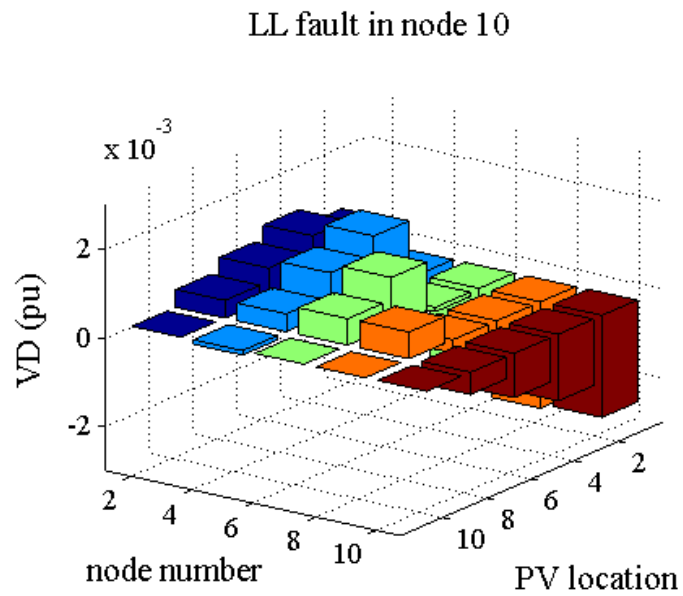
Figure 3.10. Sensitivity analysis results for voltage profile along the feeder during an LL fault at the end of feeder (node 10).
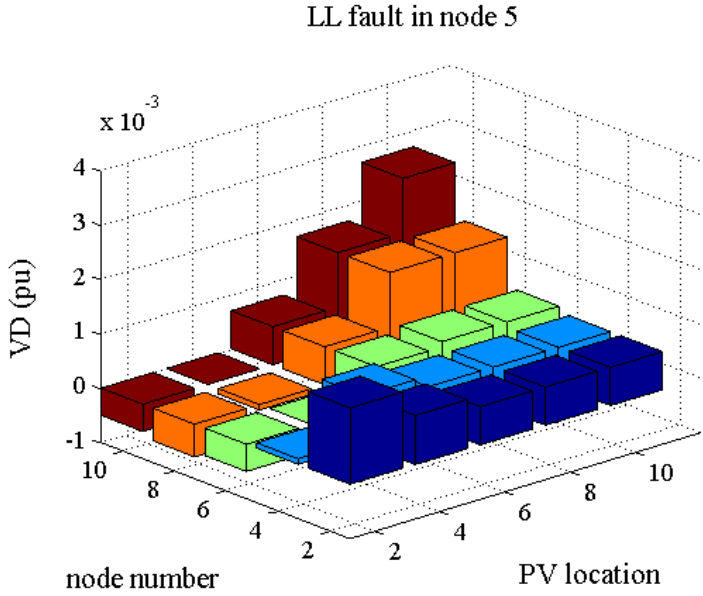
Figure 3.11. Sensitivity analysis results for voltage profile along the feeder
during an LL fault at the middle of the feeder (node 5).
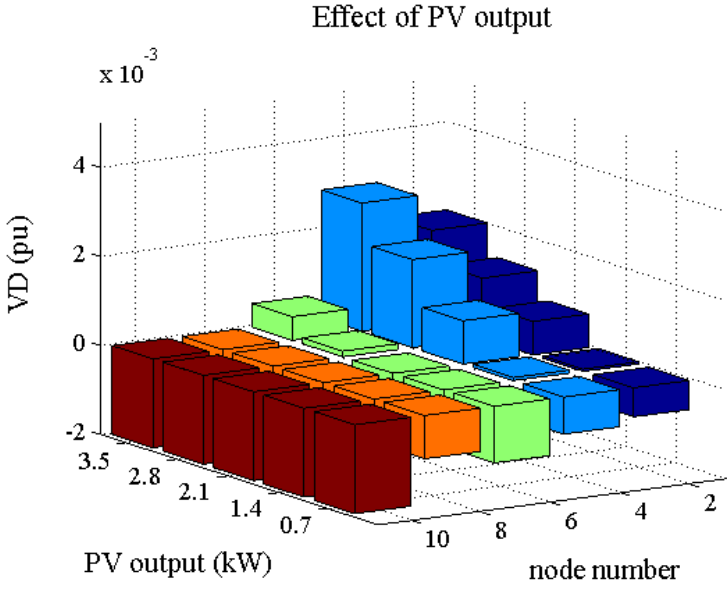
Figure 3.12. Sensitivity analysis results for the impact of PV rating on voltage
profile along the feeder during an LL fault.
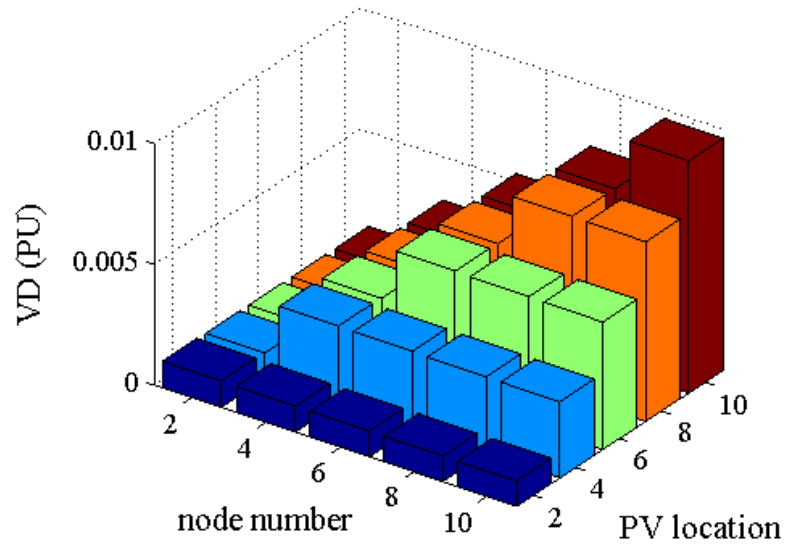
Figure 3.13. Sensitivity analysis results for voltage profile along the feeder during an LLG fault at the beginning of feeder (node 1).
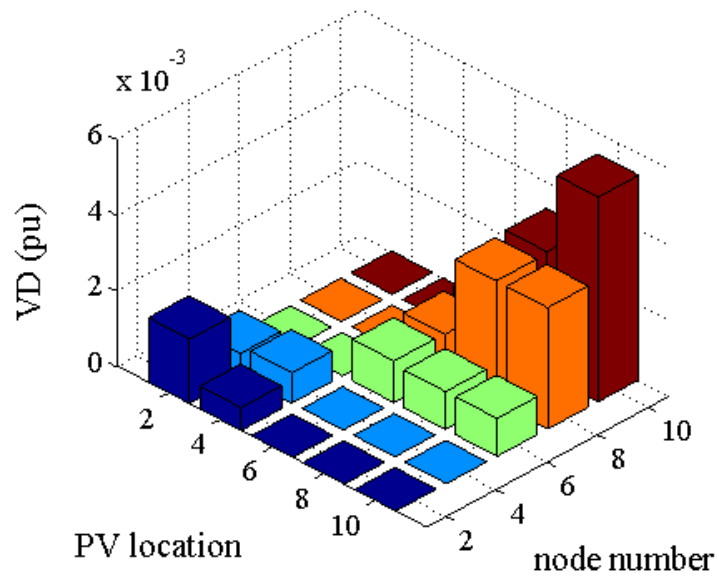
Figure 3.14. Sensitivity analysis results for voltage profile along the feeder during an LLG fault at the middle of the feeder (node 5).
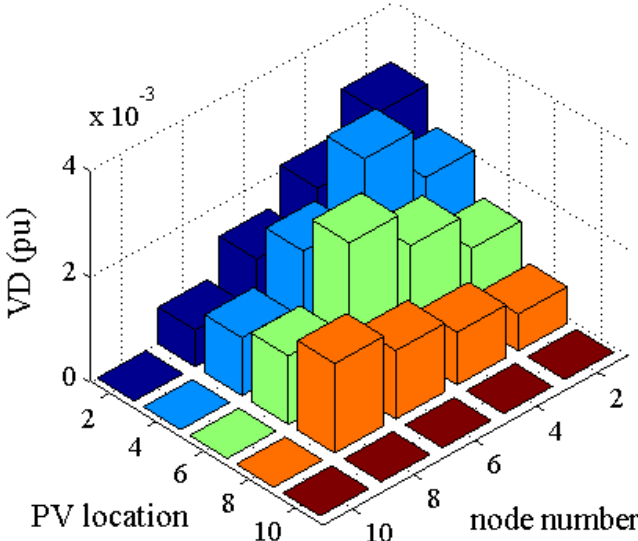
Figure 3.15. Sensitivity analysis results for voltage profile along the feeder during an LLG fault at the end of the feeder (node 10).
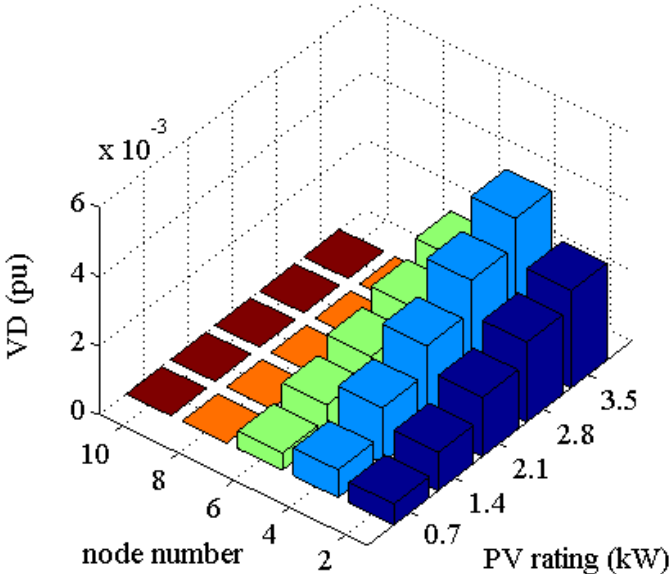
Figure 3.16. Sensitivity analysis results for the impact of PV rating on voltage profile along the feeder during an LLG fault.

48

3.4.1.3 LLG fault

Sensitivity analysis results show that VD trend for an LLG fault on the network is similar to LG faults. However, there is a small difference between the effects of PV rating in these two cases. It seems that for voltage profile along the feeder the impact of one single PV is similar to both types of faults (Figure 3.13, Figure 3.14, and Figure 3.15) but PV rating shows the same trend of impact on voltage profile on nodes but the magnitude of the effect is different for LG and LLG faults. Comparing Figure 3.8 and Figure 3.16 shows that the effect of PV rating on nodes voltage in LLG fault is less intense than LG fault. However, this difference is not considerable.

3.4.2 Fault current

Current flowing from transformer secondary side is another key factor in short circuit faults protection in distribution networks. Fuse will feel this current. Any variation in the magnitude of the current which passes from transformer secondary side will lead to deviation of tripping time of fuse. This deviation is investigated in this section in the presence of a PV in the system.

3.4.2.1 LG faults

Let us again consider a 2 kW PV with 150% current limiting during the fault. The fault and PV location vary from node 1 to 10. Let us define the fault current difference (FCD) as the fault current in PV-available case minus the fault current at No-PV case. Similarly, let us define the transformer current difference (TCD) as the current sensed at the transformer secondary in PV-available case minus the No-PV case during the short-circuit fault.

For the faults at the downstream of the PV, as the fault moves towards the EOF, the FCD decreases (Figure 3.17). This decrase can be explained by the variation of the voltages of the nodes as a result of fault location which consequently affected the current that is supplied by the distribution transformer. For the faults at the upstream of PV, as the fault moves from BOF towards the PV location, the FCD increases (Figure 3.17). The highest FCD is observed when the fault occurs at the same node that the PV is connected to.
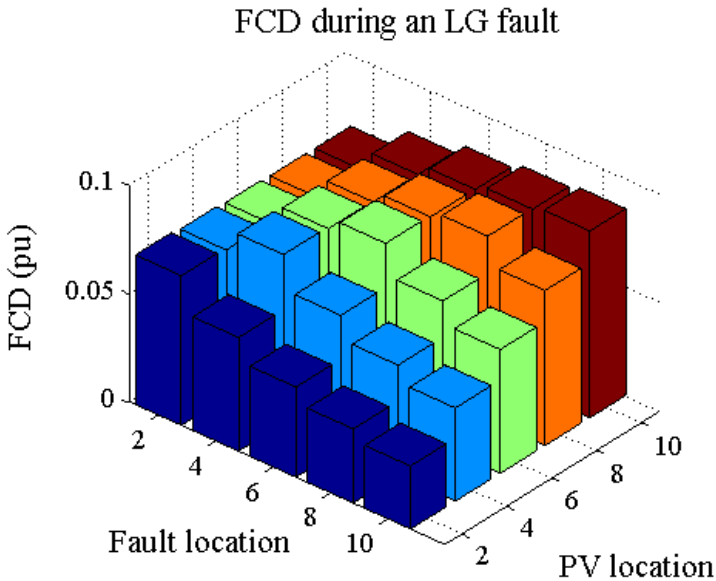
Figure 3.17. Sensitivity analysis results for fault current during an LG fault.
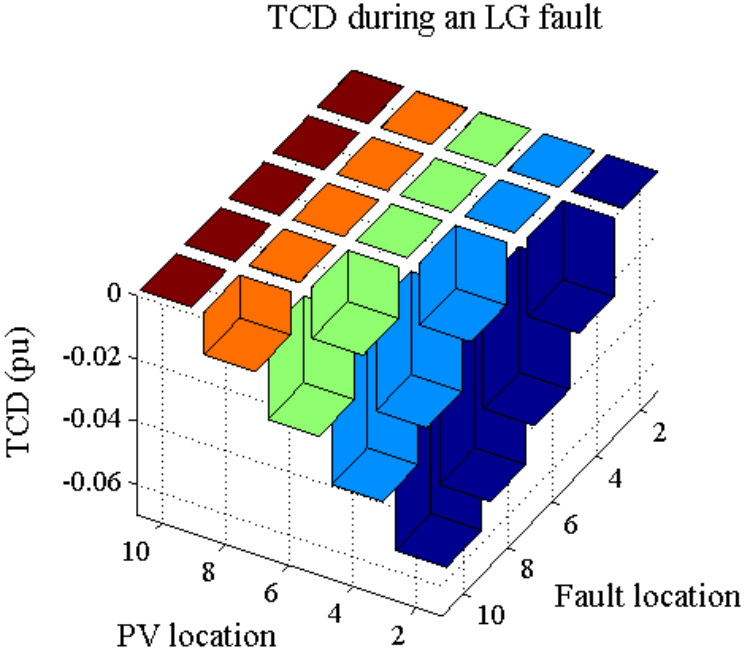
Figure 3.18. Sensitivity analysis results for transformer current during an LG fault.

Figure 3.19. Sensitivity analysis results for effect of PV rating on fault current during an LG fault.
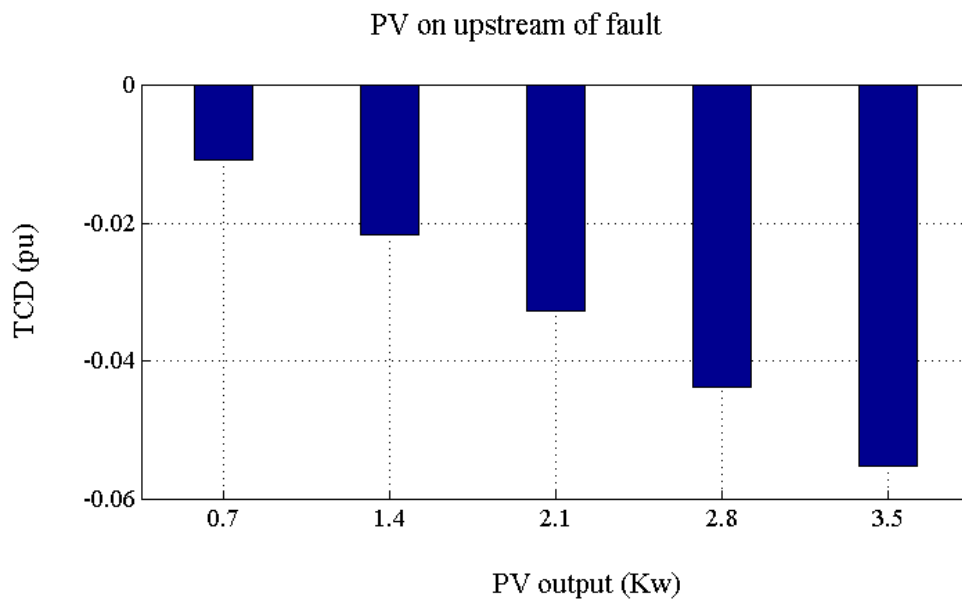
Figure 3.20. Sensitivity analysis results for effect of PV rating on transformer current during an LG fault.

When the PV is in the upstream of fault, current sensed at the transformer secondary in the PV-available case is lower than the No-PV case (Figure 3.18).

51

Hence the TCD is negative. This is due to the fact that the voltage at PV connection point is greater compared to NO-PV case, which leads derive less current from source. When the PV is at the downstream of fault, there is no difference between transformer secondary current in No-PV and PV-available cases; hence, the TCD is zero (Figure 3.18), because the PV does not affect the voltage at the upstream side of the fault. As the PV is closer to feeder beginning nodes, the transformer secondary current is much less than that of the No-PV case.

Now, let us assume an LG fault at node 8 where a PV, located at node 4, has a rating of 0.7 to 3.5 kW. As the PV rating increases, the FCD becomes greater (Figure 3.19) while the higher reduction in the TCD is observed (Figure 3.20).

3.4.2.2 LL fault

For an LL fault at the beginning nodes of feeder regardless of the PV location, the fault current in the PV-available case is higher than the No-PV case; hence, FCD is positive. FCD is negative when the fault is at the end nodes of the feeder (Figure 3.21).

For the cases in which the fault is at the end nodes of the feeder, as the PV is relocated from the BOF towards the fault location, FCD increases. However, FCD is constant if the PV is at the downstream of fault.

For the cases in which the fault is at the beginning nodes of the feeder, as the PV is relocated from the BOF towards the fault location, FCD decreases. However, FCD is zero if the PV is at the downstream of fault.

For an LL fault, the transformer secondary current in the PV-available case is less than the No-PV case; thus, TCD is negative (Figure 3.22). This is due to the fact that the voltage at the node in which the PV is located increases because of the PV; thus, the current supplied by the distribution transformer reduces. For the LL faults, as the PV is relocated from the BOF towards the fault location, TCD decreases. However, it is constant if the PV is at the downstream of fault (Figure 3.22).

Now, let us assume an LL fault at node 8 where a PV, located at node 4, has a rating of 0.7 to 3.5 kW. In such a case, for lower PV ratings (e.g. lower than 2.8 kW), FCD is negative while it is positive for higher PV ratings (e.g. 3.5 kW). As the PV rating increases, FCD decreases (Figure 3.23). For lower PV ratings (e.g. lower than

1.4 kW), TCD is positive while it is negative for higher PV ratings (e.g. higher than
2.1 kW). As the PV rating goes high, TCD increases for higher PV ratings but
decreases for lower PV ratings. (Figure 3.24)
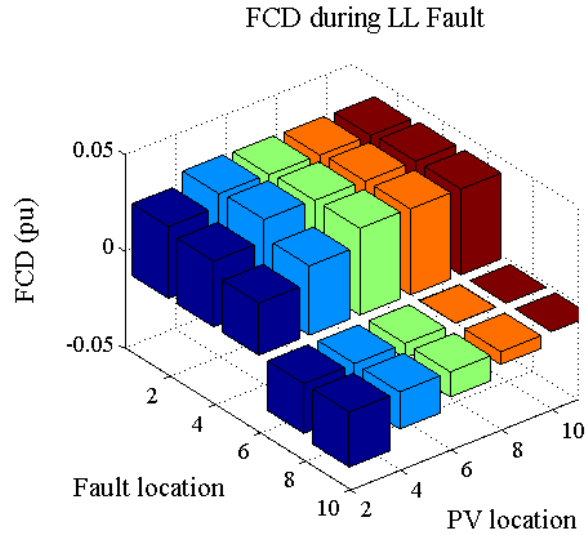
Figure 3.21. Sensitivity analysis results for fault current during an LL fault.
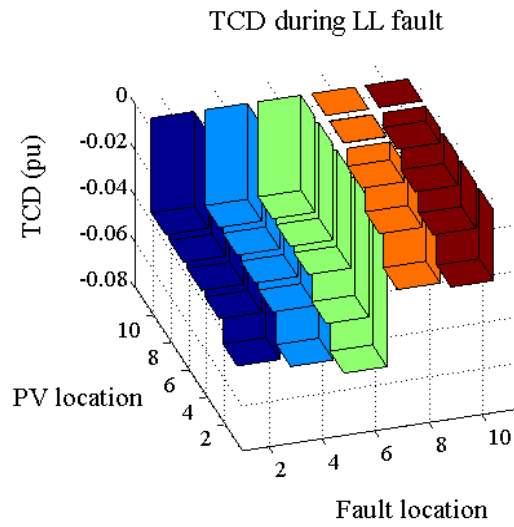
Figure 3.22. Sensitivity analysis results for transformer secondary current during an
LL fault.

53
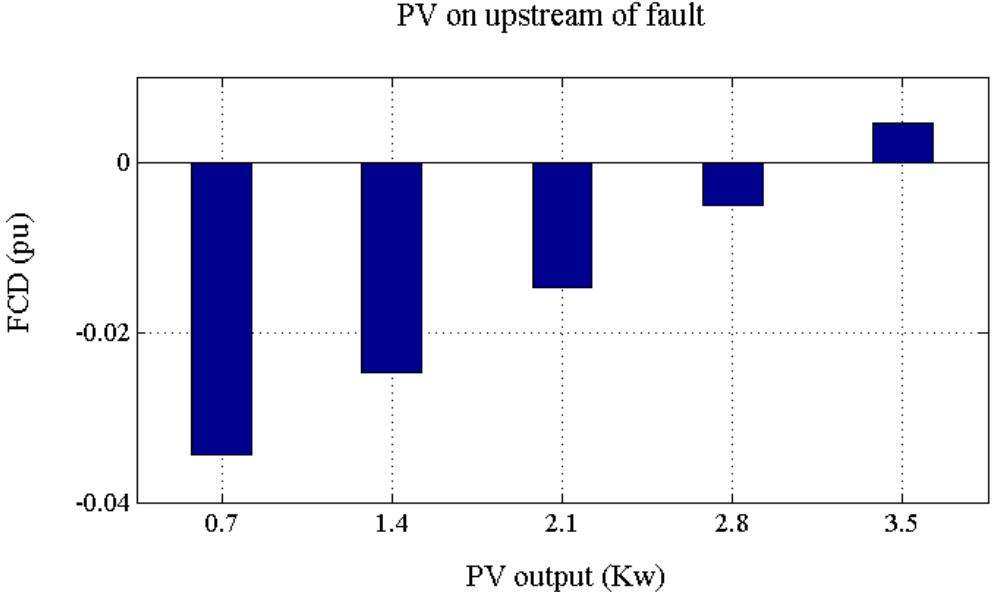
Figure 3.23. Sensitivity analysis results for PV rating effect on fault current during an LL fault when PV is located on upstream of fault.
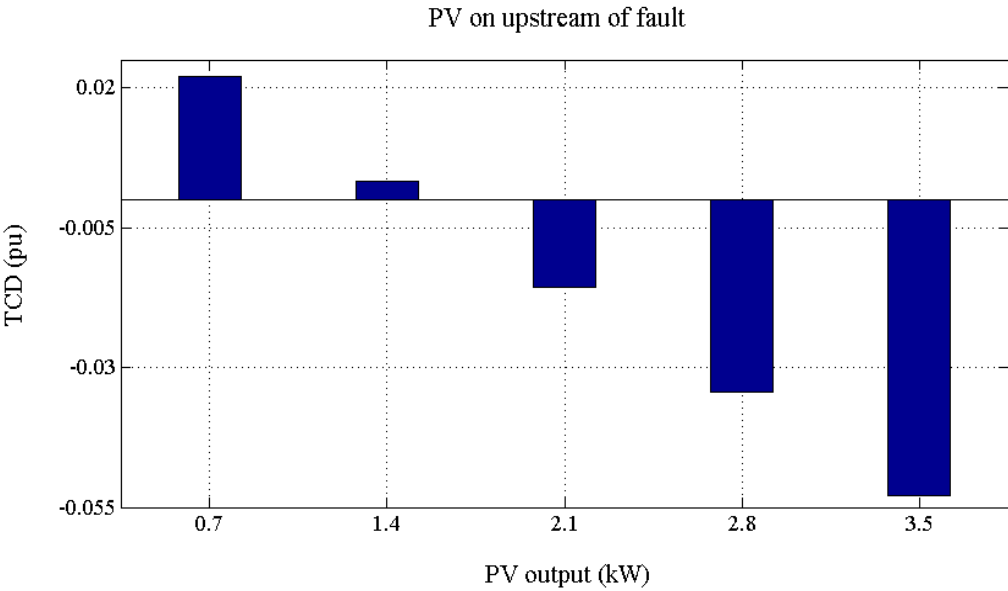
Figure 3.24. Sensitivity analysis results for PV rating effect on transformer current during an LL fault when PV is located on upstream of fault.
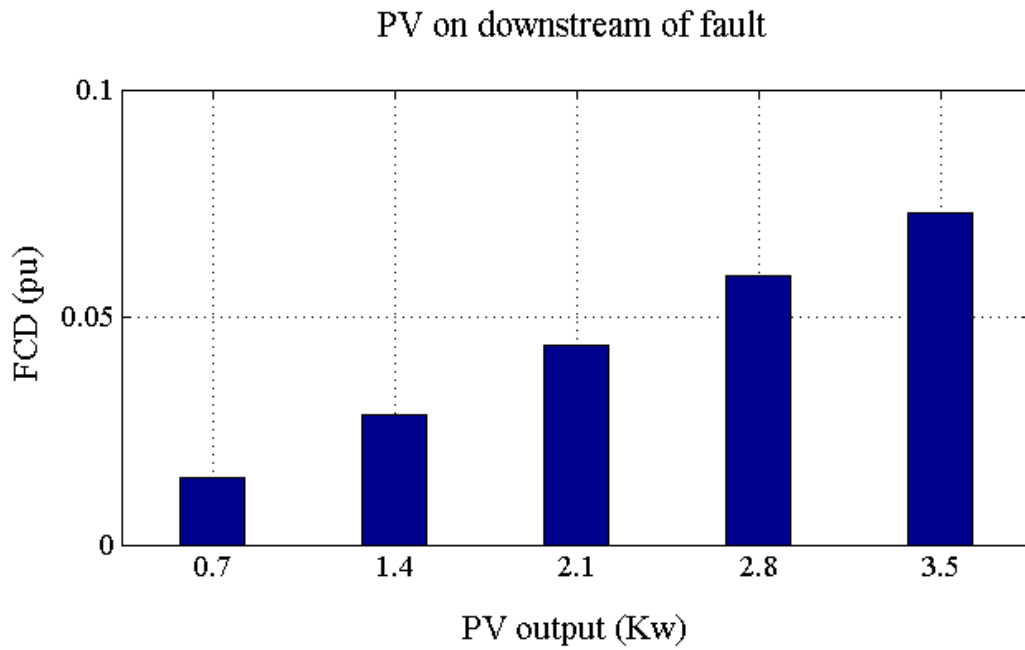
Figure 3.25. Sensitivity analysis results for PV rating effect on fault current during
an LL fault when PV is located on downstream of fault.
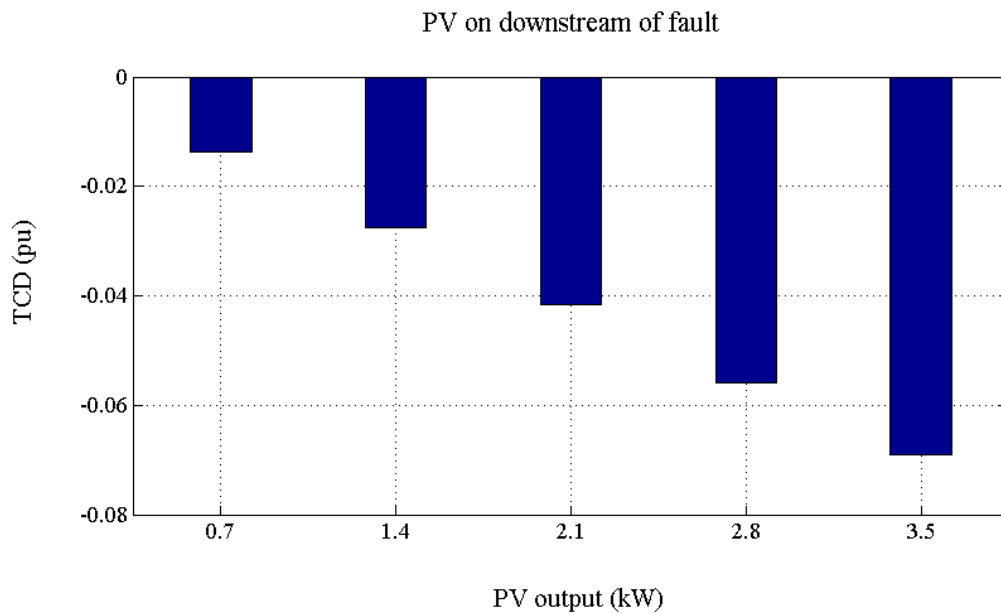
Figure 3.26. Sensitivity analysis results for PV rating effect on transformer current
during an LL fault when PV is located on downstream of fault.

Now, let us assume an LL fault at node four while the PV is at node 8. In such a case, FCD is always positive and increases as the PV output power goes high (Figure 3.25). However, as the PV rating increases, TCD increases, and it is negative for all PV outputs (Figure 3.26). This can be explained by this fact that when the PV is located at the downstream of fault location, the voltage of the node in which the fault is applied is higher than the No-PV case. This difference becomes larger as the PV rating is higher and consequently, the current supplied by the distribution transformer reduces. Also, the voltage of PV connected point increases and the current supplied by the transformer reduces.

3.4.2.3 LLG fault

For an LLG fault, FCD increases as the PV is closer to the fault location; however, it is almost constant if the PV is at the downstream of fault (Figure 3.27). During an LLG fault, if the PV is at the downstream of fault, TCD is zero. However, if the PV is at the upstream of fault, TCD reduces as the PV is relocated from the BOF towards the fault location. Assuming the PV is located at one node, TCD increases as the fault location varies from the PV towards the EOF (Figure 3.28).

Now, let us assume an LLG fault at node 8 where a PV, located at node 4, has a rating of 0.7 to 3.5 kW. In such a case, FCD is negative and increases as the PV rating goes high (Figure 3.29). However, it is almost constant for PV ratings of higher than 2.1 kW. TCD is also negative and increases as the PV rating goes high (Figure 3.30)
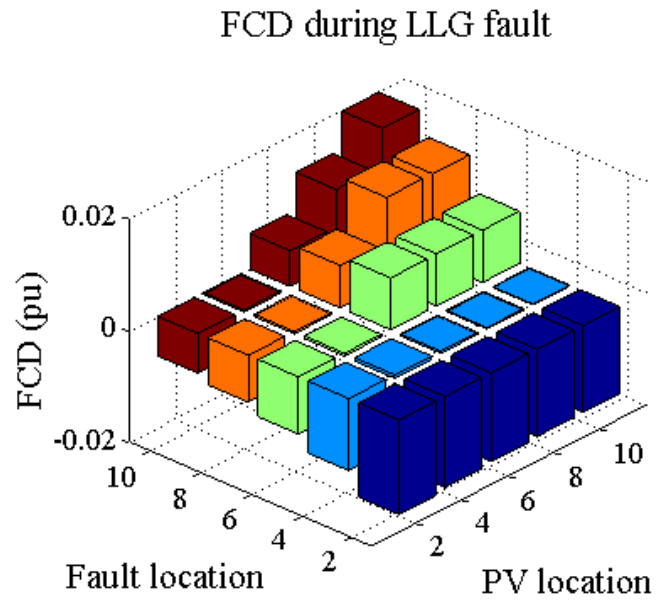
Figure 3.27. Sensitivity analysis results for fault current during an LLG fault.
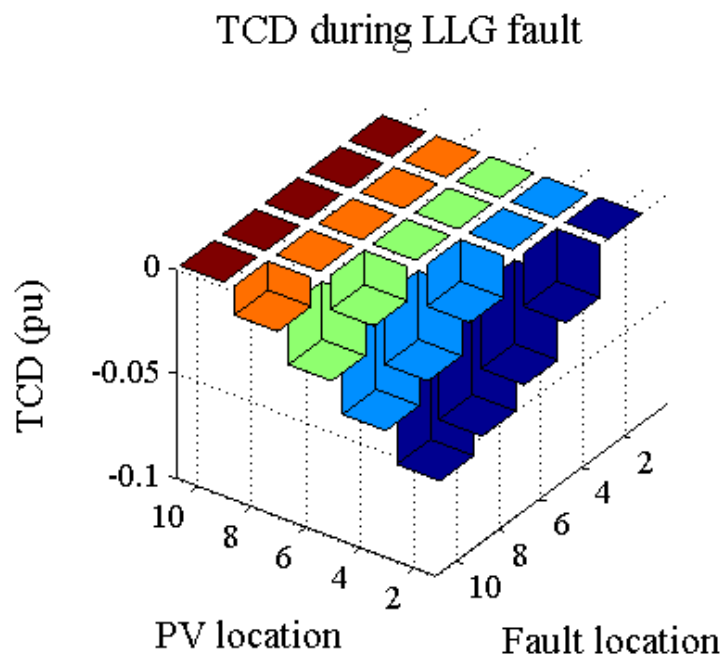
Figure 3.28. Sensitivity analysis results for transformer current during an LLG
fault.

57
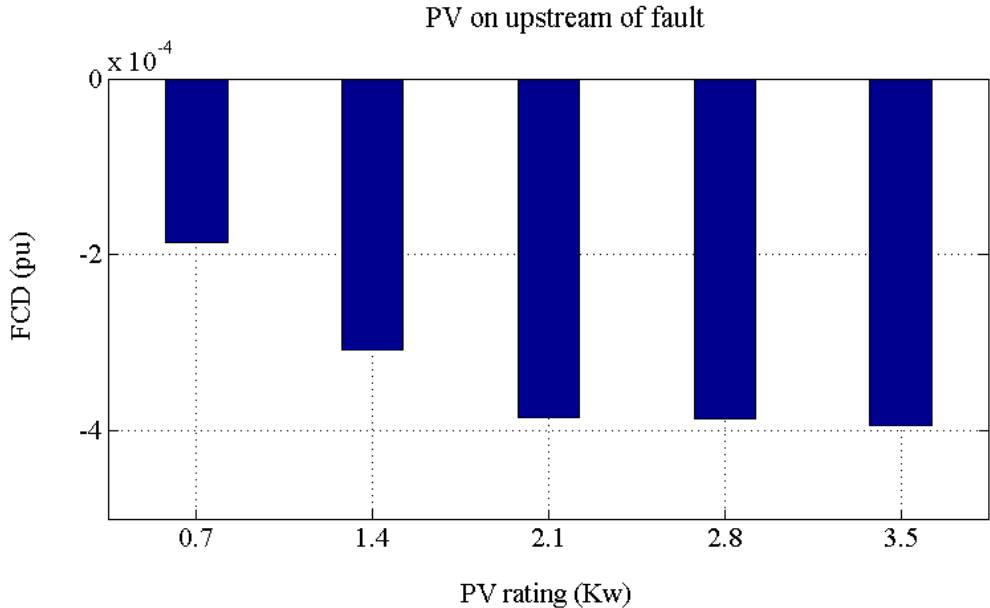
Figure 3.29. Sensitivity analysis results for effect of PV rating on fault current during an LLG fault.
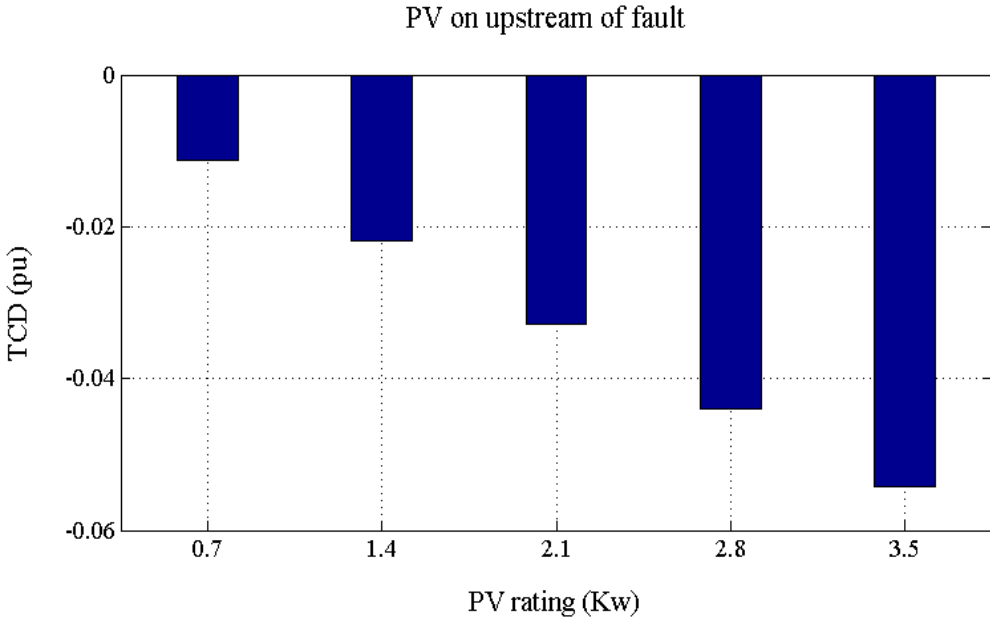
Figure 3.30. Sensitivity analysis results for effect of PV rating on transformer current during an LLG fault.
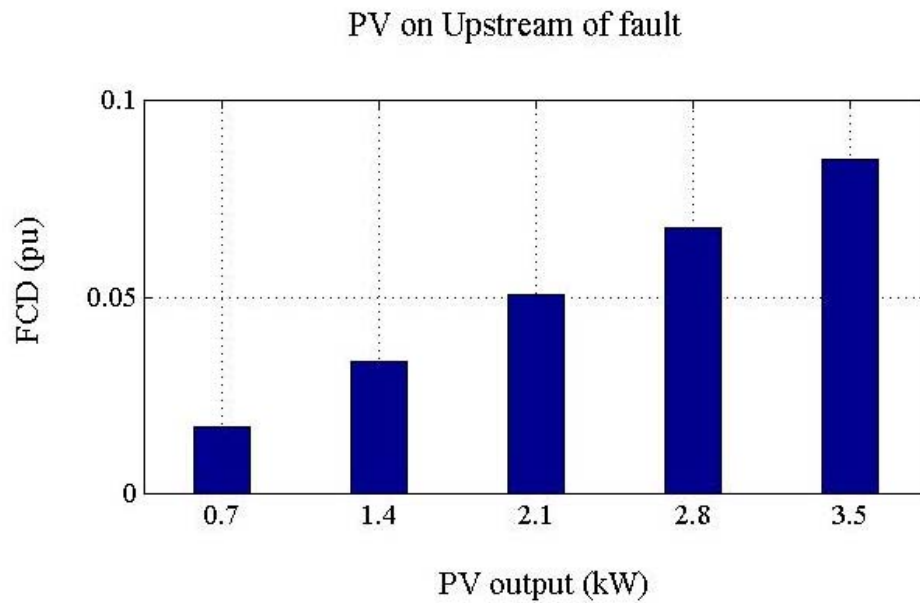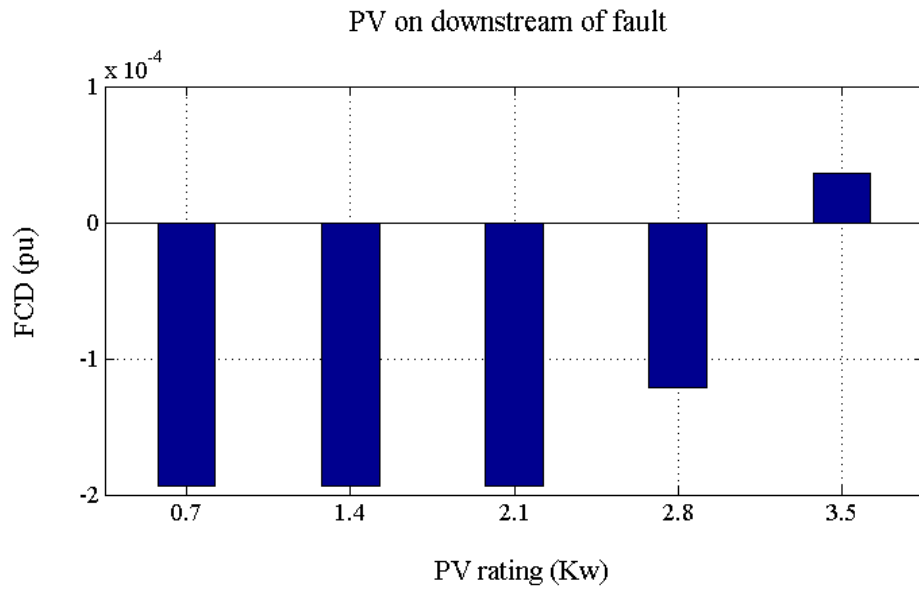
Figure 3.31. Sensitivity analysis results for effect of PV rating on fault current
during an LLG fault.
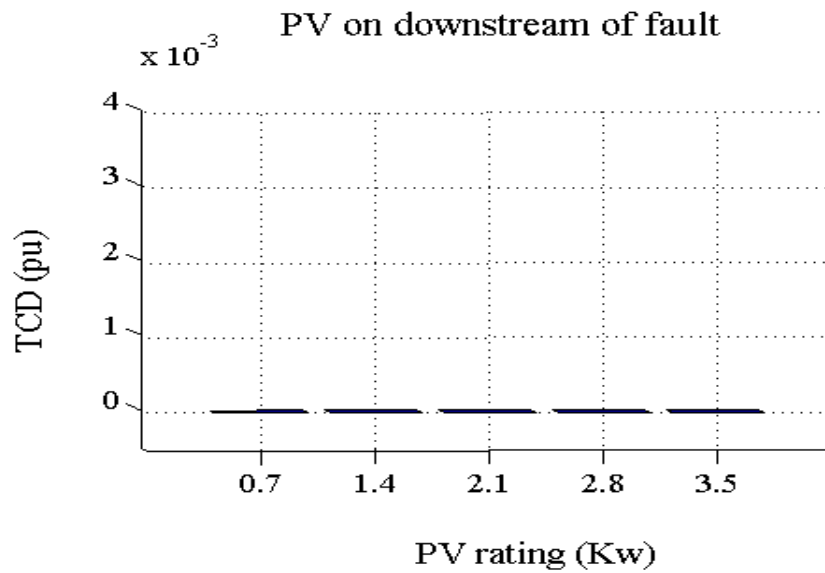
Figure 3.32. Sensitivity analysis results for effect of PV rating on transformer
current during an LLG fault.

59

Let us now assume an LLG fault at node 4 when the PV is at node 8. In such a case, FCD is negative and almost same if the PV rating is lower than 2.8 kW while it is positive for PV ratings of higher than 3.5 kW (Figure 3.31). The reason for this fact can be explained trough analysis of PV rating impact on voltage of connected node and its relationship with other nodes voltage via kirchhoffs voltage rule (KVL) and kirchhoffs current rules (KCL). So it means that until the PV rating has not exceeds an specific value, the equations and relationships between different parameters of load flow affecting variables changes such a way that they leads in reduction of fault current. However, beyond a specific value of PV rating (here 2.8 kW) the equations and balance of parameters in load flow varies such that it leads in increase of fault current and accordingly higher FCD. TCD in this condition is zero for all PV ratings (Figure 3.32).

3.5 Discussion on results

The sensitivity analysis shows that the voltages of nodes, the transformer secondary current, and the level of short circuit fault (SCF) depend on the SCF and PV location along the LVF. It is seen that the presence of a PV at SCF upstream has different impacts on these three parameters, compared to the case in which the PV is at SCF downstream. It is also observed that these effects are not similar for LG faults, LL fault, and LLG faults.

The results of the sensitivity analysis demonstrate that the SCF level is always higher when a PV is present in the LVF for an LG fault but it may be lower or greater in LL fault and LLG fault, depending on the SCF and PV location. Interestingly, it can be understood that the PV rating has entirely different impact on the transformer secondary current and SCF level even in the same fault type and location as well as the same PV location.

During LG faults and LLG faults, the current observed at the secondary of the distribution transformer is reduced when a PV is present in the network, and a larger difference is seen when the short circuit fault is closer to the EOF. However, for LL faults, a greater change is seen when the SCF is at the MOF. As the current sensed at

60

the transformer secondary is reduced, the operation time of the switch-fuse is expected to be delayed slightly.

The next chapter will focus on the analysis of distribution systems protection in the presence of mass amount of PVs and in different penetration level of PVs. In fact chapter four will reveal that what the effect of high numbers of PVs and their rating is on the main parameters of protective system in distribution network. This study will be carried out thorough statistical analysis. All possible scenarios will be covered in this study for different type of fault.

3.6 Summary

The sensitivity analysis is carried out in this chapter and impact of one single PV in different rating on voltages of nodes, and current of transformer and fault current is observed. The analysis is carried out for various fault locations (downstream and upstream of PV connection point). The FCD, TCD, and VD variables respectively show the dissimilarity between these three parameters in the network with and without a PV. However, the detail of variations of these parameters regarding PV rating and fault and PV location was addressed in this chapter. Through the sensitivity analyses, it is concluded that the SCF level can increases by 10% when a PV is present in the LVF while the transformer secondary current may decrease by 7%.

Chapter 4. Stochastic Analysis of PV Penetration Impact on Protective Devices of LV Distribution Network

4.1 Introduction

In the previous chapter, the research presented a sensitivity analysis to evaluate the contribution of PVs on the short-circuit fault current, current sensed at the secondary of the distribution transformer as well as the voltage profile along the feeder during short-circuit faults.

The rating and location of the PVs in addition to the fault location and type are considered as the variables of this analysis. The research in this chapter is expanded to consider the impact of multiple PVs with different ratings, penetration levels and random (unequal) distribution among the three phases of the network. This is carried out with the help of a Monte Carlo-based stochastic analysis. The stochastic analyses are carried out in MATLAB. The outcomes of this analysis are summarized to provide a better understanding of the impact of single-phase rooftop PVs on residential feeders during short-circuit faults. In summary, this chapter aims to answer the following questions:

- How strong is the impact of a rooftop PV on the current that is observed at the secondary side of the distribution transformers during short-circuit faults in the LV feeder?
- How strong is the impact of a rooftop PV on the voltages of the nodes along the LV feeder, during short-circuit faults?

- What are the impact of different penetration levels and ratings of rooftop PVs on
  the two above parameters?

The Monte Carlo-based stochastic analysis of the system in the presence of
multiple PVs, with different ratings, installation points along the LV feeder,
penetration level and numbers of the PVs in each phase of the system are provided in
Section 4.3. Maximum allowed penetration level based on new criterion is presented
in Section 4.4. The results of the analyses are discussed in Section 4.5 while
Section 4.6 summarizes and highlights the general conclusions and findings of the
study.

4.2 Case study network

The studied network in this section is same as the network that we considered in
the previous chapter. So let us again give a brief about the structure and specification
of this network to remind its detail which represents a typical Australian urban
residential network as shown in Figure 3.1. As it mentioned before, in Australia,
residential LV feeders are mostly three-phase 4-wire MEN systems and are supplied
by three-phase Dyn distribution transformers. The distribution transformer is
supplied by a three-phase MV feeder. All houses are assumed to be single-phase
loads. The LV feeders are protected by LV switch-fuses at the secondary side of the
distribution transformer to protect the system in case of short-circuit faults in the LV
feeder. In Australia, the distribution transformers are usually in the range of 25 to
630 Kva and the LV feeders are usually 400 meters long.

4.3 Stochastic analysis

A deterministic analysis is not comprehensive due to the randomness in PV rating
and installation point as well as the fault location and impedance [50]. For example,
considering the condition of fault just for one specific case will not reflect the true
and reliable results for that parameter. It means without applying the stochastic
analysis methods it is not possible to judge fairly about the impact of one particular
parameter on output. Therefore, a Monte Carlo analysis (MCA)-based stochastic
analysis is carried out in this thesis to investigate and predict the short-circuit current

of the feeder and the voltage profile along the feeder [51]. The uncertainties considered in the MCA research are:

- the penetration level of PVs in the network and per phase,

- the installation point (node) of PVs in each phase,

- the ratings of PVs,

- the fault location, and

- the fault impedance.

while the outputs of the MCA analysis are

- the fault current, and

- the voltage at each node along the feeder.
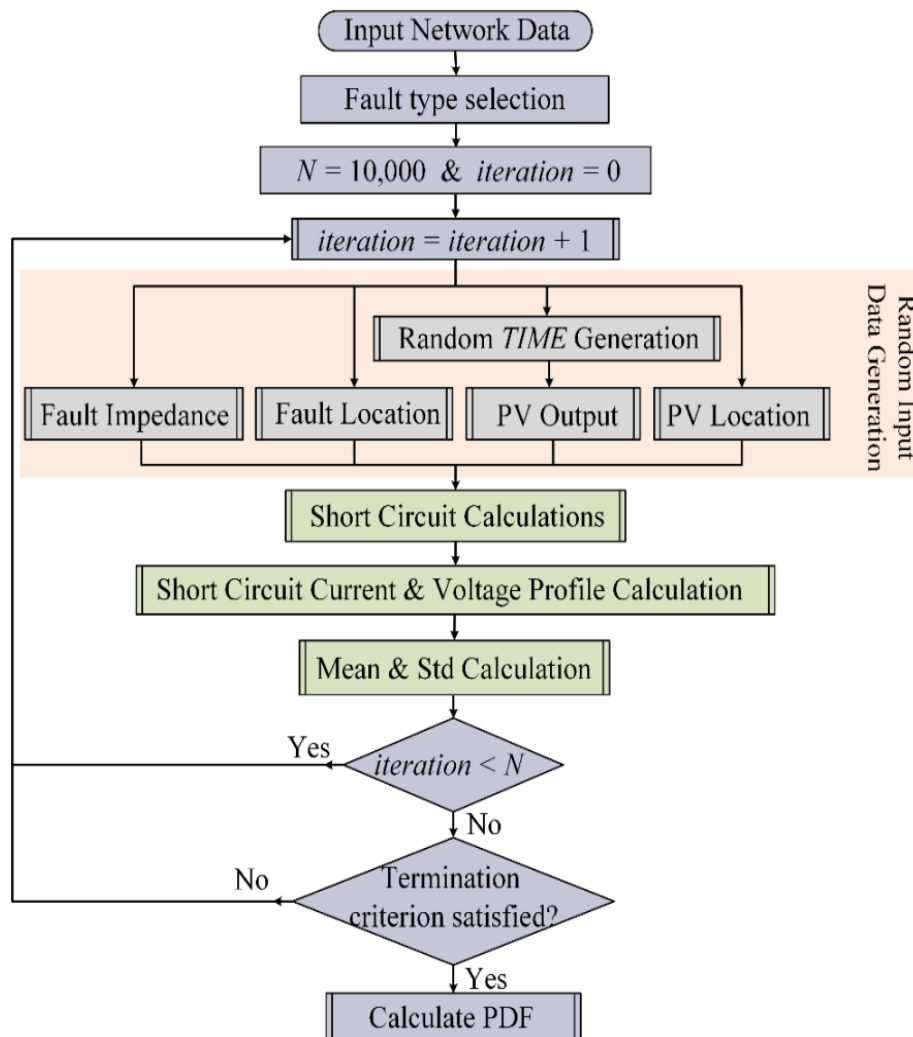
Figure 4.1. Flowchart of the developed Monte Carlo analysis.

This study will determine that how strong is the effect of each above-mentioned
parameters on short circuit fault current and voltage profile of feeder in LV
distribution network. The results will be presented in the form of table, and standard
deviation and average of outputs will be discussed. So this study will show that what
should be our expectation to the variation of amplitude of short circuit fault current
and voltage of different points of distribution feeder due to variation in each of input
parameters.
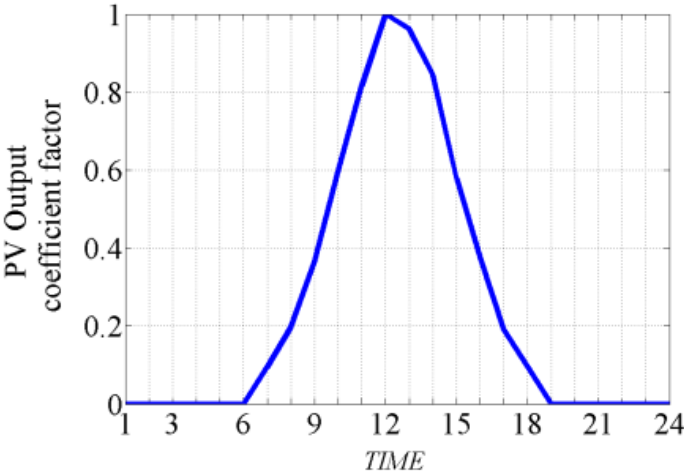
Figure 4.2. Normalized available power from the PVs during the day.
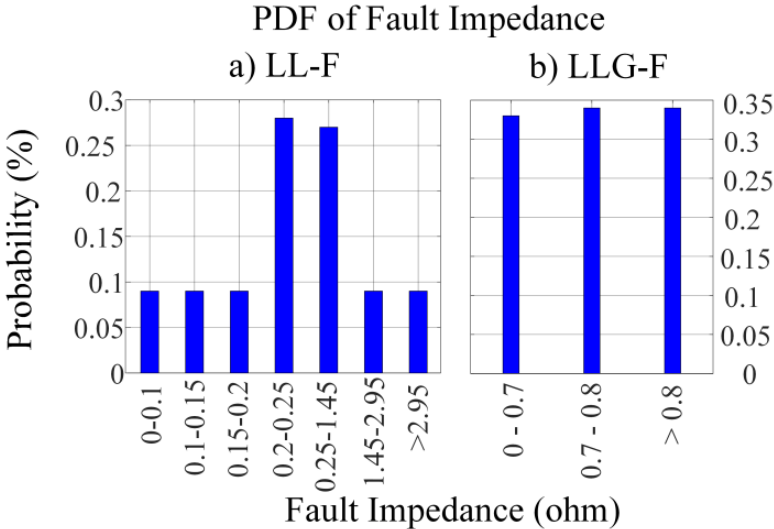
Figure 4.3. Considered fault impedance PDF for   a) LL   and   b) LLG faults.

For instance, it will be clarified that if the penetration level of rooftop PVs
increases from 20% to 80%, what will be the consequences of this variation in terms

of voltage of nodes in the distribution network. Similarly, the effects of other parameters such as PV rating, fault impedance, and fault location will be illustrated. However, the achieved results are statistical results and are more reliable than results of one specific case study.

The more variation in average results of the output parameter, the stronger the impact of input. Also, the higher the standard deviation of output, the more diverse the output result and it means that variation of that particular parameter as a contribution may lead to very diverse and different output (short circuit current or voltage profile of feeder). Figure 4.1 illustrates the flowchart of the developed stochastic analysis.

The *Time* parameter is considered to reduce and eliminate the non-desired combinations of the inputs for the stochastic analysis, which represents the time of the analysis over the 24-hr period and is normalized in [0-1] range, as shown in Figure 4.2. In this study, the sunlight availability is assumed between 6 am and 19 pm while the PVs generate their maximum output at 12 pm with the coefficient factor of 1, considering the solar radiation in Perth, Australia [52]. *Time* is utilized to select correlated random values for the instantaneous output current available from PVs while the other inputs of the MCA are considered independent from *Time*. Alternatively, the method proposed in [53-54] can be utilized to determine the PV output power based on solar irradiance.

Only PV installation point and PV rating are assumed to have discrete values while the other inputs are considered continuous. The output power of the PVs is assumed to have a normal distribution with an average of 2.5 kW and a variance of 0.8 kW, based on the ratings of the PVs installed in Perth, Australia. PV installation point and fault location are assumed to have a uniformly distributed probability over the LV feeder length (i.e. 400 m in this study which is the typical LV feeder length in Perth, Australia).

Uniform distribution over 0-0.3 Ω is considered for the impedance of the LG faults while the impedance of the LL and LLG faults are assumed with the probability density function (PDF) values shown in Figure 4.3a and Figure 4.3b [43].

The algorithm shows that how this method works. In each iteration, input data including fault impedance, fault location, PV rating and PV locations are chosen randomly according to appropriate PDF and calculation is carried out to achieve

short circuit current and feeder voltage in different nodes. Then average and STD of outputs will be calculated. Then, if the algorithm checks the termination criteria and if it meets the termination criteria, the algorithmic computation will stop. If termination criteria are not satisfied, the computation continues and chooses another set of input parameters to perform the next iteration. The termination criteria of the MCA is chosen based on achieving an acceptable convergence for the average and variance of the desired outputs (i.e. short-circuit current at fault location and node voltages along the feeder). For this, the MCA simulation is deemed converged when a confidence degree of 95% is achieved. However, a minimum of N=10,000 trials is utilized to avoid premature convergence. Once the Monte Carlo method is converged, the PDF is defined of all desired outputs.

4.4 Maximum allowed PV penetration level (PPL)

Based on the findings from the stochastic analysis, the study aims to investigate the maximum allowable PPL in a residential LVF from the SCF perspective (note that other considerations such as the maximum voltage rise and maximum harmonic distortion in the LVF should also be considered when selecting a general limit). To this end, different criteria may be defined. This study has determined the maximum allowable PPL considering two criteria, namely switch-fuse operation probability (SOP), and PV disconnection probability (PDP). The SOP illustrates the probability of operation of the switch-fuse (at the secondary of the distribution transformer) in the case of an SCF, while the PDP depicts the probability of disconnection of PVs of the LVF after an SCF because of voltage deviation at the connection point of the PV, according to IEEE Standard 929-2000 [55]. From the MCA-derived PDF for node voltages (considering its EAV and STD), the probability of observing a voltage higher than 1.1 or below 0.88 per-unit (pu), i.e., the thresholds for the disconnection of a PV according to [55], is calculated and referred to as the PDP. Similarly, using the derived PDF for the current sensed at the transformer secondary (considering its EAV and STD), the probability of observing a current higher than 1.25 pu (i.e., the threshold for the operation of the switch-fuse) is calculated, and referred to as the SOP. These two indices are expressed for different PPLs at various SCF types. From the SCF perspective, the maximum allowable PPL is then determined as the

corresponding PPL for the minimum probability of the successful operation of the switch-fuse or the disconnection of PVs, after an SCF in the LVF.

4.5 Stochastic analysis results

The stochastic analysis evaluates the effect of multiple PVs at different locations and phases, different PV penetration levels and instantaneous output power of PVs during all types of faults. After the MCA method is converged, the PDF is defined and the average (referred to as 'mean') and standard deviation (referred to as 'STD) of each output from all iterations are recorded. In this study, transformer secondary current and voltages at each node are the desired outputs, for which their mean and STD values are presented instead of their PDF figures. The results of each study is presented in this Section and discussed further in the following Section.

4.5.1 LG fault

The MCA is carried out for an LG fault assuming 50% penetration level for PVs. Depending on the parameter *Time*, the instantaneous output power of the PVs is different in the Monte Carlo iterations. The results of this analysis are given in Table 4.1.This table only shows the results for the node at BOF (node 1), MOF (node 5) and EOF (node 10). As seen from this table, the expected average voltage at each node increases slightly as the PV rating goes high. This is true for all nodes in this phase. Note that there is no significant variation in STD due to the change in PV ratings. Another MCA is carried out assuming all PVs have an output power of 2 kW with a 150% current limiting while different PV penetration levels are considered.

The results of this analysis are given in Table 4.2. This table shows that the expected average voltage at each node increases as the PV penetration level goes high, but this increase is not considerable. Also, as the PV penetration level goes

Table 4.1 Monte Carlo results for node voltages (pu) at phase A, for various PV
ratings during LG faults assuming a PV penetration level of 50%.

PV [kW]	V_1		V_5		V_{10}	
	mean	STD	mean	STD	mean	STD
0.7	0.748	0.1742	0.557	0.2236	0.486	0.2513
1.4	0.749	0.1739	0.560	0.2239	0.490	0.2525
2.1	0.751	0.1736	0.563	0.2247	0.493	0.2537
2.8	0.754	0.1746	0.567	0.2255	0.496	0.2543
3.5	0.756	0.1751	0.570	0.2247	0.499	0.2539

Table 4.2 Monte Carlo results for phase A node voltages (pu) for different PV
penetration levels during LG faults.

Penetration [%]	V_1		V_5		V_{10}	
	mean	STD	mean	STD	mean	STD
20	0.748	0.1733	0.558	0.2229	0.488	0.2516
40	0.749	0.1745	0.561	0.2242	0.489	0.2518
60	0.750	0.1760	0.563	0.2253	0.490	0.2536
80	0.755	0.1756	0.569	0.2258	0.497	0.2549
100	0.758	0.1763	0.571	0.2265	0.501	0.2552

Table 4.3 Monte Carlo results for current in the transformer secondary (pu) during
LG faults assuming a PV penetration level of 50%.

PV [kW]	Current		Penetration [%]	Current	
	mean	STD		mean	STD
0.7	6.9221	2.9889	20	6.9381	2.9884
1.4	6.9364	2.9944	40	6.9336	2.9904
2.1	6.9421	2.9819	60	6.9490	2.9949
2.8	6.9227	3.0054	80	6.9040	3.0230
3.5	6.9328	3.0312	100	6.9050	3.0412

high, the STD for node voltages slightly increases. Both of these MCAs are repeated to investigate the expected PDF of the current sensed in transformer secondary during the fault. The results of these analyses are given in Table 4.3. This table shows that PV rating and penetration levels do not modify the expected current in transformer secondary during an LG fault. In addition, the increase in STD with respect to the increase of PV rating and penetration level is not significant.

4.5.2 LL fault

Let us consider an LL fault, assuming 50% penetration level for PVs. Table 4.4 shows that the expected average voltages for each node decrease as the PV rating goes high. This is valid for all nodes. The STD of the node voltages also goes high as the PV rating increases.

Table 4.5 shows the MCA results of node voltages in different PV penetrations, assuming all PVs have an output power of 2 KW with a 150% current limit. From this table, it can be seen that with an increase in PV rating and penetration level, the average and STD of voltages of the nodes go high.

Table 4.6 shows the transformer current as the output of the MCA. This table indicates that the average and STD of transformer current increases as PV rating or penetration level goes high.

Table 4.4 Monte Carlo results for phase C node voltages (pu) for different PV outputs during LL faults penetration level of 50%.

PV [kW]	V_1		V_5		V_{10}	
	mean	*STD*	*mean*	*STD*	*mean*	*STD*
0.7	0.9552	0.0693	0.8639	0.1193	0.8354	0.1400
1.4	0.9475	0.0687	0.8537	0.1191	0.8238	0.1401
2.1	0.9395	0.0677	0.8425	0.1187	0.8115	0.1394
2.8	0.9316	0.0669	0.8319	0.1175	0.7999	0.1383
3.5	0.9262	0.0651	0.8250	0.1165	0.7923	0.1373

Table 4.5   Monte Carlo results for phase C node voltages (pu) for different PV
penetration levels during LL faults.

Penetration [%]	V_1		V_5		V_{10}	
	mean	STD	mean	STD	mean	STD
20	0.9551	0.0702	0.8641	0.1202	0.8360	0.1405
40	0.9482	0.0697	0.8551	0.1192	0.8255	0.1399
60	0.9425	0.0668	0.8462	0.1183	0.8157	0.1392
80	0.9331	0.0658	0.8340	0.1172	0.8020	0.1386
100	0.9246	0.0650	0.8230	0.1167	0.7900	0.1378

Table 4.6   Monte Carlo results for current in the transformer secondary (pu) during
LL faults during LL faults at PV penetration level of 50%.

PV [kW]	Current		Penetration [%]	Current	
	mean	STD		mean	STD
0.7	4.8637	2.9879	20	4.8413	2.9862
1.4	4.8810	2.9948	40	4.8655	3.0103
2.1	4.8927	3.0241	60	4.9017	3.0168
2.8	4.9465	3.0275	80	4.9224	3.0206
3.5	4.9534	3.0289	100	4.9327	3.0293

4.5.3 LLG fault

Let us consider an LLG fault, assuming 50% penetration level for PVs. The
results are shown in Table 4.7. From this table, it can be seen that the expected
average and STD of the BOF node voltages increase as the PV rating goes high.
However, these values decrease for the MOF and EOF nodes.

Table 4.8 shows the MCA results for different PV penetration levels. From this
table, it can be seen that the expected average voltage in BOF nodes increase as the
PV penetration level goes high. However, this value decreases for the MOF and EOF
nodes. The STD of voltages in all nodes increases as PV penetration goes high.

Table 4.7   Monte Carlo results for phase C node voltages (pu) for different PV ratings during LLG faults and PV penetration level of 50%.

PV [kW]	V_1		V_5		V_{10}	
	mean	STD	mean	STD	mean	STD
0.7	0.5354	0.0917	0.4625	0.0583	0.4469	0.0700
1.4	0.5393	0.0930	0.4604	0.0568	0.4413	0.0683
2.1	0.5418	0.0942	0.4577	0.0565	0.4355	0.0679
2.8	0.5461	0.0965	0.4552	0.0561	0.4294	0.0667
3.5	0.5487	0.0973	0.4534	0.0556	0.4251	0.0662

Table 4.8   Monte Carlo results for phase C node voltages (pu) for different PV penetration levels during LLG faults.

Penetration [%]	V_1		V_5		V_{10}	
	mean	STD	mean	STD	mean	STD
20	0.5357	0.0913	0.4626	0.0536	0.4467	0.0687
40	0.5395	0.0926	0.4599	0.0539	0.4405	0.0689
60	0.5423	0.0938	0.4568	0.0546	0.4347	0.0694
80	0.5468	0.0963	0.4554	0.0550	0.4294	0.0695
100	0.5489	0.0971	0.4533	0.0552	0.4244	0.0699

Table 4.9 Monte Carlo results for current in transformer secondary (pu) during LLG faults at PV penetration level of 50%.

PV [kW]	Current		Penetration [%]	Current	
	mean	STD		mean	STD
0.7	8.7255	2.8067	20	8.7538	2.8227
1.4	8.7156	2.8037	40	8.7405	2.8111
2.1	8.7041	2.7928	60	8.6751	2.7859
2.8	8.6715	2.7885	80	8.6642	2.7756
3.5	8.6608	2.7770	100	8.6464	2.7676

Table 4.10 SOP results for different fault types.

Fault	Penetration [%]	Rating (kW)	SOP[%]
LG	From 20 to 100	0.7 to 3.5 kW	97
LL	From 20 to 100	0.7 to 3.5 kW	89
LLG	From 20 to 100	0.7 to 3.5 kW	99

Table 4.9 shows the transformer current as an output of MCA. This table shows
that the average and STD of transformer current decrease as PV rating or penetration
level goes high.

Also Table 4.10 illustrates the calculated SOP to each fault type. It can be seen that
the SOP is same for all penetration levels in every fault type, varying from 99% and
97% in the case of LLG and LG respectively to 89% in the case of LL faults. Based
on this table, it can be concluded that the switch-fuse at the transformer secondary
will detect the SCF in the LVF successfully with a probability of over 89%.

Also, Table 4.11 lists the expected average voltage (EAV) of each node of the
LVF for different PPLs under various SCF types. Through this chart, it can be seen
that the phase voltages on the faulted phase are below the threshold of 0.88 pu for
both LG-Fs and LLG-Fs, regardless of the PPL. However, the EAV of the nodes at
the BOF is above the threshold. Using the corresponding PDFs, the PDP is also
calculated for each node of the LVF, and listed in Table 4.12. From this analysis, it
can be seen that the PVs in the faulted phase will disconnect according to [55] in the
case of LG-Fs and LLG-Fs with a probability of over 89%. However, this probability
is between 52-63% in the case of LL-F. In this type of SCF, the impact of the PPL is
more tangible, and it increases for large PPLs.

Table 4.11. Expected average voltage in all nodes of the LVF [%] in various PV penetration levels and different faults and the expected number of non-disconnected PVs after the fault.

Fault	PV Penetration [%]	V_1	V_2	V_3	V_4	V_5	V_6	V_7	V_8	V_9	V_{10}	Non-Disconn-ected PVs
LG	20	74.8	68.3	63.1	58.8	55.8	55.4	52.6	50.6	49.2	74.8	0
	40	74.9	68.4	63.3	59.0	56.1	55.5	52.8	50.8	49.4	74.9	0
	60	75.0	68.8	63.7	59.5	56.3	56.0	53.4	51.4	50.0	75.0	0
	80	75.5	68.9	63.8	59.6	56.9	56.0	53.6	51.6	50.2	75.5	0
	100	75.8	69.4	64.4	62	57.1	56.8	54.1	52.1	50.7	75.8	0
LL	20	95.5	92.4	89.8	88.2	86.4	85.1	84.3	83.8	83.5	83.6	4
	40	94.8	91.6	89.0	87.3	85.5	84.2	83.3	82.8	82.5	82.5	3
	60	94.2	97.0	88.0	85.9	84.6	83.0	82.2	81.6	81.3	81.5	3
	80	93.3	89.9	87.2	85.0	83.4	82.0	81.1	80.5	80.2	80.2	2
	100	92.4	89.1	86.3	841	82.3	81.1	80.2	79.6	79.2	79.0	2
LLG	20	53.5	59	48.9	47.3	46.2	45.4	45.0	44.7	44.6	44.6	0
	40	53.9	51.1	48.9	47.2	45.9	45.0	44.5	44.2	44.1	44.0	0
	60	54.2	51.3	48.9	47.1	45.6	44.8	44.1	43.8	43.6	43.4	0
	80	54.6	51.5	49.0	47.0	45.5	44.4	43.7	43.2	43.0	42.9	0
	100	54.8	51.7	49.0	46.9	45.3	44.0	43.2	42.7	42.5	42.4	0

Table 4.12. The probability of observing a voltage of higher than 88% in each node along the LVF in various PV penetration levels and different faults.

Fault	PV Penetration [%]	Expected PDP in the each Node										Expected PDP in the LVF [%]
		1	2	3	4	5	6	7	8	9	10	
LG	20	77.7	84.9	88.9	91.4	92.6	92.1	93.1	93.7	94.0	94.1	90.3
	40	77.4	84.5	88.7	91.2	92.3	92.0	92.9	93.5	93.9	94.0	90.1
	60	77.0	84.1	88.2	90.7	92.1	91.5	92.5	93.1	93.5	93.8	89.7
	80	76.2	83.8	87.9	90.4	91.6	91.2	92.2	92.9	93.2	93.4	89.3
	100	75.6	83.3	87.5	90.1	91.4	90.9	92.0	92.6	93.0	93.2	89.0
LL	20	14.3	48	49.3	49.9	55.3	59	61	62.1	62.7	62.4	52.4
	40	16.5	48.3	49.6	52.6	58.3	61.8	63.8	64.8	65.4	65.3	54.7
	60	17.7	48.8	50.0	57.7	61.3	65.4	67.0	68.1	68.6	68.0	57.3
	80	21.1	49.1	50.4	61.1	65.2	68.4	70.2	71.2	71.6	71.5	60.0
	100	25.0	49.5	50.8	64.4	68.7	71.0	72.7	73.5	74.1	74.5	62.5
LLG	20	99.9	100	100	100	100	100	100	100	100	100	99.9
	40	99.9	100	100	100	100	100	100	100	100	100	99.9
	60	99.9	100	100	100	100	100	100	100	100	100	99.9
	80	99.9	100	100	100	100	100	100	100	100	100	99.9
	100	99.9	100	100	100	100	100	100	100	100	100	99.9

4.6 Discussion

The ratio of STD to the EAV or expected average current represents the data diversity in each of the conducted MCA studies. Results of

Table 4.1 to Table 4.8 show that this ratio is below 18% for LL and LLG faults while it is in the range of 23-52% for LG faults. It can also be seen that this ratio is in the range of 7-24% when the SCF is at the BOF while it is in the range of 12-40% and 15-52% for the SCFs at the MOF and EOF, respectively. Thus, it can be concluded that the SCF impedance and location (with the assumed PDFs) are the dominant inputs than the PV rating and PPL. Also, it can be concluded that as the SCF is located closer to the far end nodes of the LVF, the data diversity increases as other inputs also become more influential. Likewise, from Table 4.3 this ratio is determined to be in the range of 32-62% which again emphasizes that SCF location and impedance are the dominant inputs.

Table 4.13 summarizes the results of the MCA for three types of SCFs and shows the impact of PV rating and PPL increase on the EAV of the nodes along the LVF, and the average of the transformer secondary current. The stochastic analysis results demonstrate that the EAV of the PDF of the transformer secondary current increases during LL and decreases in LLG fault, for large PV ratings or PPLs. However, it does not demonstrate a particular trend for LG faults.

An increase in PPL leads to an increase of the EAV of the nodes in LG fault while it causes a decrease in these parameters during LL fault. Similarly, the growth in PV rating results in an increase of this parameter in case of the LG but a decline for LL faults. On the other hand, in the case of LLG, for large PV ratings or PPLs, the EAV of nodes increase at BOF and decrease at the MOF or EOF.

It is to be noted that the stochastic analysis considers different parameters of SCF location and impedance, PV installation point and rating, and PPL as the input and its outcome illustrates the combined impact of all inputs. As seen from results tables which were shown on previous sections, the outcomes of the MCA are not too different when varying the PPL from 0 to 100%. This implies that other inputs (mainly the SCF impedance and location) have a stronger impact on the outcome as they are directly related, while the outcomes are not directly influenced by the PPL.

On the other hand, the output currents of the PVs are limited to 150% of their nominal current during SCFs, and the variation of the PPL does not change it significantly when compared with the SCF level of the network. Thereby, it is seen that the PPL is not a strong measure when evaluating the performance of an LVF under SCFs.

The results showed in Table 4.10 demonstrates that the SOP is above 89% for LG, LL and LLG faults irrespective of the PPL. On the other hand, Table 4.12 indicates that the PDP is above the same level for LG and LLG faults while it is between 52-63% for LL faults. Thereby, considering only the SOP criterion, even at a PPL of 100%, the switch-fuse at the transformer secondary will detect the SCF in the LVF successfully with a probability of over 89%. However, considering the PDP criterion for all considered SCF types, a PPL of below 80% will result in the disconnection of the PVs on the faulted phase with a probability of approximately 52-57% while this number rises to 60-63% for a PPL of above 80%.

Table 4.13 summarizes the results of MCA for three types of faults. This table shows the impact of PV rating and penetration level on the average of feeder node voltages and transformer secondary current.

Table 4.13. Summary of stochastic analysis for different faults in the network.

Fault	Monte Carlo Output			Expected Average	STD
LG	Transformer Current	PV Rating	↑	～	～
		Penetration Level	↑	～	↑
	Voltage	PV Rating	↑	↑	～
		Penetration Level	↑	↑	↑
LL	Transformer Current	PV Rating	↑	↑	↑
		Penetration Level	↑	↑	↑
	Voltage	PV Rating	↑	↑	↑
		Penetration Level	↑	↓	↓
LLG	Transformer Current	PV Rating	↑	↓	↓
		Penetration Level	↑	↓	↓
	Voltage	PV Rating	↑	↑↓↓	↑↓↓
		Penetration Level	↑	↑↓↓	↑

↑ consistent increase, ↓ consistent decrease, ～ no trend

↑↓↓ increase at beginning nodes and decrease at middle and end nodes

The stochastic analysis results demonstrate that the expected average of the pdf of transformer secondary current increase during LL fault and decreases in LLG fault, as the PV rating or penetration level goes high. For LG faults, the mean of the pdf of transformer current does not demonstrate a specific trend as the PV rating or penetration level goes high.

An increase in PV penetration level leads to an increase of the mean of the pdf of node voltages in LG faults while it leads to a decrease in these parameters during LL faults. The increase in PV rating results in an increase of the mean of node voltages for LL and LG faults. For LLG faults, as PV rating or penetration level goes high, the average of pdf of node voltages increase at the beginning nodes and decrease at the middle and end nodes.

The following chapter is dedicated to analyze the disconnection of PVs in the case of fault occurrence. The chapter five will discuss the condition that leads in unsuccessful disconnection of PVs during the fault. In addition, the disconnection of PVs in detail will be studied and different effective parameters on disconnection of PVs will be investigated. Parameters such as fault impedance, fault location, fault type and grounding system.

4.7 Summary

This chapter has evaluated the contribution of residential single-phase rooftop PVs on the SCFs in the supplying LVFs. The effect of PVs on the voltage profile along the LVF and the current sensed at the secondary of the distribution transformer is studied during LG, LL and LLG faults. To consider the uncertainties in PV rating, location and PPL as well as the SCF location and impedance, a stochastic analysis is carried out.

Three parameters of SCF level, transformer current, and voltages of the nodes along the LVF are investigated during the SCFs. The results of the stochastic analysis show that the expected average current at transformer secondary and EAV of the nodes along the LVF are not influenced strongly by the PV ratings and PPLs, and it is seen that the SCF location and impedance are the dominant factors to be considered.

Based on the outcomes of the MCA, two criteria were defined to evaluate the impact of the PV rating and PPL on the probability of the successful detection of the SCF by the switch-fuse at the transformer secondary and the disconnection of the PVs. These criteria show that with a probability of over 89%, the switch-fuse will detect the SCF while the PVs will disconnect with a probability of 52-57% if the PPL is below 80% which rises to 60-63% for a PPL of above 80%

.

Chapter 5. Disconnection of Rooftop PVs under Different Types of Short Circuit Faults

5.1 Introduction

One important issue to be investigated in electricity networks with rooftop PVs is that whether it is possible for some PVs to continue to supply power to the feeder when the upstream network is lost, particularly in a situation where there are many PV systems on the feeder. This islanding mode of operation could increase distribution system reliability if properly designed without compromising safety of personnel. In the past, many utility regulations mandated that all downstream distributed generators must disconnect. But technology and knowledge about the risk of operating DGs under such circumstances are now much clearer and an informed judgement to continue to operate downstream DGs is an issue that is subject matter of many grid connection standards. This is a research gap that this paper focuses on.

To facilitate higher penetration of single-phase rooftop PVs in electric networks, the protection issues of these networks should be evaluated in more details. In this regard, this chapter concentrates on the LV feeders to which the single-phase rooftops PVs are connected. The voltage profile along the feeder after a short-circuit fault in the LV feeder is analyzed carefully. Within this period, the disconnection time and disconnection sequence of the rooftop PVs are also scrutinized. Several parameters such as the impedance of fault (IoF), location of fault (LoF) and PV generation capacity to residential load demand ratio (GDR) are included within this study. The voltages of nodes along the feeder are observed during the first few cycles after fault-occurrence on the LV feeders. Another aim is to compare the footprint of

network earthing on the disconnection time of PVs. So in this chapter, a comparison of the voltage profile along the feeder in multiple earthed neutral (MEN) [56] and non-effectively grounded (NEG) [57] systems after a short-circuit fault will be presented. The single-phase (1Φ) faults, which are the most common type of faults in distribution networks [43] as well as three-phase faults are considered in the analyses of this paper. The open-conductor fault is also briefly discussed. The main contributions of this chapter are:

- evaluate and discuss the disconnection time and sequence of single-phase rooftop PVs distributed in different phases during an LG and three phase faults,

- investigate the importance of IoF and LoF on the disconnection time of rooftop PVs after an LG and three phase faults,

- investigate the correlation between the disconnection time of PVs and a high GDR under short-circuit scenarios,

- compare the consequence of NEG and MEN systems on the disconnection time of rooftop PVs in an LV feeder with 100% penetration of rooftop PVs,

- define the conditions under which rooftop PVs may not be disconnected after an LG or three phase fault in LV feeders.

The rest of the chapter is organized as follows: Section 5.2 introduces the network under consideration. The research methodology is discussed in Section 0, and the results of the analyses are presented in Section 5.4 and 5.5. Section 5.6 presents a discussion on the findings of the research. The general conclusions are highlighted in the last section as a summary.

5.2 Network under consideration

Let us consider the network of Figure 5.1, which schematically represents a typical Australian urban LV distribution network used for supplying residential loads. This network is selected as a case study in this research. It is assumed that a three-phase, three-wire MV feeder supplies a three-phase, four-wire LV feeder through a three-phase Dyn distribution transformer [58]. The residential houses are assumed to be single-phase loads, connected to the LV feeder. The network above is

Table 5.1 Technical data of the network under consideration

Distribution Transformer: 150 Kva, 11 Kv/ 415 V, 50 Hz, Dyn-type, Z = 5%
MV feeder: 11 Kv L-L rms, 2 km, ACSR 50 mm^2 bare conductor, three-phase three-wire system, $R = 2.16$ Ω/km, $X = 2.85$ Ω/km
LV feeder: 415 V, 400 m, AAC 75 mm^2 bare conductor, three-phase four-wire system with ABCN horizontal configuration on 120 cm crossarms [58] and a total of 400 meter length, 10 nodes with a distance of 40 meter from each other, $R = 0.452$ Ω/km, $X = 0.27$ Ω/km
PV systems: PF = 1, η =100 %, $I_{max\ at\ Fault} = 150\%\ I_{rated}$
Residential Demand: Single-phase constant-impedance loads, $S = 4.4$ Kva, PF = 0.95 lagging

composed of 30 houses, and assumed to be equally distributed among the three phases. The parameters of the network under consideration are given in Table 5.1.

In this research, to consider a worst case scenario, it is assumed that the penetration of single-phase rooftop PVs is 100%. It is to be noted that the PV penetration level is defined as the ratio of the output AC power of the PV systems versus the network peak load [59]. A similar network is used by majority of the European and Asian utilities to supply the urban residential loads. It is to be noted that this network is different from the networks of North American countries [60]. The new and properly designed LV feeders are in the form of MEN type where the neutral wire is earthed at the secondary of the distribution transformer as well as at the premises of each load [61], as seen from Figure 5.2 (a). However, old LV feeders or LV feeders developed without proper engineering supervisions may be in the form of a NEG system. Thus, the neutral wire in the LV feeder is assumed to be grounded only at the distribution transformer but not at every residential load premises, as seen from Figure 5.2(b), when considering a NEG system. While iin the case of MEN systems it is also grounded at each residential units (through an earthing resistance).

The rooftop PVs are assumed as constant single-phase power sources, operating at unity power factor, based on IEEE Recommended Practice for Utility Interface of PV Systems [62]. Furthermore, the maximum current output of the PVs is limited to

150% of the nominal value [63], during the faults. Each PV is assumed to be 4.4 kW, which is approximately the median of the most common rooftop PVs sizes in Perth, Western Australia [64]. Also, in this research it is assumed that the protection system of the PV systems are based on under/over voltage scheme, as highlighted in the datasheet of PV systems that are commercially available in Australian market [63,65-66].

Loads of the networks are assumed as single-phase constant impedance type, distributed equally among the phases. Each load is assumed to be 4.4 Kva with a power factor of 0.95 lagging, which is equal to the after diversity maximum demand (ADMD) of townhouses and villas in Perth, Western Australia [67].

(a)

(b)
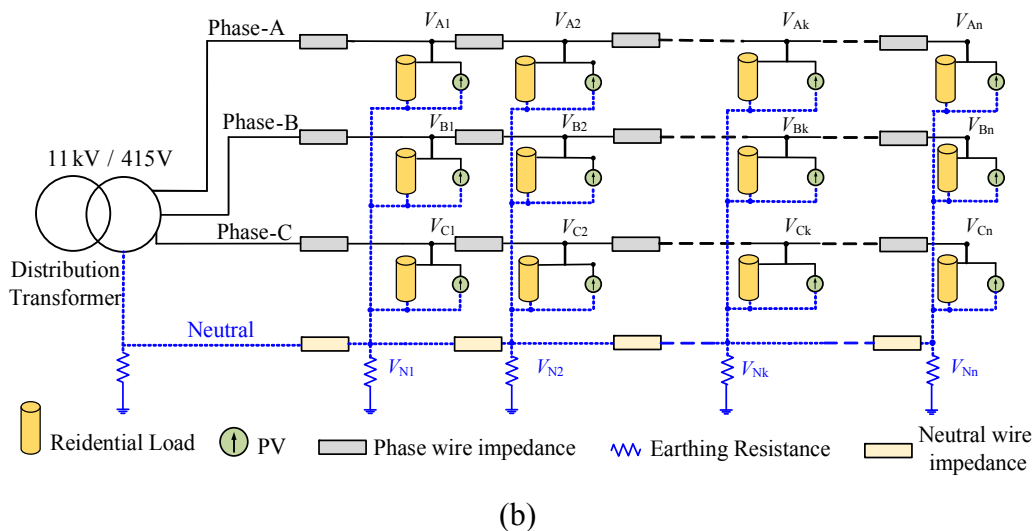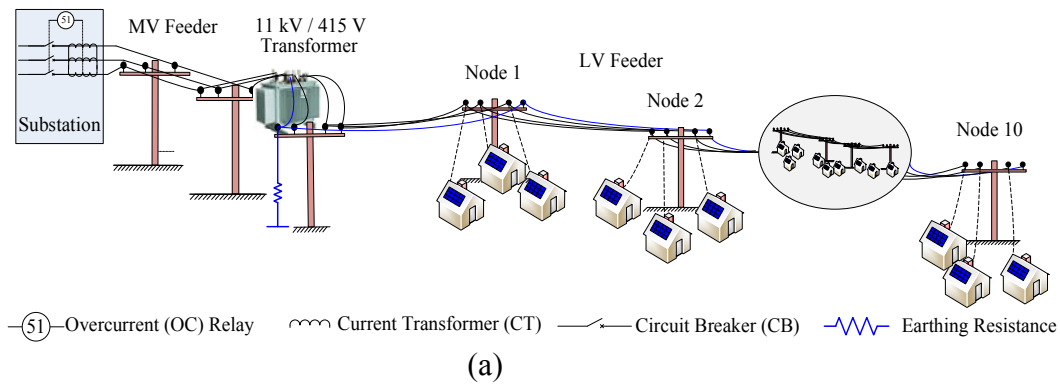
Figure 5.1. (a). Schematic diagram of the three-phase, four-wire LV feeder with high penetration of rooftop PVs, supplied from an MV feeder,
(b) single-line diagram of the LV feeder.
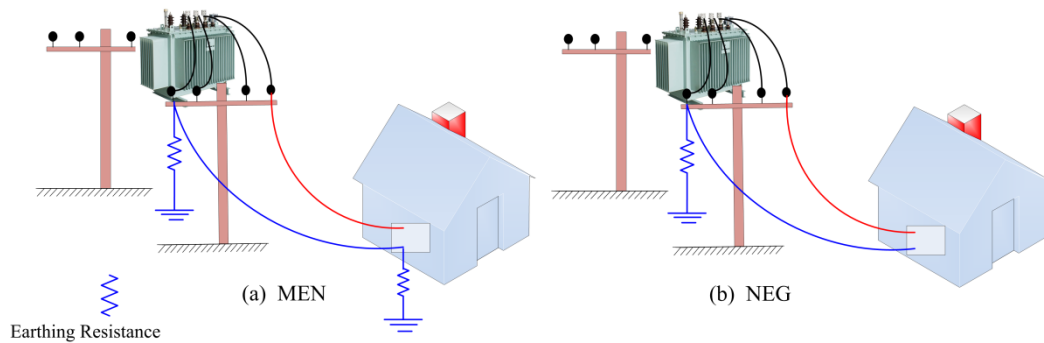
Figure 5.2. Schematic diagram of different earthing systems in an LV feeder:
(a) MEN system, (b) NEG system.

AS mentioned earlier, the LV feeder is composed of 30 houses and is supplied by a 150 Kva distribution transformer. Three houses are assumed to be supplied from each pole, where the poles are located at a distance of 40 meters from each other as shown in Figure 5.1(a).

5.3 PV disconnection after a fault and important parameters

PV systems should isolate from the LV feeders if a short-circuit fault occurs in the network. If they are not isolated, the LV feeder may remain energized by the PV systems, even if the upstream circuit breaker has operated. Under such a scenario, if the output power of the PV systems is potentially equal to or greater than the minimum load of the network, a risk of islanding exists; although no national or international records are available [35]. Islanding can lead to the damage of the electrical equipment and hazards for the utility personnel. Although this can be a rare situation but proper protection schemes should be utilized to prevent such cases. IEEE Recommended Practice for Utility Interface of PV Systems [55] defines the normal operating voltage boundaries for the rooftop PVs of smaller than 10 kW. Based on [55], the rooftop PVs should be isolated and disconnected from the LV feeder and do not energize it, if the voltage of the feeder drops below 88% of the nominal value. In a similar fashion, the PVs should also get isolated if the voltage of the feeder rises above 110% of the nominal value. This standard also highlights that the PV systems should disconnect if frequency variations are observed in the LV feeder. Australian standard for grid connection of energy systems via inverters [68]
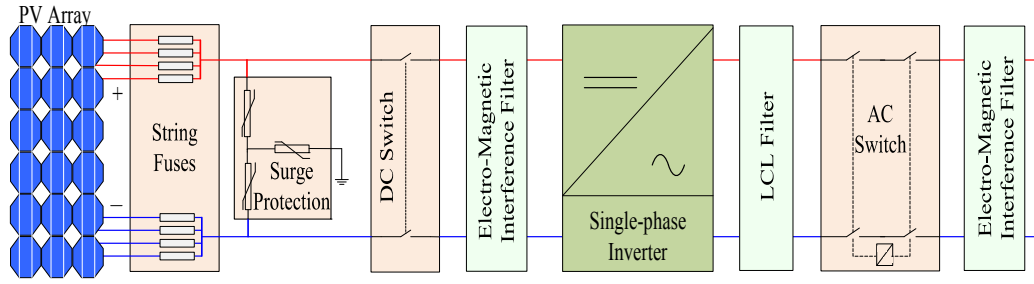
 Figure 5.3. Schematic internal structure of a rooftop single-phase PV system.

provides a similar guideline for the disconnection of PV systems in the case of abnormal voltage and frequency deviations in the network. The maximum allowable

time for disconnection of the PVs depend on the level of the voltage drop, as given in Table 5.2 for both of these standards. In the rest of this chapter, the levels defined by [55] are only considered.

Table 5.2 Maximum disconnection time of rooftop PV in response to feeder abnormal voltages [55, 68]

IEEE Recommendation (IEEE Std 929-2000)		Australian Standard (AS4777-2013)	
Condition (%)	Maximum tripping time (cycle)	Condition (%)	Maximum tripping time (cycle)
50% < V < 88% or 110% < V < 137%	120	V < 78% or V > 113%	100
V < 50%	6		
V > 137%	2		
59.3 < f < 60.5 Hz		47.5 < f < 52 Hz	100

Figure 5.3 illustrates schematically the internal structure of a typical single-phase rooftop PV system that are available in Australian market [66]. These PV systems are usually equipped with different types of protection functions such as surge protection, overvoltage protection, deep discharge protection, reverse current protection and short circuit protection of the module and overcurrent and over temperature protection for their PV array and dc sides. On the other hand, they are required to be equipped with techniques to prevent islanding in the LV feeders. Thus, the PV systems usually have passive anti-islanding protection functions such as

Table 5.3 Protection functions available in some of the PV systems in Australia

Protection Function	Schneider (Clipsal)	ABB (PVS300)	C1energy Catalyst (SPH40)	EATON (SG00210)
Overcurrent (Overload, Short-circuit)	✓	✓	✓	✓
Under/over voltage	✓	✗	✓	✓
Reverse current	✓	✗	✓	✗
Over temperature	✗	✓	✗	✗
Deep discharge	✗	✗	✓	✗

under/over voltage, under/over frequency, the rate of change of frequency, voltage phase jump and harmonics [70].

Among these, under/over voltage and under/over frequency are the most common protection functions for the PV systems that are commercially available in Australian market.

Table 5.3 illustrates a comparison among the available protection functions of different PV systems that are available in the Australian market. On top of the passive anti-islanding protection functions, active islanding protection functions such as frequency shift, frequency instability, power variation, negative sequence current or impedance monitoring can also be utilized [69].

On the other hand, PV systems are usually equipped with low voltage ride through (LVRT) capability [71-72], based on which the PV systems continue to supply power if the voltage in the LV feeder drops below the nominal value, especially in the case of temporary short-circuit faults. It is been cited in [72] that a delay time of 0.2 or 0.5 second is used to avoid unnecessary disconnection of the PV systems in such cases in the grid codes of different countries. If the fault is not cleared and the voltage drop is not recovered within this period, the PV system then disconnects from the LV feeder.

It is expected that following an LG short-circuit fault in the LV feeder, the voltage along the feeder in the faulty-phase will drop quickly while the voltage in the other (healthy) phases will rise. The level of voltage drop in the faulty phase mainly

depends on the fault impedance. The present-day concern of utilities is that the high PV generation to load demand ratio, network earthing as well as the fault impedance and location may cause the voltage drop not to be below 88% of the nominal voltage. If it happens so, the rooftop PVs will not detect any abnormal voltage in the feeder and will not disconnect. This will allow the PVs to continue to feed the fault. Under such scenarios, the voltage in the healthy phases may also not rise above the threshold of 110%; hence the PVs on the normal phase(s) may continue to supply the fault via the distribution transformer. The scenario mentioned above will continue until the upstream circuit breaker, which is usually controlled by an inverse definite minimum time (IDMT) over current relay, trips. After circuit breaker tripping, the voltages in both faulty and healthy phases will significantly drop, leading to the disconnection of the PVs that are still connected. It is worth mentioning that there is a possibility that the fault current to be very small, resulting in being non-detectable with normal overcurrent relays. Thus, the fault will continue to be fed by the upstream network and PVs. These scenarios and situations will be investigated in Sections 5.4.

In the case of three phase faults, it is expected that all three phases show a similar trend to the faulty phase of the feeder under LG fault. This scenario and the PVs disconnection following a three phase fault are investigated in Section 5.5.

It is to be noted that although recently developed LV feeders are usually in the form of MEN, the old LV feeders may be NEG. Each of these earthing systems, might have a strong footprint on the voltage profile along the feeder, during LG or three phase short-circuit faults.

To understand the network situation during an LG or three phase short-circuit fault, this research considers the network of

Figure 5.1 and evaluates the voltage along the feeder and the disconnection time of the PVs based on the following 4 parameters:

- PV generation capacity to load demand ratio (GDR),
- the impedance of fault (IoF),
- location of fault (LoF) along the feeder,
- network earthing system.

Several simulation study cases are developed and examined in PSCAD/EMTDC to evaluate the network performance, a few of which provided in Sections 5.4 and 5.5. To analyze each parameter, the selected cases are re-examined assuming the other parameters as constant and the results (i.e. the voltage along the feeder following an LG or three-phase short-circuit fault as well as the disconnection time and sequence of the PVs) are recorded. At the end, the results are tabulated and evaluated.

5.4 Disconnection of PVs during single-phase faults

This section focuses on the disconnection time and sequence of single-phase rooftop PVs after an LG short-circuit fault in the LV feeder. Let us consider the network of Figure 5.1 with the GDR of unity. An LG short-circuit fault is applied at the middle of the feeder (i.e. LoF = node 5 can range from 1 to 10) on phase-a where the IoF is assumed (e.g. IoF = 2 Ω). The disconnection time of the PVs depends on the time that the voltage of their point of common coupling (PCC) drops below 88% or rises above 110% of the nominal voltage. Assuming the network at steady-state condition, the fault occurs at $t = 0$. The voltages of the faulty phase drop below 88% of the nominal value immediately; hence, all of the PVs within phase-a disconnect simultaneously at $t = 0.0048$ s. Immediately after fault-occurrence, the voltages of the healthy phases increase. As an example, in one study, the voltage of node 1 in phase-b and nodes 1-4 in phase-c increase above 110% of their nominal value at $t = 0.0060$ s and 0.0075 s; thereby the PVs connected to these nodes disconnect at these times. The rest of the PVs connected to phase-b and c disconnect in the same fashion before 0.0137 s. Thus, all PVs disconnect in less than a cycle after fault occurrence. It is to be noted that no LVRT was considered in this analysis. However, if the PVs have the LVRT feature, the PVs will disconnect in one cycle after the delay time of the LVRT (i.e. 0.2 or 0.5 s based on the grid codes of different countries [72]). The upstream circuit breaker, which has an extremely inverse characteristic and a time multiplier setting (TMS) of 0.02 opens at $t = 1.306$ s. The schematic disconnection time of the PVs for the case study is shown in Figure 5.4. This network is now analyzed in detail considering different IoFs, LoFs and GDRs, as discussed below:
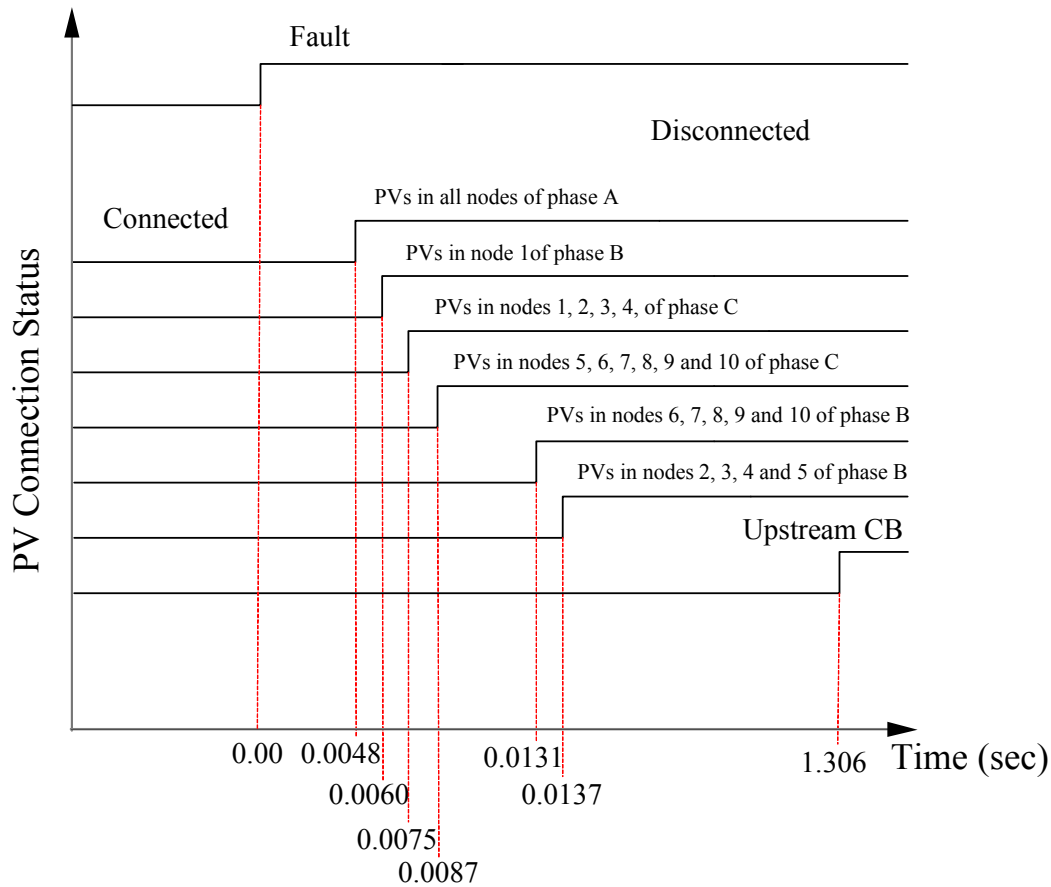
Figure 5.4. Disconnection time and sequence of PVs and upstream circuit breaker after an LG fault.

5.4.1 Impact of impedance of fault

Let us consider the network of Figure 5.1 with the GDR of unity. A LG short-circuit fault is applied at the middle of phase-a (i.e. LoF = node 5). In this study, the IoF is varied from a very small (e.g. 0.002 and 0.2 Ω) to small (e.g. 1 and 2 Ω) and high (e.g. 20 Ω) values. The voltage profile along the feeder between fault-occurrence and the disconnection time of PVs or the opening time of the upstream circuit breaker is shown in Figure 5.5. The results are recorded for the MEN and NEG systems, separately. The left-hand graphs of Figure 5.5 show the voltages in an NEG system while the right-hand graphs show the voltages in an MEN system. From this figure, it can be seen that the voltage of all nodes of the faulty phase drop below the limit of 88% for all IoFs except IoF = 20 Ω. Hence, all of the PVs in the faulty

phase disconnect after fault-occurrence. This is valid for both MEN and NEG systems; however, the voltages of the NEG system remain slightly higher than those for the MEN system. This figure also shows that for high impedances IoFs (e.g. 20 Ω) in the MEN system, the voltage of the healthy phases (phase-b and c in this case) rest within the normal operation bandwidth of 88% to 110%; Thus, the PVs connected to the healthy phases will not disconnect and will continue to feed the fault. This is true for the IoFs larger than 1 Ω in the NEG system. In the case of high impedance LG short-circuit faults (e.g. 20 Ω), the PVs in both healthy and faulty phases remain connected to the LV feeder and keep feeding the fault until the upstream circuit breaker trips.

It is worth mentioning that the voltages shown in Figure 5.5 are recorded at one specific moment (i.e. between fault-occurrence and the first disconnection time of PVs or the upstream circuit breaker). Thus, this figure does not illustrate the voltages after the disconnection of the first set(s) of PVs. Thereby, even if the voltages of some nodes is within the nominal bandwidth of 88% to 110% in Figure 5.5, their voltages may exit this bandwidth after the disconnection of the other PVs. Hence, the disconnection time and sequence of the PVs should also be studied.

To study the disconnection time of PVs and their sequence in the presence of different IoFs, the recorded results are represented in radar charts of Figure 5.6. In this type of charts, the radius of circles represents the disconnection time while the numbers around the circles refer to the node numbers. It is to be noted that the considered LV feeders are radial, as illustrated in

Figure 5.1(b) and the circular alignment of the nodes should not be interpreted as a loop topology. The top row of this figure represents the NEG system while the bottom row represents the MEN system. It can be seen from this figure that the PVs connected to both healthy and faulty phases do not sense the fault and do not disconnect when the IoF is higher than 2 Ω for both MEN and NEG systems. The radar charts of Figure 5.6 also show that for each IoF, all of the PVs in one phase operate at the same time roughly (i.e. in less than half a cycle difference). The disconnection time increases as the IoF becomes larger. This figure also shows that for the MEN system, the disconnection time is almost same for both faulted and

healthy phases. It is noteworthy that this time is larger for the NEG system versus the MEN system.

5.4.2 Impact of location of fault

To investigate the influence of the LoF on the voltage profile along the feeder and also the disconnection time and sequence of the rooftop PVs, the previous evaluation is repeated. (i.e a short-circuit fault is applied on phase-a where the GDR is unity) assuming that the IoF is very small (i.e. 2 mΩ) while the LoF is varied from the beginning of the feeder towards its end. In the rest of this paper, LoF = 1, 5, and 10 respectively represents the fault at the beginning (i.e. node-1), middle (i.e. node-5) and the end (i.e. node-10) of the LV feeder.

The voltage profile along the feeder in this case is shown in Figure 5.6. This figure shows that for all cases of LoF = 1, 5 and 10, the voltage of the nodes in the faulty phase are very close to each other and all are lower than 20% of the nominal value in the MEN and less than 40% of the nominal value in the NEG system. Hence, it is expected that the PVs within the faulty phase will disconnect regardless of the fault location along the feeder. Following fault occurrence, the voltages of the nodes in the healthy phases rise above the threshold of 110% and thus their PVs will also disconnect.

Figure 5.5. Voltage profile along the feeder during LG fault between fault-occurrence and the PV upstream circuit breaker tripping for different IoFs.

An interesting issue can be observed in the results of the NEG system. As it can be seen from Figure 5.7, the voltage of some of the nodes in phase-b in the NEG system does not rise above the 110% threshold even for a very small IoF of 2 mΩ. Thus, the PVs connected to the middle and end nodes of this phase will not be disconnected under such conditions. The situation will be even worse when the IoF is larger. Figure 5.7 presents the disconnection time of the PVs in radar charts. This figure shows that all of the PVs in both healthy and faulty phase disconnect almost at the same time (i.e. within few millisecond differences but within the same cycle) and this time is not affected strongly with the LoF. This is valid for both of the MEN and NEG systems.
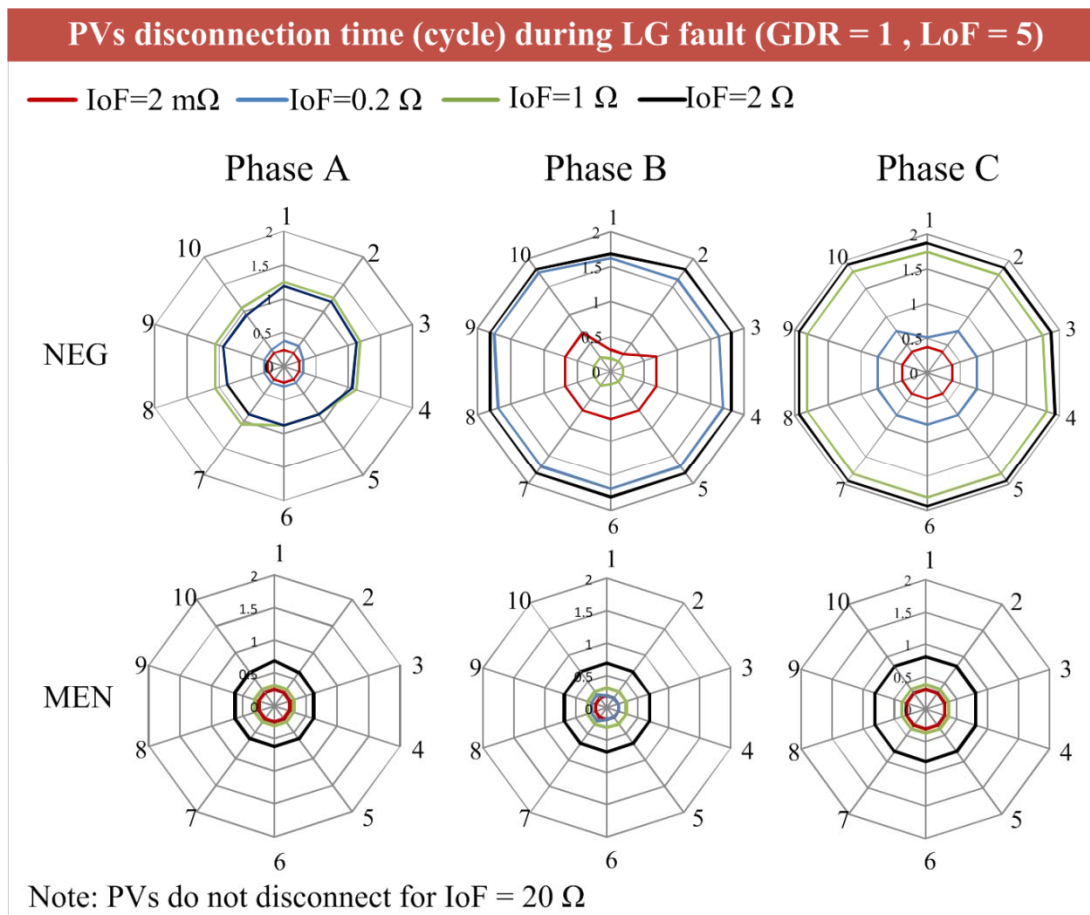
Figure 5.6. Disconnection time and sequence of PVs after LG fault for different IoFs.

5.4.3 Impact of generation to demand ratio

To analyse the importance of the GDR on the voltage profile along the feeder as well as the disconnection time and sequence of the rooftop PVs, the previous study is repeated (i.e a short-circuit fault is applied on phase-a with IoF = 2 mΩ and LoF = 5) where the GDR is varied from 50% to 200% in steps of 50.

The voltage profile along the feeder for this case is shown in Figure 5.9. This figure shows that for all different considered GDRs, the voltages of all nodes in the faulty phase are very close to each other and all are lower than 10% of the nominal value in the MEN and less than 25% of the nominal value in the NEG system. Hence, it is expected that the PVs within the faulty phase will disconnect regardless of the GDR level. Following fault-occurrence, the voltages of the nodes in the healthy phases rise above the threshold of 110%. These voltages are also very close to each other, and the PVs connected to these nodes will disconnect.

Figure 5.10 presents the disconnection time of the PVs in radar charts. It is seen from this figure that as the GDR level increases, the disconnection time of the PVs connected to the healthy phases reduces. This is valid for both of the MEN and NEG systems. The disconnection time of the PVs connected to the faulty phase does not illustrate a specific trend as the GDR level varies; however, all of the PVs disconnect in less than a cycle after fault occurrence.

Figure 5.7. Voltage profile along the feeder during LG fault between fault-occurrence and the PV upstream circuit breaker tripping for different LoFs.

Figure 5.8. Disconnection time and sequence of PVs after LG fault for different LoFs.
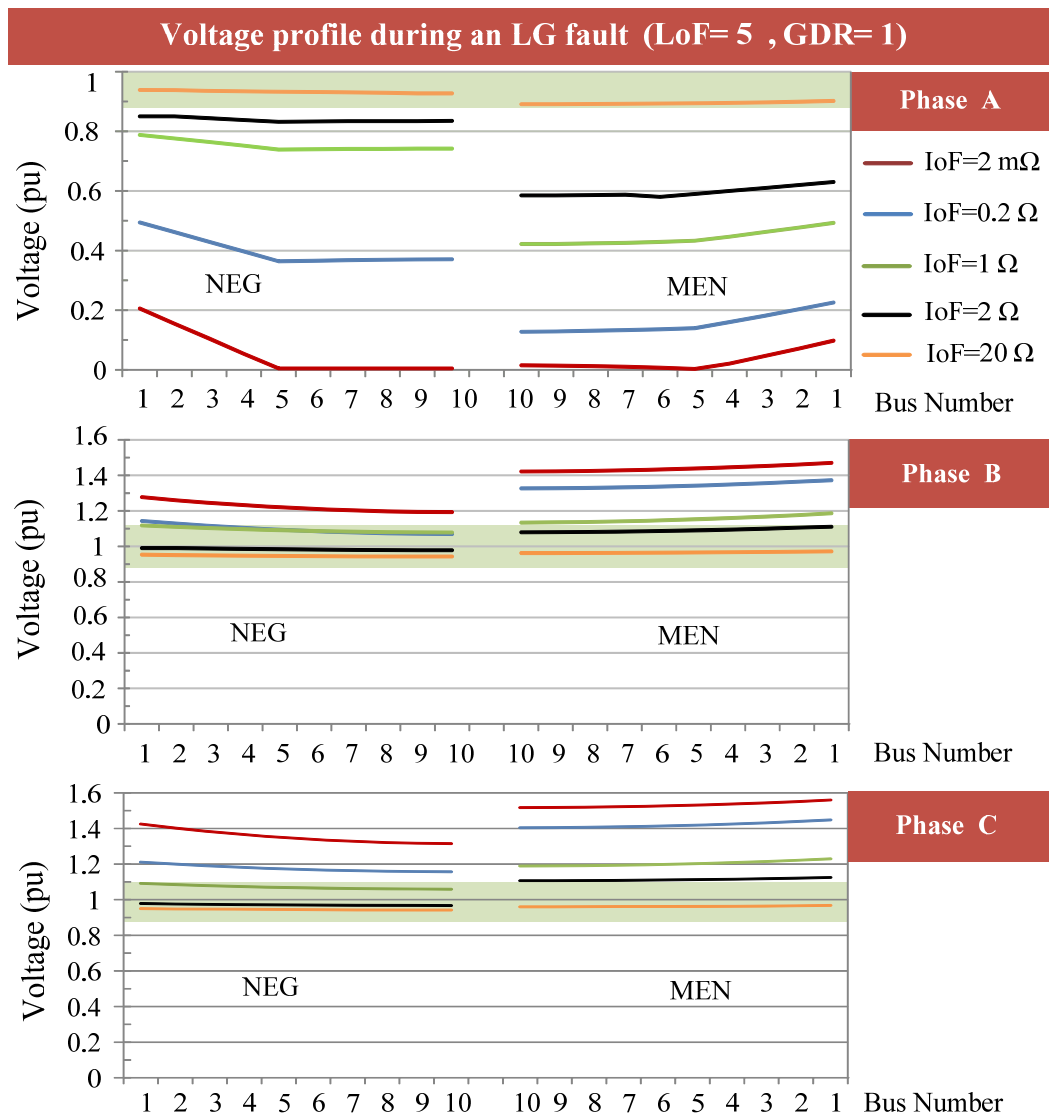
Figure 5.9. Voltage profile along the feeder during LG fault between fault-occurrence and the PV upstream circuit breaker tripping for different GDRs.
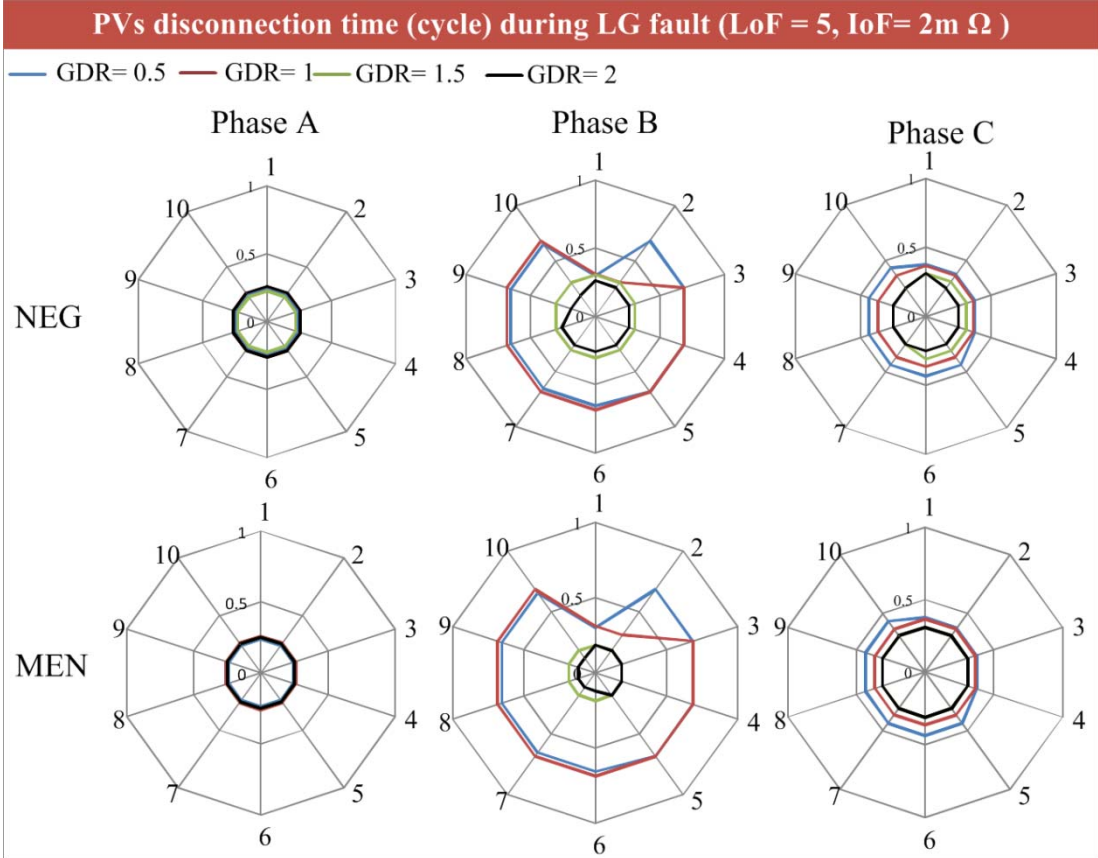
Figure 5.10. Disconnection time and sequence of PVs after an LG fault for different GDRs.

5.4.4 Disconnection of PVs during three-phase faults

This section focuses on the disconnection time and sequence of single-phase rooftop PVs after a three phase fault in the network. Let us consider the network of

Figure 5.1 with the GDR of unity. A three-phase short-circuit fault is applied at LoF = 5 with an IoF = 2 mΩ. The disconnection time of the PVs depends on the time that the voltage of their PCC drops below 88% of the nominal voltage. Immediately after fault occurrence, the voltages of all nodes along all phases drop below 88% of the nominal value; hence, all of the PVs disconnect almost simultaneously in less than a cycle. The upstream circuit breaker opens within two cycles after fault occurrence. The schematic disconnection time of the PVs in the considered study case are shown in Figure 5.11.

This network is now analyzed in details considering different IoFs, LoFs and GDRs. A study similar to Section 5.4 is repeated for this type of fault, as discussed below:

PVs disconnection time and sequence during a three phase fault in MEN network (IoF=2 Ω , LoF=5 , GDR=1)
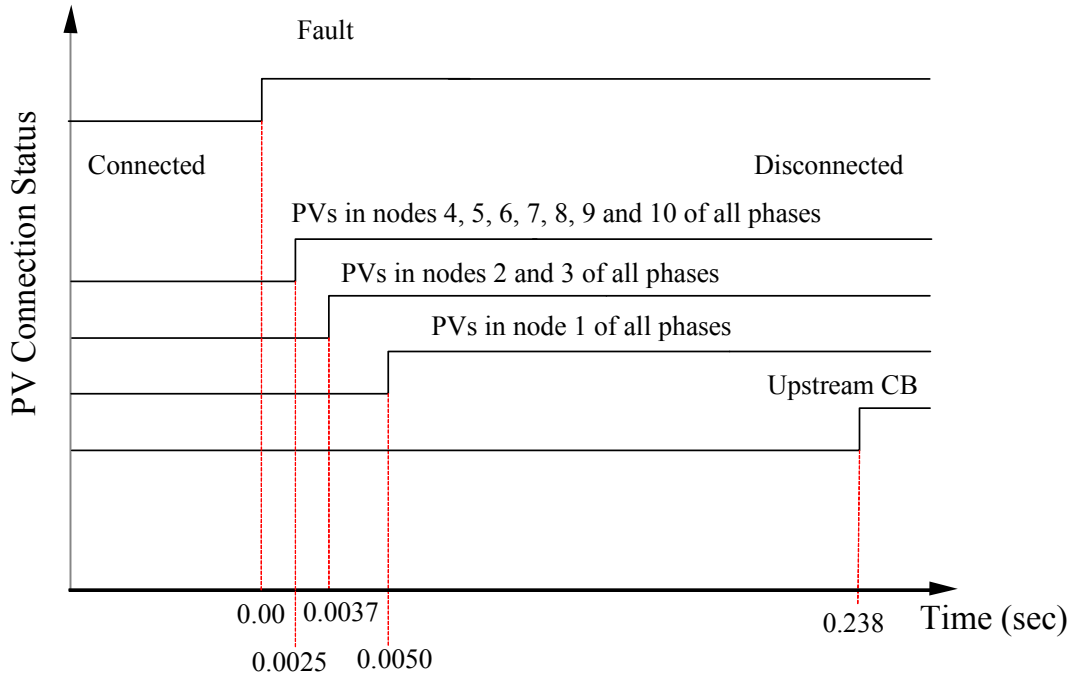
Figure 5.11. Disconnection time of PVs and upstream circuit breaker during a three phase fault.

5.4.5 Impact of impedance of fault

Let us consider again the network of Figure 5.1 with the GDR of unity. A three-phase short-circuit fault is applied at the middle of the feeder (i.e. LoF = 5) where the IoF is varied from 0.002 to 20 Ω. The voltage profile along the feeder between fault-occurrence and the disconnection time of PVs or the opening time of the upstream circuit breaker is shown in Figure 5.11(a). From this figure, it can be seen that the voltage of all nodes in all phases drop below the limit of 88% for all IoFs except IoF = 20 Ω. Hence, all of the PVs in the feeder disconnect after fault-occurrence except the conditions that the IoF is very large. This is valid for both MEN and NEG systems.

99

To examine the disconnection time of PVs and their sequence in presence of different IOFs, the recorded results are represented in the radar chart of Figure 5.12(a). It can be seen from this figure that none of the PVs disconnect when the IoF is higher than 2 Ω. This figure also shows that for each IoF, all PVs in one phase disconnect at the same time roughly (i.e. with almost less than half a cycle difference). Note that Figure 5.12 illustrates the results for phase-A only, but the results are identical for all three phases. It is also worth mentioning that the PVs that are connected to the very first nodes (e.g. node-1 to 2) of the LV feeder may not sense the fault and thus may remain connected even for an IoF = 2 Ω since their PCC voltage does not drop below the 88% limit (see Figure 5.11(a)).

5.4.6 Impact of location of fault

The previous examination is repeated to analyze the significance of the LoF assuming the GDR is unity and IoF = 2 mΩ. The LoF is varied from the beginning of the feeder towards its end. The voltage profile along the feeder for this case is shown in Figure 5.12(b). This figure shows that the voltage of all nodes of the feeder are below the 88% limit for all different LoFs. Hence, all of the PVs in the LV feeder disconnect within less than half a cycle after fault occurrence, as seen from the radar chart of Figure 5.13(b). This is valid for both MEN and NEG systems.
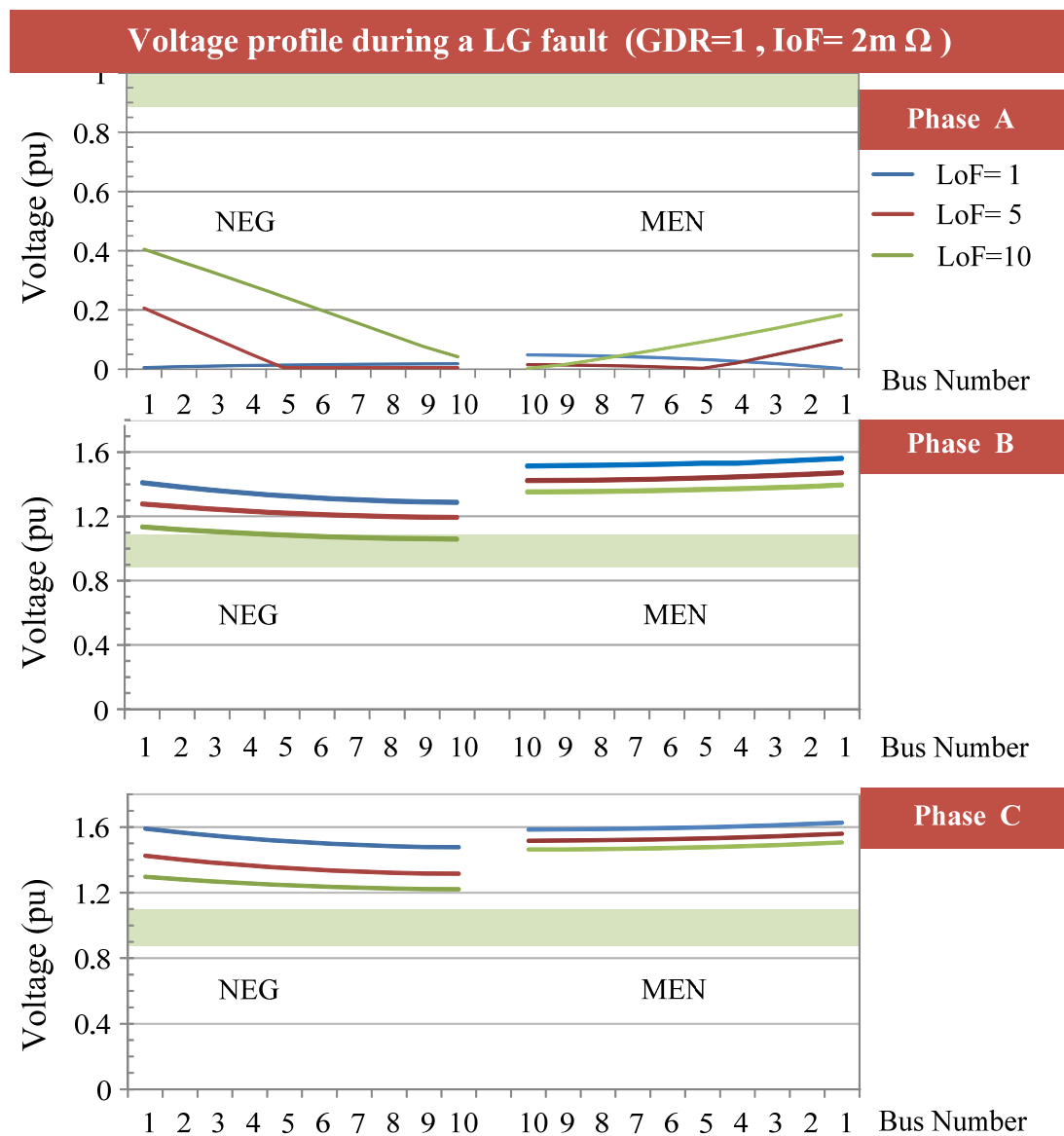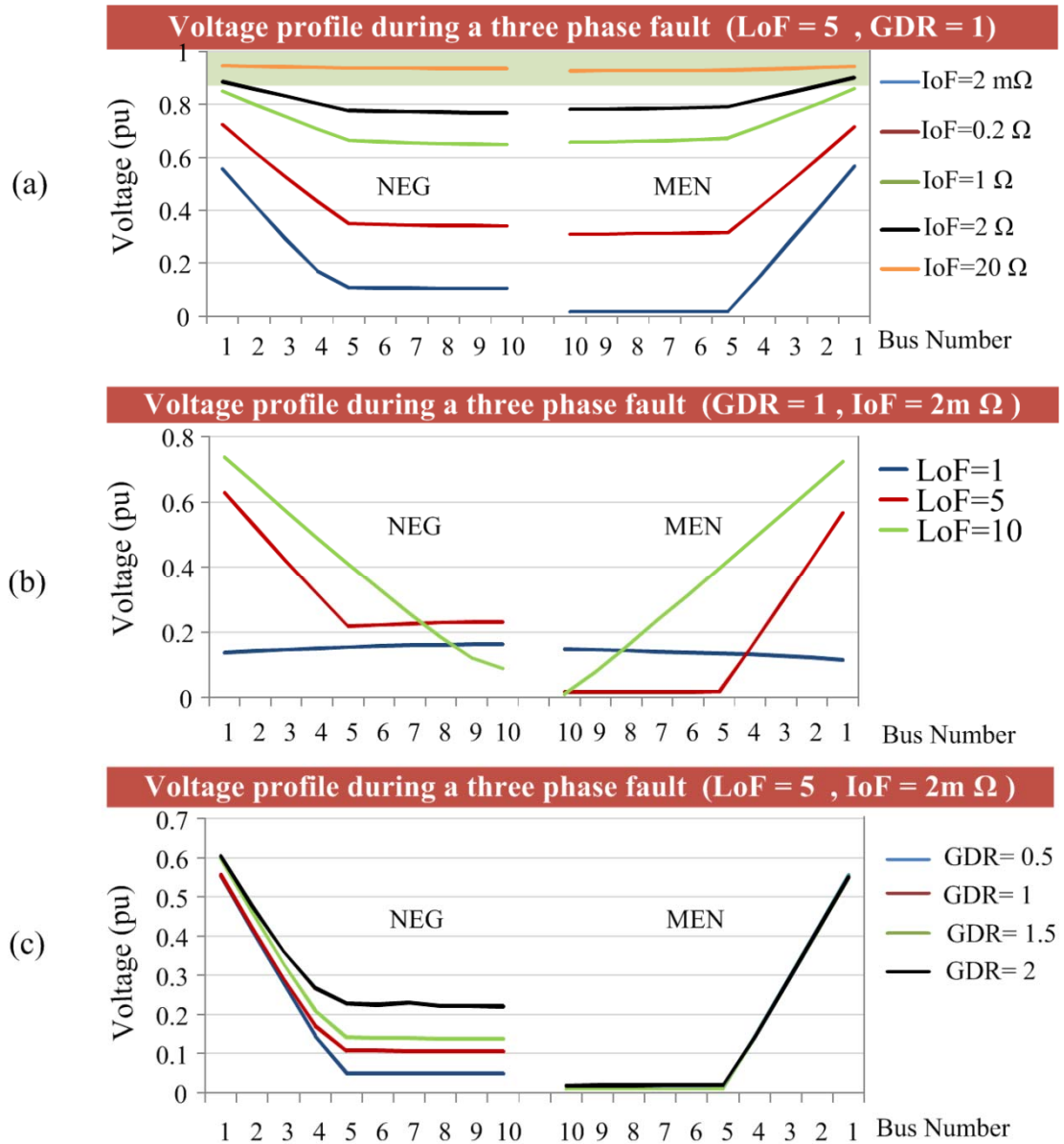
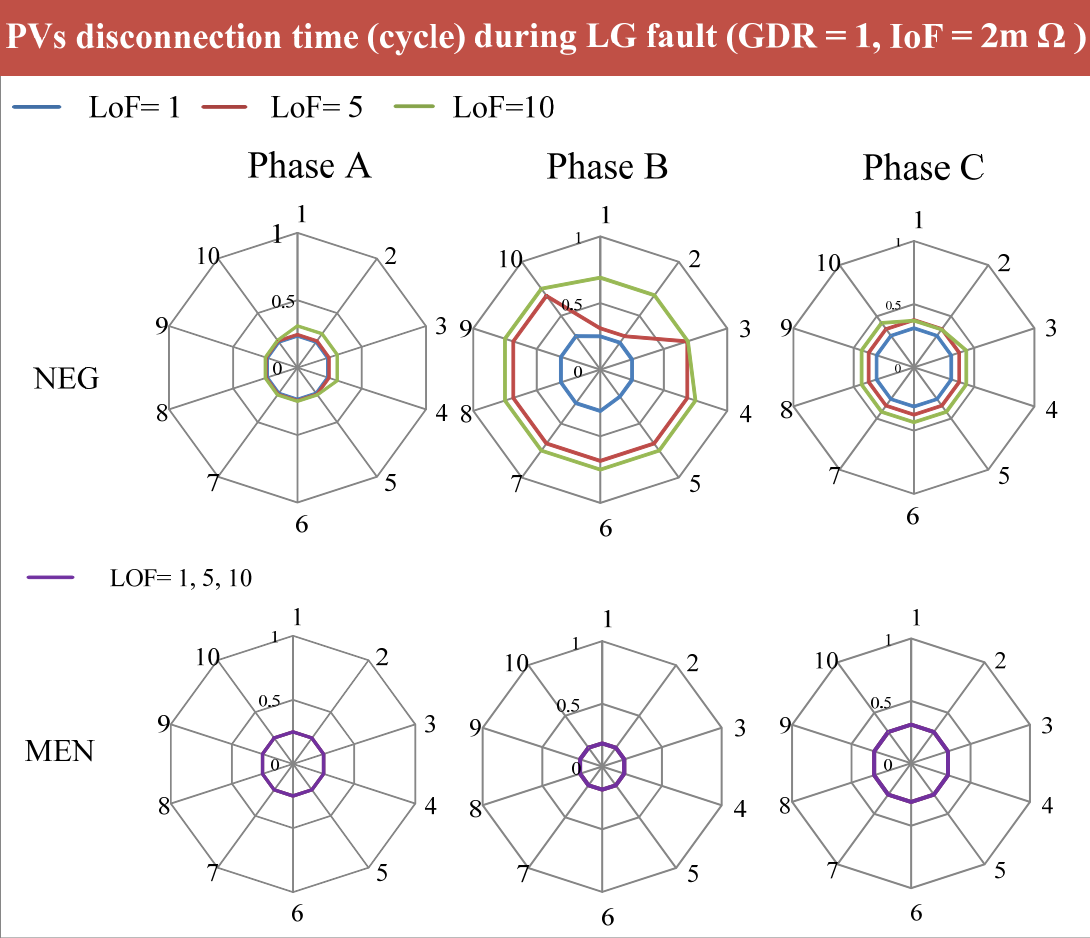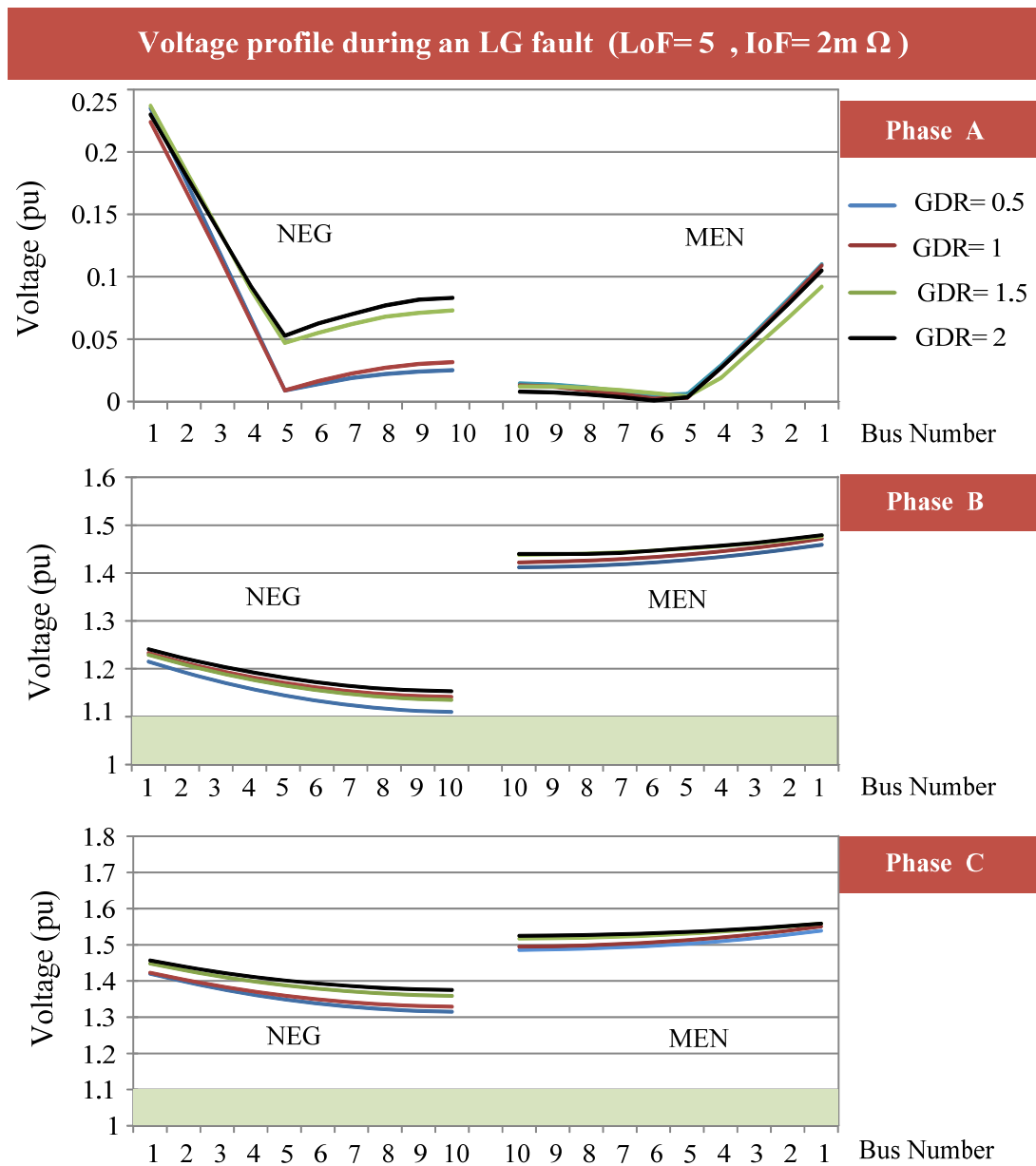Figure 5.12. Voltage profile along the feeder during a three phase fault between fault-occurrence and the PV upstream circuit breaker tripping time for different: (a) IoFs, (b) LoFs, (c) GDRs.

5.4.7 Impact of generation to demand ratio

To analyze the consequence of the GDR on the voltage profile along the feeder as well as the disconnection time and sequence of the rooftop PVs, the previous work is repeated assuming an IoF of 2 mΩ and LoF = 5 where the GDR is varied from 50% to 200% in steps of 50. The voltage profile along the feeder for this case is shown in Figure 5.12(c). This figure shows that for all different considered GDRs, the voltage

of all feeder nodes fall below the 88% limit and thus all PVs disconnect within less than half a cycle after fault-occurrence, as seen from the radar chart of Figure 5.13(c). It is to be noted that in this case, the voltage of the nodes is slightly higher for the NEG system when compared with the MEN system. However, it does not affect the disconnection time of the PVs.
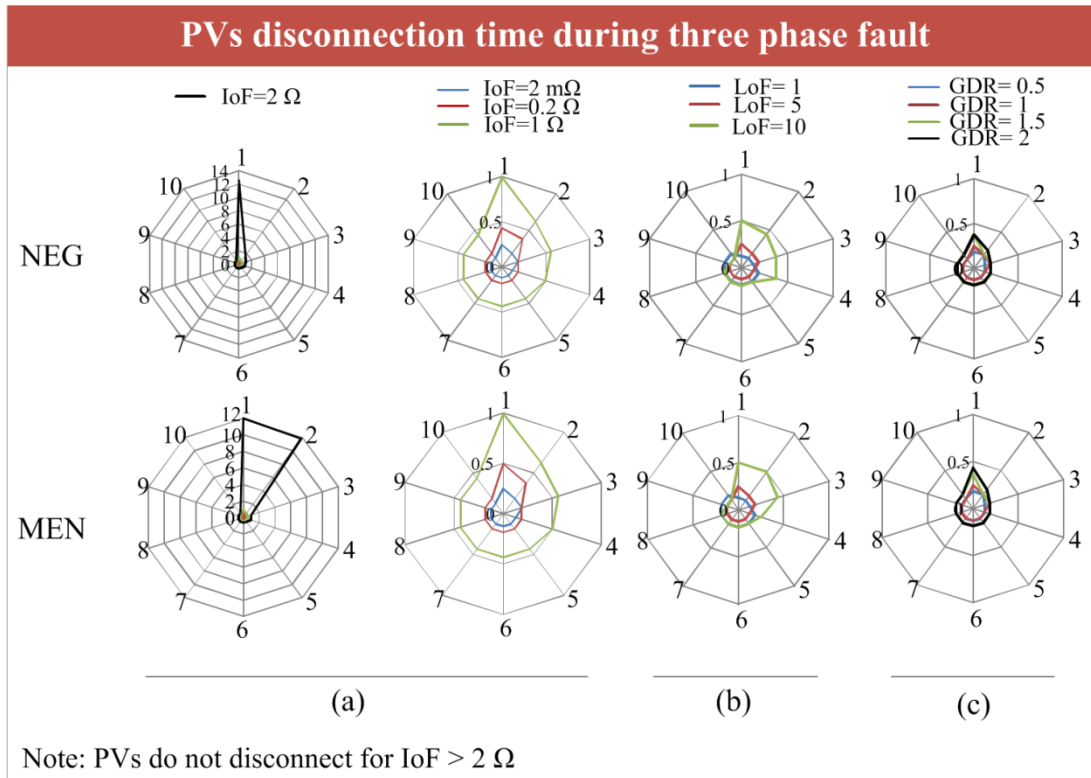
Figure 5.13. Disconnection time and sequence of PVs during a three phase fault for different: (a) IoFs, (b) LoFs, (c) GDRs.

5.5 Extreme conditions

To expand the studies for extreme conditions, the previously studied cases are re-examined under extreme conditions. The objective of this analysis is to determine whether the PVs will be disconnected even under the extreme conditions.

Section 5.4.2 shows that when the LoF is at node 10, the results are more extreme than when the LoF is at node 1 and 5. This analysis was conducted with an IoF of 2 mΩ. This case is re-examined when the IoF is increased to 2 Ω. The results of this analysis are illustrated in Figure 5.14(a). This figure shows that in such an extreme condition, all PVs disconnect successfully in a MEN system while the PVs that are

connected to the end nodes of the healthy phases in an NEG system remain connected until the upstream circuit breaker operates. It is only at this time that those PVs disconnect.

Section 5.4.3 illustrated that when the GDR is 2, the results are more extreme. This analysis was also conducted with an IoF of 2 mΩ. This case is re-examined when the IoF is increased to 2 Ω. The results of this analysis are illustrated in Figure 5.14(b). This figure shows that in such an extreme condition, all PVs disconnect successfully in a MEN system while only the PVs that are connected to the far end nodes of the healthy phases of an NEG system disconnect successfully. Thus, all of the PVs connected to the faulty phase and the beginning and middle nodes of the healthy phases remain connected until the upstream circuit breaker operates, after which they disconnect.

To consider the worst case scenario, another study is carried out which is a combination of all extreme conditions, i.e. the IoF is 2 Ω, GDR is 2 and the LoF is at node 10. The result of this case is illustrated in Figure 5.14(c). This figure shows that all of the PVs in the MEN system disconnect successfully while almost all of the PVs in the NEG system fail to disconnect until the operation of the upstream circuit breaker.

The case of Section 5.5 is re-analysed when the LoF is at node 10 while the IoF is increased from 2 mΩ to 2 Ω. The results of this analysis are illustrated in Figure 5.15(a). This figure shows that in both MEN and NEG systems, only the PVs that are connected to the far beginning nodes of the network disconnect successfully and all other PVs remain connected until the upstream circuit breaker operates.

The case of Section 5.4.3 is also re-analysed when the GDR is 2 and the IoF of is increased from 2 mΩ to 2Ω. The results of this analysis are illustrated in Figure 5.15(b). This figure shows that in both MEN and NEG systems, none of the PVs in the system disconnect before the operation of the upstream circuit breaker.
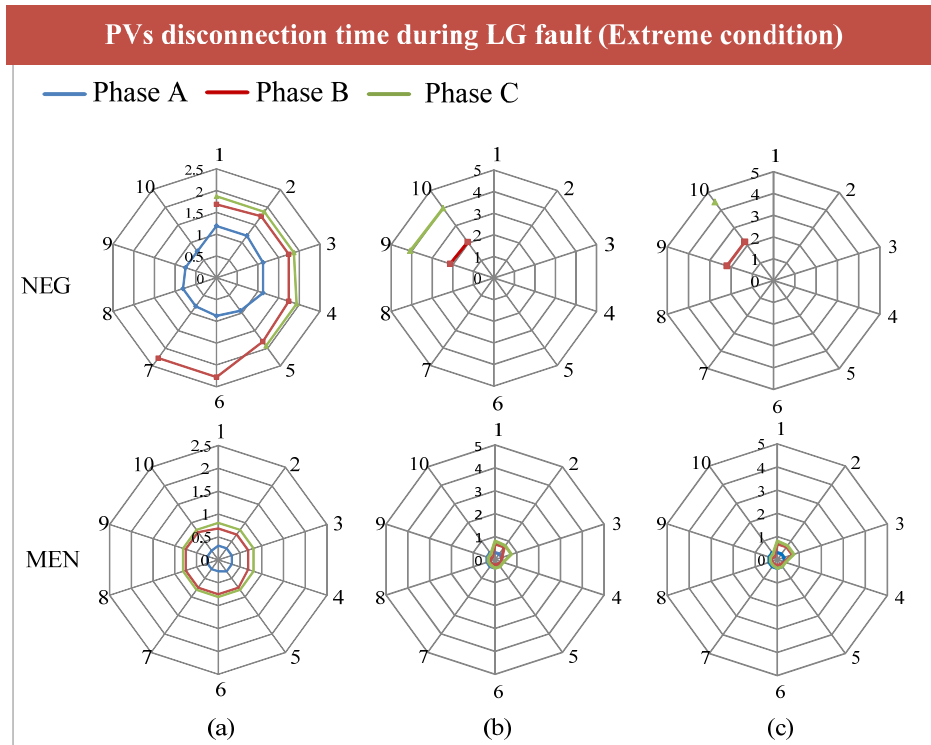
Figure 5.14. Disconnection time and sequence of PVs during an LG fault for some extreme cases: (a) LoF extreme case, (b) GDR extreme case, (c) worst case scenario.
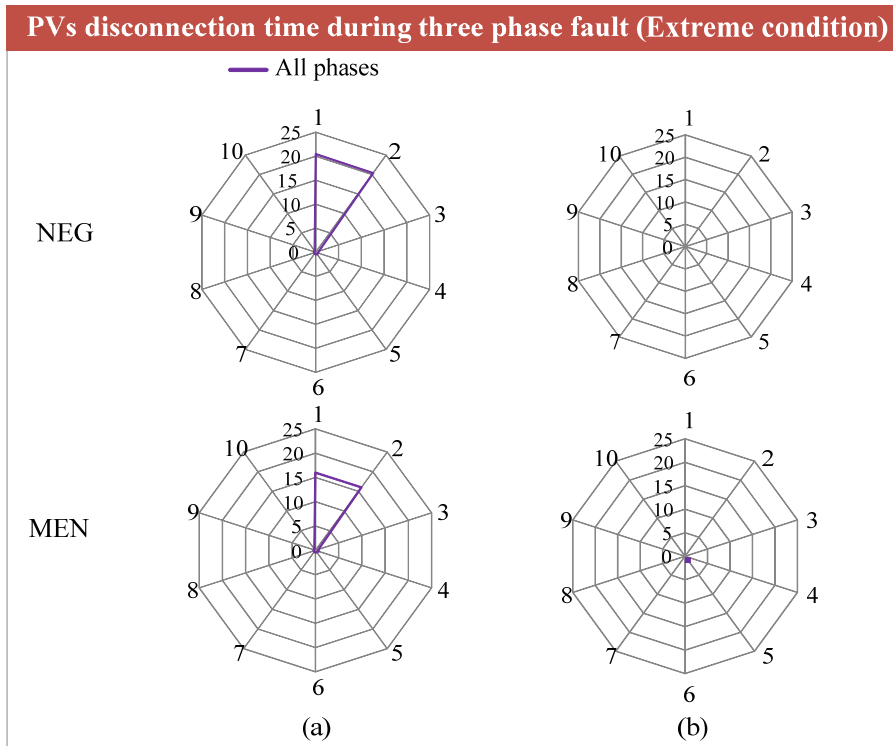
Figure 5.15. Disconnection time and sequence of PVs during a three phase fault for some extreme cases: (a) LoF extreme case (b) GDR extreme case.

5.6 Discussions

The carried out study demonstrates that following a LG short-circuit fault, all of the PVs that are connected to the faulty phase sense the fault and disconnect in an MEN system since their voltages drop below 88% of the nominal voltage immediately, except the cases with large IoFs (e.g. IoF = 20 Ω). However, these PVs may fail to disconnect before the operation of the upstream circuit breaker for an IoF $\geq 2 \ \Omega$, if the GDR is high (e.g. GDR = 2) or when the fault is at the end of the feeder (e.g. LoF = 10).

The results show that except the cases that an LG short-circuit fault is at the beginning nodes of the feeder (e.g. LoF = 1), the level of voltage drop in the MEN systems is much larger than the NEG system. In MEN systems, the PVs of the faulty phase disconnect in less than two cycles after the fault or after the delay time allowed for LVRT, if the fault impedance is small (i.e. less than 2 Ω). It was also revealed that the location of the fault, when varied from the beginning of the feeder towards its end as well as the ratio of the generation capacity of PVs versus the load demand, when varied from 50% to 200%, does not have a significant effect on the disconnection of the PVs in MEN systems. However, they have some effects in the NEG systems and lead to unsuccessful disconnection of the PVs. Moreover, it was revealed that there is a possibility for the PVs that are connected to the faulty phase not to disconnect, if the network is NEG or if the IoF is high (e.g. 20 Ω).

The conducted analysis also demonstrates that the voltages of all nodes along the healthy phases, in the case of an LG short-circuit fault, rise above the nominal voltage immediately after fault occurrence. The level of voltage rise is higher for the MEN systems compared to the NEG system. Once the voltage magnitude rises above 110% of the nominal voltage, the PVs connected to the healthy phases disconnect. The examinations show that this usually happens in less than a cycle after fault occurrence or after the delay time allowed for LVRT. For the healthy phases, it was noticed that the fault impedance has a significant effect on the PVs disconnection. As an example, the results revealed that for fault impedances larger than 2 Ω for the MEN system and larger than 0.2 Ω for the NEG system, the voltage profile along the healthy phases does not rise above 110%. Also, it is revealed that the location of the

fault and the ratio of PVs generation to load demand do not have a strong effect on the disconnection of PVs in MEN systems.

It is to be reminded that the analysis carried out in Section 5.4 assumed a solid grounded system (i.e. an earthing resistance of zero ohms) for the MEN system. When the analysis was repeated assuming a 2 Ω earthing resistance at every earthing point, the variations in the voltage profiles along the feeder did not exceed 3.28 % compared to the zero ohms earthing resistance. Thus, the maximum deviation in the disconnection time of the PVs was less than 10% of a cycle.

The analysis revealed that in the case of a three-phase short-circuit fault, the PVs in all phases disconnect in MEN systems in less than a cycle after fault occurrence or after the delay time of LVRT, since their voltages drop below the 88% limit. However, there are a few exceptions such as when the fault impedance is very large (e.g. 20 Ω), or when GDR is high (i.e., 2) even for an IoF of 2 Ω. It was also revealed that there is a possibility for the PVs not to disconnect in NEG systems.

It is to be noted that the analyses carried out in Section 5.5 assumed a three-phase short-circuit fault. When these analyses were repeated for a three phase-to-ground fault, the variations in the voltage profiles along the feeder did not exceed 25% compared to the three-phase faults. Thus, the maximum deviation in the disconnection time of the PVs was less than 40% of a cycle.

The extreme cases of Section 5.6 illustrate that using PV systems with only under/over voltage protection function may lead to a failure in the disconnection of PV systems from the LV feeder in the case of both MEN and NEG systems during three-phase short-circuit faults.

It was noticed that the PVs that had failed to disconnect based on the under/over voltage protection function will disconnect only when the upstream circuit breaker operates. It was seen that after the operation of the upstream circuit breaker all PVs are disconnected and no islanding issue was observed.

It is worth mentioning that the open-conductor faults were also examined in this research. The studies exposed that the voltage of all the nodes in the downstream of the open conductor point drop below the 88% limit immediately after fault occurrence; thus all of the PVs that are connected to those nodes disconnect. This is

only observed for the faulty phase, and no problem arises in the healthy phases or the upstream of the fault point of the faulted phase.

Chapter six will focus on effects of PVs installation on medium voltage distribution network and its protection system. However the method of study will be different from chapter four as the protective devices in MV network are different with LV one. However, the influential factors still are more or less same. Furthermore, the effect of PVs on coordination of main and back up relays has been scrutinized and the variation of high impedance fault threshold as a result of increase in PV penetration level has been studied in next chapter.

5.7 Summary

This chapter investigates the disconnection time of single-phase rooftop PVs following a single-phase or a three-phase short-circuit fault on the low voltage feeders. The research focuses on a three-phase, four-wire low voltage feeder, with 100% PV penetration. Several parameters are contemplated including the location of the fault, the impedance of the fault and the ratio of the PVs generation capacity to the load demand. Moreover, the influence of the network earthing system is also investigated.

The analysis reveals that for a MEN system, during a single-phase short-circuit fault, the PVs in the faulty phase sense the fault and disconnect immediately in less than a cycle after fault-occurrence or after the required delay time for LVRT since the voltage of their PCC drops below the limit of 88%. Similarly, the PVs located in the healthy phases sense the fault and disconnect as the voltage of their PCC rises above the 110% threshold. An exception is when the fault impedance is relatively large (e.g. 20 ohms or more). However, if the LV feeder is not effectively grounded, there are situations in which the PVs may not disconnect.

The study also discovered that in the case of three-phase and three-phase-to-ground faults, depending on the system earthing type, the location and impedance of the fault and the ratio of the PVs generation capacity versus the load demand, there are situations in which the PVs do not disconnect following the fault. These PVs

remain connected until the upstream circuit breaker operates, after which they disconnect successfully.

There may be situations in which the PVs fail to disconnect and continue to feed the fault until the upstream circuit breaker operates. These situations are more probable in NEG systems or when the fault impedance is high in MEN systems. Thus, only utilizing the under/over voltage protection function will not guarantee the successful disconnection of PVs in such situations. Hence, newer fault detection algorithms should be developed and evaluated for rooftop PVs which can sense the fault and disconnect the PVs, irrespective of the fault impedance, network earthing type and the PV penetration level, before allowing higher PV penetration levels in LV feeders.

Chapter 6. PV Penetration Level Impact on Protective Devices of MV Distribution Network

6.1 Introduction

In last three chapters, the effects of PV and different penetration levels on LV distribution networks and its protection system was discussed. In this chapter the analysis of PVs impact on MV distribution system protective devices will be presented. As it was discussed in chapter one, some papers have paid attention to effects of PV plants on distribution networks in MV level. However they have made some basic inappropriate assumption in their procedure, and these wrong assumptions have made a strong impact on their results. For example, reference [36] has considered the fault impedances in their study much bigger than its real values and hence the results have been affected significantly. Hence, to have a precise and comprehensive study on the impact of PV penetration on protective devices at MV level, dynamic fault impedance will be applied which presents more accurate results in fault analysis.

Another point that will be clarified in this section is the impact of penetration level of PVs on normal load current of the feeder and its impact on pick up current of relays in overcurrent protection. In addition, the effect of loading and demand in the network together with penetration level on pickup current of relays are discussed in this chapter. Also, the time difference variation between main and backup relays will be investigated in the presence of various PV penetration levels.

This thesis tries to fill this gap and makes the impacts of high penetration of single phase PVs on MV distribution network clearer. To this ends, the research will cover the following points;

- The impact of PV penetration level and demand ratio on normal current of relays installed on the residential feeder.

- Analysis of PV penetration level impact on high impedance fault threshold and fault detection success rate without high impedance relays.

- Implementation of dynamic impedance fault to simulate the fault conditions to make the results more precise and realistic.

- Presenting the difference of the analysis results in the presence of bolted faults and simulated dynamic arc impedance.

- Analysis of PV penetration level impact on operation time difference of the main and backup relays. (to monitor whether the coordination time interval is lost or not)

6.2 Case study network

In this chapter, an MV distribution network has been selected to be the study case. This network similar to many of distribution networks has the radial structure. This network includes one (132:11 Kv) transformer with rating of 3 MVA and twelve (11:0.415 Kv) distribution transformers with rating of 200 Kva and each LV transformer is feeding the 30 houses. The distribution transformers are usually in the range of 25 to 630 kva, and the LVFs are 400 meters long, distributed through 10-12 poles, with a distance of 30-40 meters from each other. In fact, this is the typical Australian residential network and each house consumes about 4.4 kva as a maximum power that one specific house needs. The rating of transformers and other specification of the network are presented in Table 6.1. Schematic diagram of this network is shown in Figure 6.1. The network is simulated in PSCAD software.

The residential rooftop PVs in Australia are single-phase units (composed of PV cells, inverters, and disconnectors). They have a nominal rating of 1-5 kW (depending on the financial status of the householders). The number of rooftop PVs connected to each phase of the system is random as the utilities do not have a regulation for balancing the number of rooftop PVs among the phases when

Table 6.1 Specifications of MV network under study.

Substation Transformer: 3MVA, 132 Kv/ 11 Kv, 50 Hz, Dyn-type
Distribution Transformer: 200 Kva, 11 Kv/ 415 V, 50 Hz, Dyn-type, Z = 5%
MV feeder: 11 Kv L-L rms, 8 km, ACSR 50 mm^2 bare conductor, three-phase three-wire system, $R = 2.16$ Ω/km, $X = 2.85$ Ω/km [37]
LV feeder: 415 V, 400 m, AAC 75 mm^2 bare conductor, three-phase four-wire system with ABCN horizontal configuration on 120 cm crossarms [58] and a total of 400 meter length, 10 nodes with a distance of 40 meter from each other, $R = 0.452$ Ω/km, $X = 0.27$ Ω/km [37]
PV systems: PF = 1, η =100 %, Imax at Fault = 150% Irated
Residential Demand: Single-phase constant-impedance loads, ($S = 4.4$ Kva in 100% of loading), PF = 0.95 lagging

approving the connection of a rooftop PV to the system. The output current of the PV systems are equipped with a current limiting technology and protection fuses which limit their output current to 1.5 times of their nominal current [22]. The simulated MV network in this chapter consists of two relays (R1 and R2). R1 is the upstream relay in the main branch of network and R2 is the downstream one. These relays have been shown in Fig 6.1.

6.3 Impact of PV penetration on relays coordination

PV penetration level plays a major role in determination of current passing through lines in the distribution network. As these energy resources play as a current source, there is a possibility for them to feed the fault if they do not become disconnected from the network. Considering this fact, the impact of different levels of PV penetration on protective devices such as overcurrent relay which is the main protection responsible in MV distribution networks and also works based on measurement of passing current from relays is vital. In this chapter, the effects of PV penetration on relays are discussed in two main parts. The first impact of them on relays in normal operation mode and second part pays attention to operation and coordination of relays at fault condition.

6.3.1 PV penetration impact on relays current at normal operation

As the PV penetration level goes high in the distribution network and the generation from these resources increase, the balance of current at network lines is disrupted, and another combination of voltages and currents become dominant on the network according to Kirchhoff laws and basic load flow rules. The relays setting are designed and set for a normal and without PV condition. So in the case of appearance of many PVs in feeder the current equations will change and this time in normal operation state the relays will sense different current than previous state.

However, if this normal current in the new state exceeds the relay pickup current, it leads to operation of the relay in normal mode and without having a fault in the system the relays will disconnect the feeder. This does not mean anything but losing a big portion of the network and residential houses unnecessarily.

As it is known to investigate the impact of one parameter on relays in normal operation condition, it is important to pay attention to pick up currents of relays. Because when relays sense greater current than their pick up value, they will trip. However, the pickup current in overcurrent relays usually is set to 1.25 times of the load current passing from relay at installed point. On the other hand, the loading of network and the value of power which is consumed in residential houses in this network is another key factor to determine the current that passes from relays. So in this research, the value of loading is considered in analysis and in different rates of loadings the calculation and simulation are run. In fact, in this research the value of loads changes in steps of 25% from 25% to 100% of distribution transformers nominal ratings and the results for all four states are given here.

The pickup current of relays is set in NOPV mode and the presence of maximum possible loads at the network. So to determine the load current and accordingly pickup current of relays first the case with a loading rate of 100% is presented.

Table 6.2 shows the values of load current at the point of relay 1 and 2 during 100% of loading. As it is seen from this table as PV penetration level goes high, the nominal load current which passes from relays is decreasing. The table shows that in NOPV case the pickup current of R1 is selected as 156 A in R1 and 52.5 A in R2.
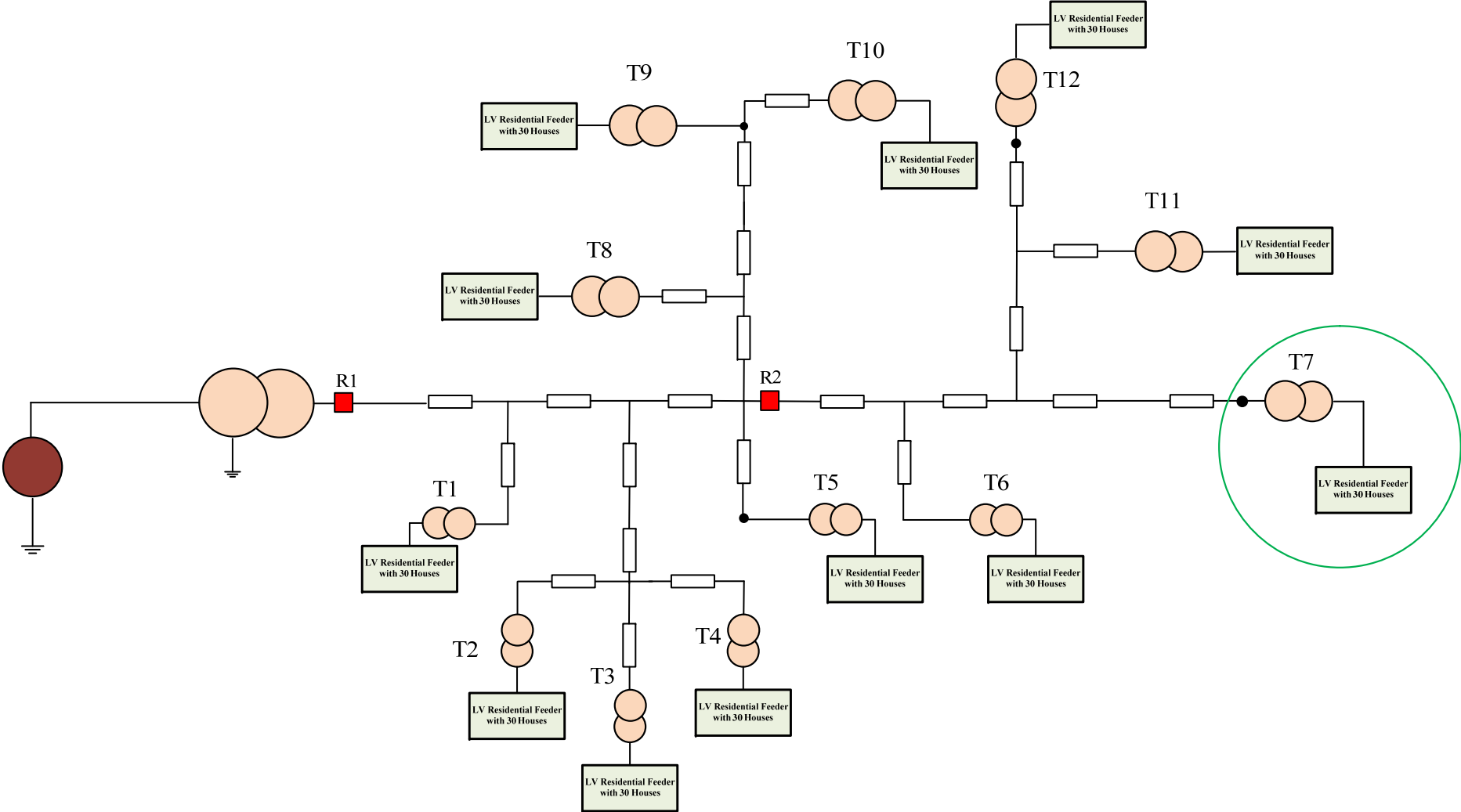
Figure 6.1 Simulated MV distribution network.
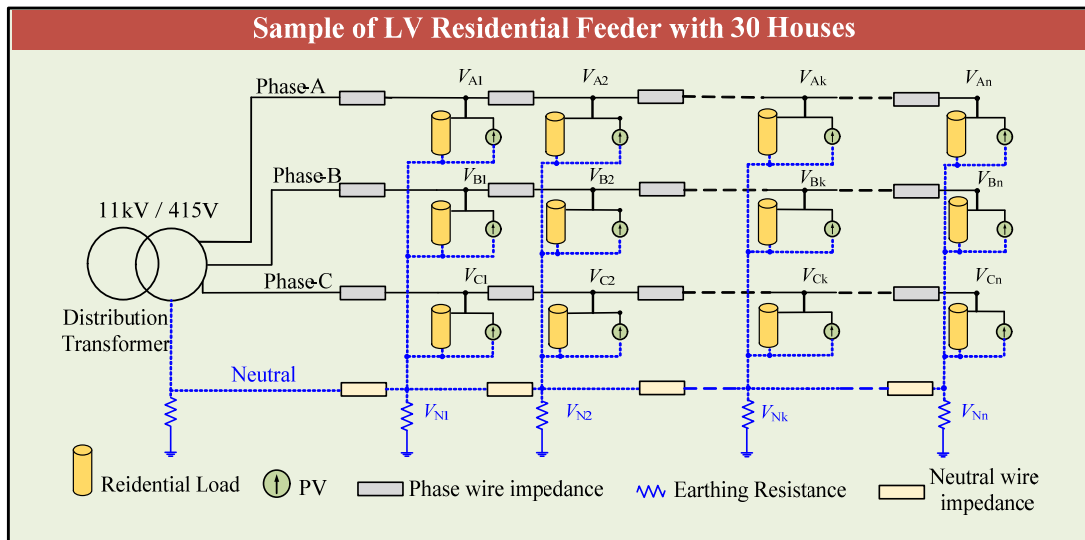
Figure 6.2. A sample of residential LV network feeding by each distribution transformers showed at Figure 6.1.

These are the setting for relays in reality and all distribution networks protective settings are made with the assumption of no PV available in the network. Accordingly, the Figure 6.3 shows the chart of results for Table 6.2.

The same analysis is carried out for penetration level of 75%, and the results for relays current and their pick up current are presented in Table 6.4. It is seen that as PV penetration increases from zero to 80% the currents of relays decrease. In the case of increase in PV penetration level to beyond the 80%, it starts to grow even when it gets to 100%. This fact shows that the minimum relays current appears in case that the PV penetration level becomes equal to loading rate and this can be verified in last table which was the results of 100% of loading. So the Figure 6.4 which shows the relevant values of Table 6.3 tells us that under the condition of 75% loading the relays current never reaches to pick up currents of relays and this means that in this condition the penetration level will not be a case even in 100% of it.

Repeating the same process for loading of 50% is giving the below results which have been presented in Table 6.4 and reflected in Figure 6.5. Again this result confirms the conclusion that we made in last part. It shows that the relays current decrease as PV penetration goes high till it gets equal to loading percentage. Then increasing the PV penetration more than loading rate will cause the increase in relays

Table 6.2 Load current of relays in different penetration levels at 100% of loading.

Load currents of relays for various PV penetration level 100% of loading (A)		
PV Penetration level	Load current (R1)	Load current (R2)
NOPV	125.0	41.6
20%	101.8	33.8
40%	79.5	26.3
60%	59.7	19.7
80%	45.3	15.0
100%	41.9	13.9
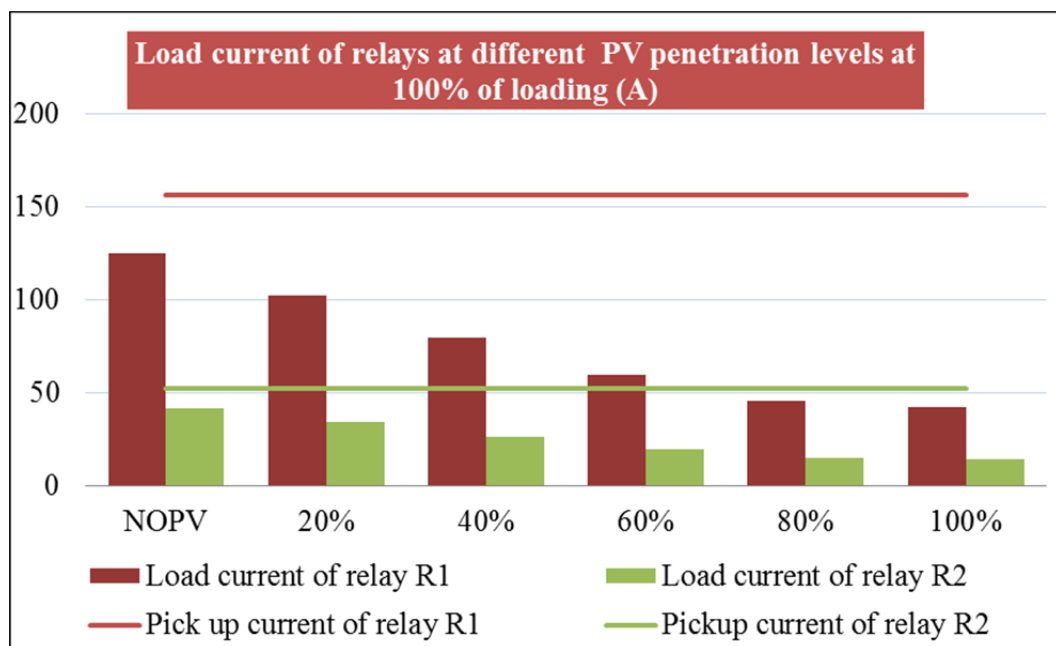
Figure 6.3. Load current of relays in different penetration levels at 100% of loading.

load currents. So according to this finding it is clearly seen that the minimum relay current is achieved at 50% of PV penetration level (from Table 6.4) as the loading rate is 50% in this case.

Table 6.3 Load current of relays in different penetration levels at 75% of loading.

Load currents of relays for various PV penetration level at 75% of loading (A)		
PV Penetration level	Load current(R1)	Load current(R2)
NOPV	91.4	30.3
20%	69.1	22.9
40%	48.6	16.1
60%	33.0	11.0
80%	30.3	10.1
100%	43.4	14.4
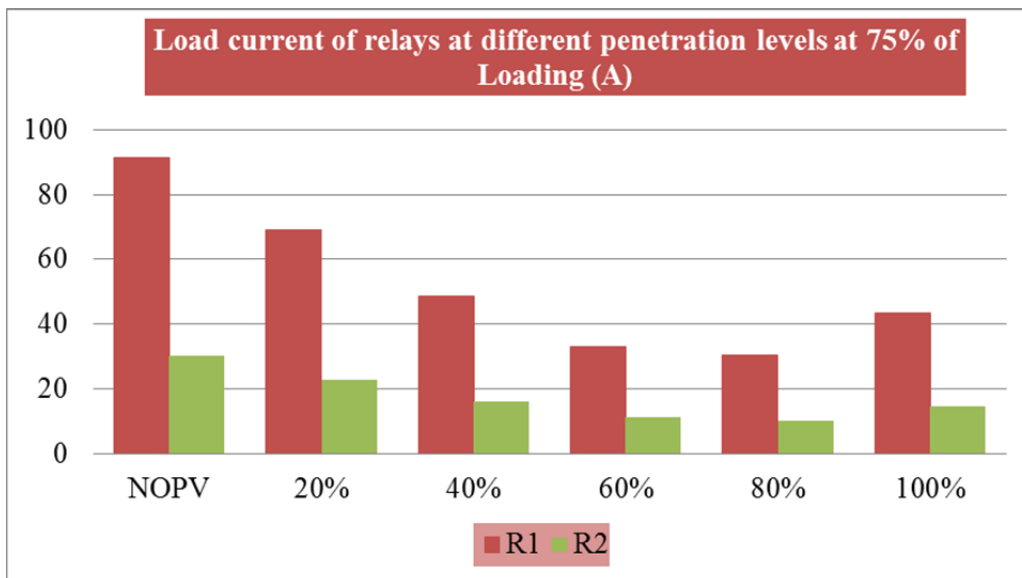
Figure 6.4. Load current of relays (R1, R2) for various penetration levels at 75% of loading

As the last step in this analysis, the simulation is run for loading rate of 25% and the results are tabulated in Table 6.5. The results also are shown in Figure 6.6. This figure indicates that the minimum relay current is observed when the PV penetration level is 25% and it is equal to loading rate.

Also, it shows that in any penetration level the relays current does not exceed the pickup current at 100% of loading rate (156.2 A for R1 and 52A for R2) and it does not bring any protection problem. As it can be seen from Figure 6.6 for all penetration levels, the normal operation current at relays connection point stays under the pickup current. (156.2 A for R1 and 52 A for R2)

Table 6.4 Load current of relays in different penetration levels at 50% of loading

Load currents of relays for different PV penetration level at 50% of loading (A)		
PV Penetration level	Load current(R1)	Load
NOPV	61.7	20.5
20%	40.0	13.3
40%	23.1	7.7
50%	20.5	6.8
60%	24.1	8.0
80%	41.3	13.7
100%	63.4	21.0

Figure 6.5. Load current of relays (R1, R2) for different penetration levels at 50% of loading

Table 6.5 Load current of relays in different penetration levels at 25% of loading

Load currents of relays for different PV penetration level at 25% of loading (A)		
PV Penetration level	Load current(R1)	Load current(R2)
NOPV	31.5	10.5
20%	12.4	4.1
40%	20.8	6.9
60%	42.4	14.1
80%	64.9	21.5
100%	88.7	29.4

117
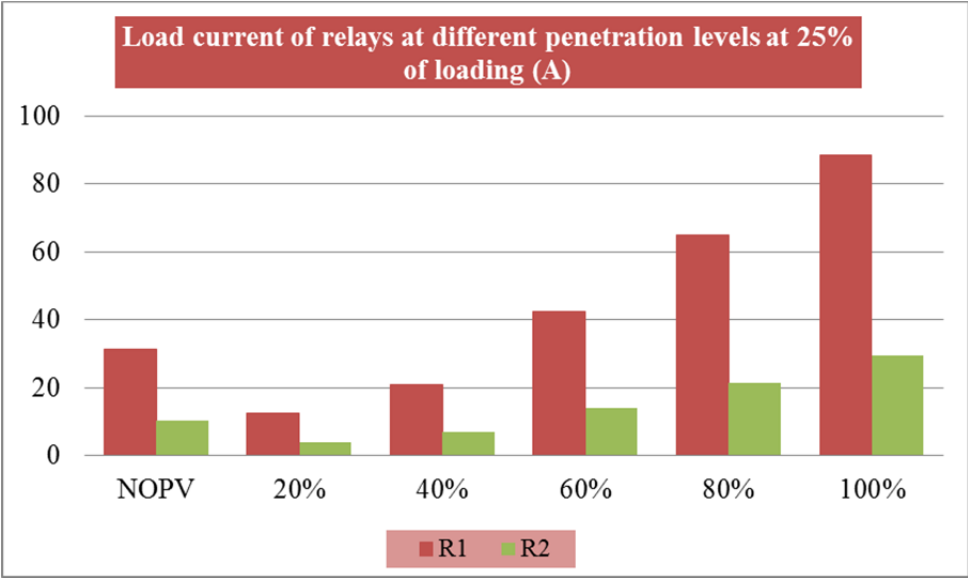
Figure 6.6. Load current of relays (R1, R2) for different penetration level at 25% of loading

Doing the four analysis for different loading rates, gives us the opportunity to show the results in one frame to compare the effect of PV penetration and loading level on relays current at the same time. Figure 6.7 and Figure 6.8 are presenting the results for relay R1 and R2 respectively. It can be seen from these figures in each loading rate, as the PV penetration level goes high the relays current decreases till the penetration level become equal to loading rate and at that point, the relays current is the minimum. Increasing the PV penetration beyond the selected loading rate results in an increase of relays current. In brief the more the difference of PV penetration level (generation of power at PVs) and loading rate (consumption of power at houses), the more the relays current at the main feeder.

According to achieved results, the current of relays are varying with a difference of generated power by PVs and consumed power of loads at the network. So let's name it Generation and demand difference (GDD) factor and the Figure 6.9 shows the result of the relay R1 current regarding GDD. In this figure GDD changes from -75% to +75% and as it is seen the minimum current of the relay is observed when the GDD is zero. As GDD increases or decreases (variation in any direction from zero) the relay current increases.
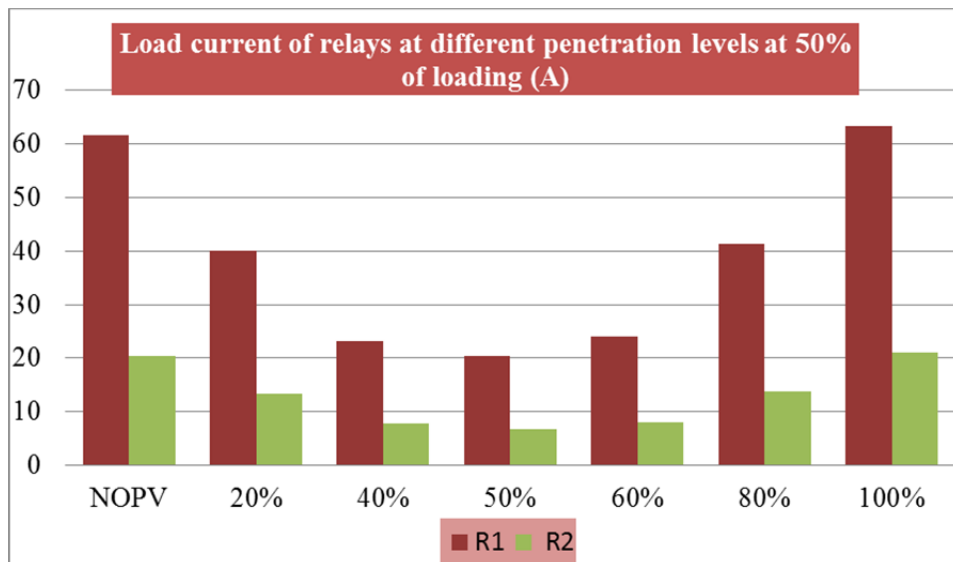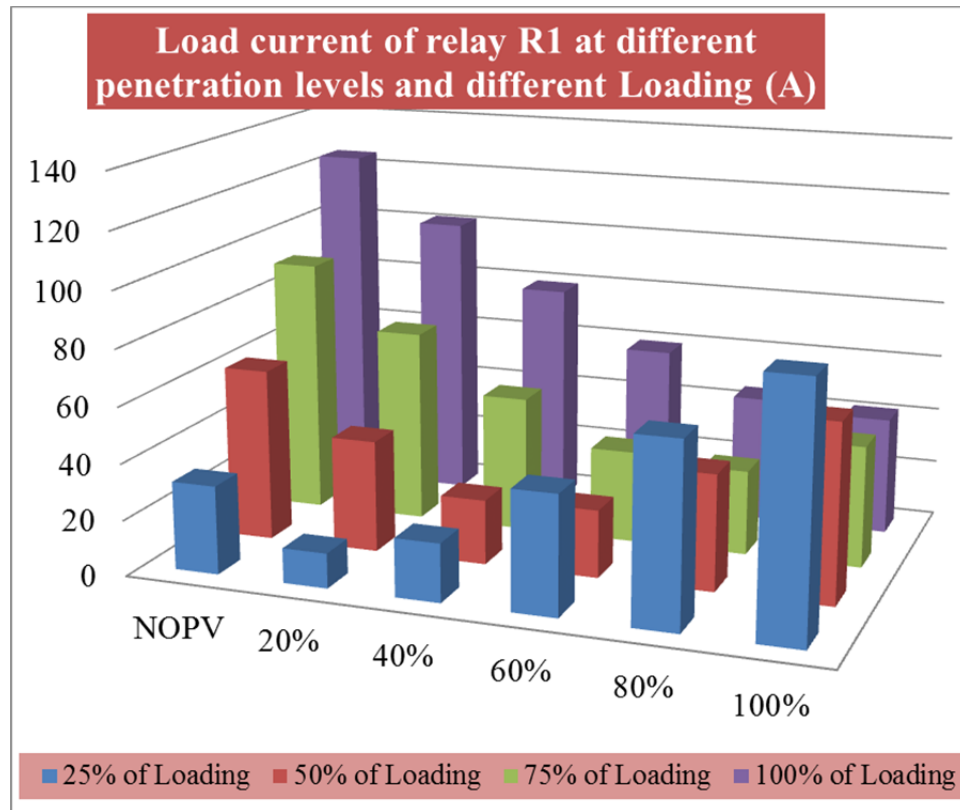
Figure 6.7. Load current of relay R1 in different penetration levels and loading.
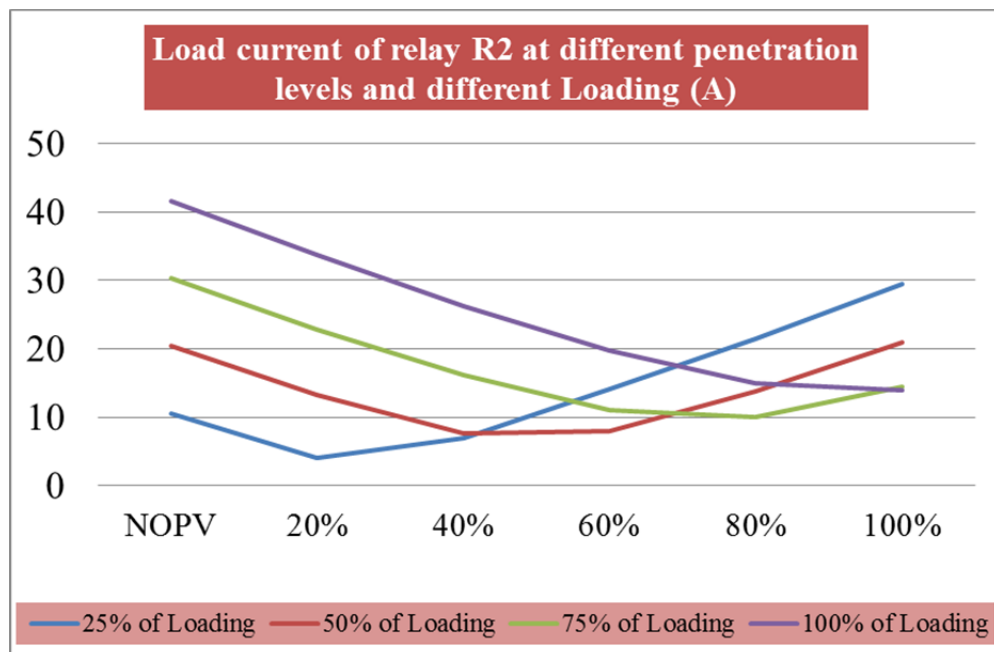
Figure 6.8. Load current of relay R2 in different penetration levels and loading.
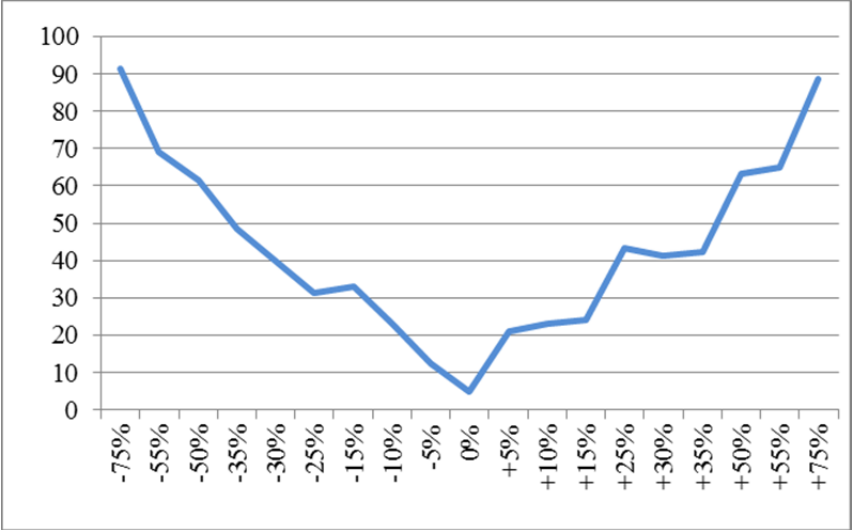
Figure 6.9. Variation of relay R1 current in terms of GDD variation

This fact shows that to consider the effect of PV penetration on protective devices in the distribution network, not only we have to pay attention to PVs generation but also considering the power consumption level in load side is a must. So it is necessary to know what the load profile in the network is when we are designing the protection system of it. On the other hand to protect system properly the worst case of loading should be taken into account.

Actually, according to this study, the worst case happens when the loading and generation level are far different. To achieve the amount of loading that lets us to increase the penetration level up to 100% without having any concern about relay pickup current the simulation has been run in different levels of loading in presence of 100% of PV penetration. The results show that the increasing the PV penetration level will not make a problem for relays in normal operation mode. It means that if the relays pick up current is set appropriately in loading maximum state and NOPV mode, for all other states of penetration level and loading, the load current will be less than pickup current of relays, and it will work well. So there is no worry in these situations about the penetration level.

6.3.2 Impact of PVs distribution along the MV feeder on relays current

Considering the results achieved in previous section, the problem is exceeding the nominal load current from specific penetration level onward in relay than its pick up current. This problem appears only in MV network, and as it was discussed in past chapters, it never occurs on LV networks. So one of the ideas to improve or change this situation is the rearrangement of PV included LV networks along the MV feeder to investigate the effect of the different distribution of PVs on relay current. In this study, this has been carried out in three different penetration levels. 25%, 50%, and 66% are the selected penetration levels to end this.

In this part, the whole of the MV feeder is divided into two main zones. The first zone is the area between two relays and the second area is covering the LV networks which are connected in downstream of R2. Figure 6.10 shows these two zones. There are 12 LV networks are feed from this MV feeder. So when the penetration level is 25%, it means that a quarter of LV networks are equipped with PVs. So, 3 LV networks out of 12 should be selected as a nominee of being PV equipped. The whole possible states to divide three networks into the two types of zones are four
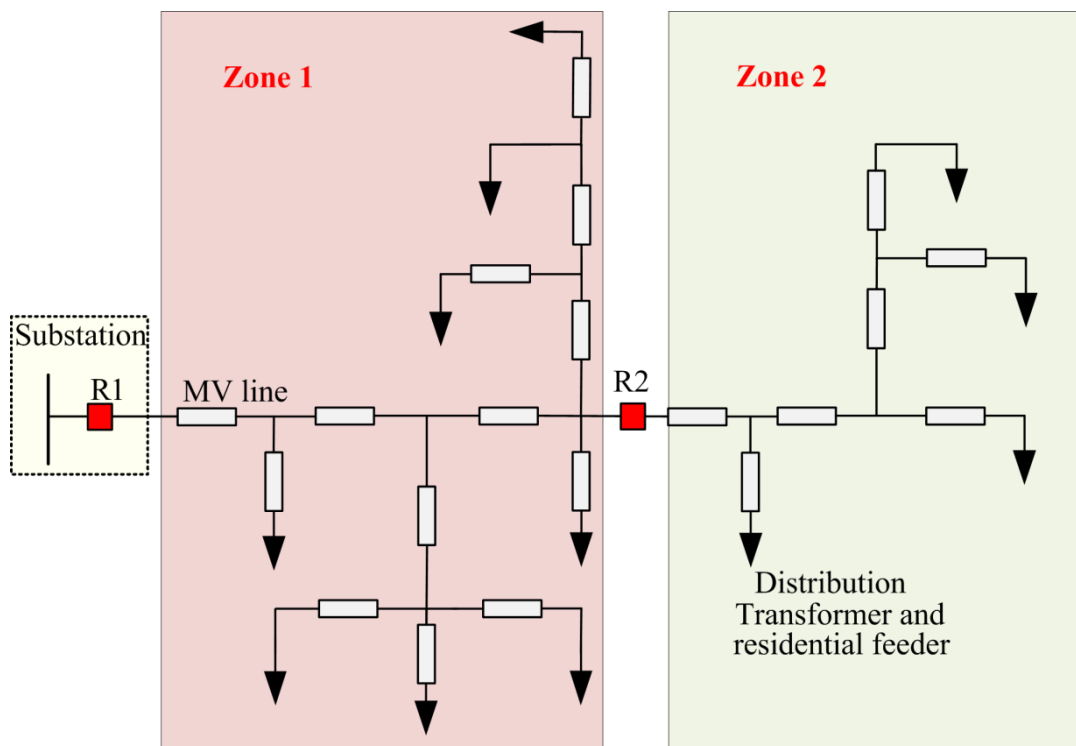
Figure 6.10. Selected zones for PV distribution along the feeder in studied

States, which are 3-0, 2-1, 1-2 and 0-3, configurations. The first digit represents for a number of PV equipped LV networks in the first zone and the second digit is showing the number of PV equipped LV networks located in the second zone. These states for 50% and 66% of penetration level will be 7 and 9 respectively and are shown in horizontal ax of Figure 6.11.

As it is seen from Figure 6.11 the different configuration of PV included networks along the MV feeder can result in various load currents in relays location. In this figure the blue line represents the pickup current setting of the relay in NOPV mode. The yellow bar chart shows the load current at relay location when the penetration level is made by the evenly distribution of PVs among all LV networks. The green bar charts represent the states that the load current sensed by relay gets lower than relays pick up current. So these are the pleased States from protection viewpoints. However as it can be seen just considering the R2 condition, penetration level can increase even up to 66% and more if the PVs are distributed appropriately among the LV feeders. For example, the relay load current still can stay less than pick up current when the PVs are distributed in forms of 6-0 or 8-1 between two zones in 50% penetration level or in the forms of 8-0 or 7-1 between two areas in 66% of PV penetration level.
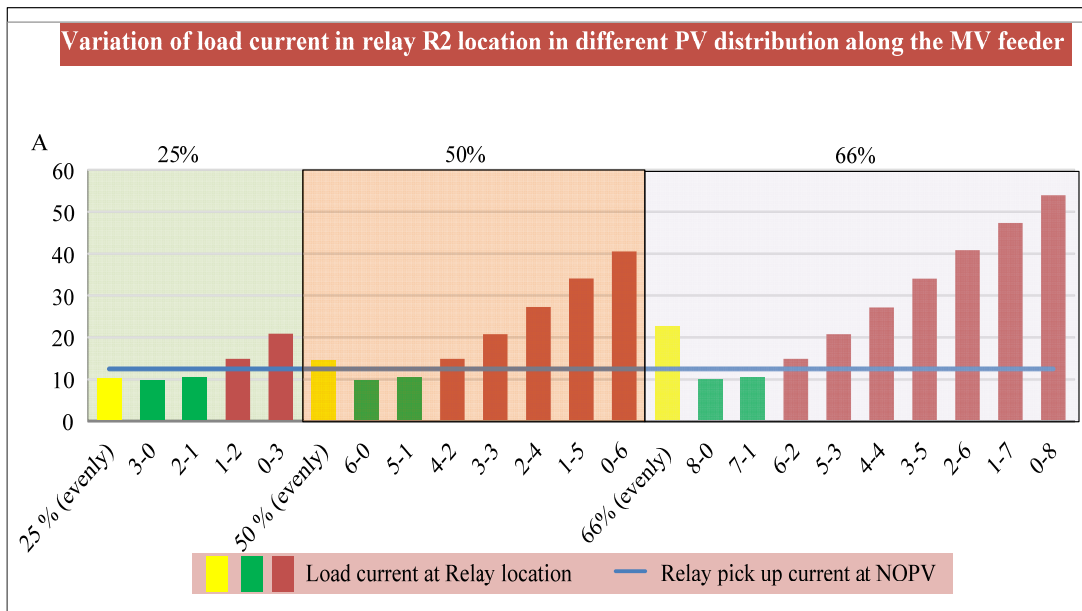
Figure 6.11. Load current at relay R2 location in different arrangements of PVs along the MV feeder.
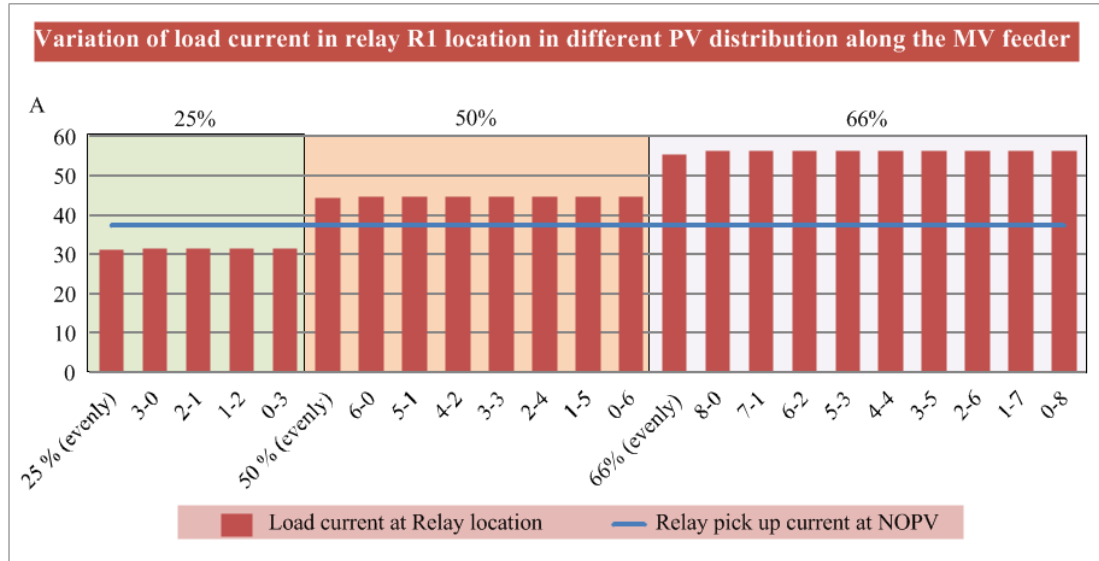
Figure 6.12. Load current at relay R2 location in different arrangements of PVs along the MV feeder.

However, for protection judgment, it is not fair that just rely on one relay condition. Considering the status of load current in R1 will lead to different results. As it is shown in Figure 6.12, changing the PVs distribution between the zones does not change the load current sensed at the R1 location. So it means by variation of PVs location only the main protection of zone 2 can be addressed and the upstream relay will not be affected.

6.3.3 Impact of PV penetration on high impedance fault

The increasingly trend of PV installation in distribution networks has made some changes in parameters that protective devices settings are set based on them. To investigate this impact and to analyze that how strong is this impact, a single phase to ground fault is applied to different points of the network and the current sensed at the both primary and backup relays in this network have been measured. These points are shown in the Figure 6.13. This figure is the same network that has been shown in Figure 6.1, and the LV networks on downstream of distribution transformer together with the transformer are shown by arrows. These tests are carried out at 10% of loading rate. Two faults have been applied on downstream of both relays (F-3, F-4) and two faults have been applied to two protective devices (F-1, F-2). The red arcs are showing the fault applied locations. According to these faults, it has been tried to

123

achieve the threshold of impedance that faults turn to high impedance fault. I.e. it is shown here that how variation of PV penetration level may change the high impedance fault threshold for the network.

Table 6.6 lists the results of this study and as it can be understood the numbers are drawn in Figure 6.14. This figure indicates
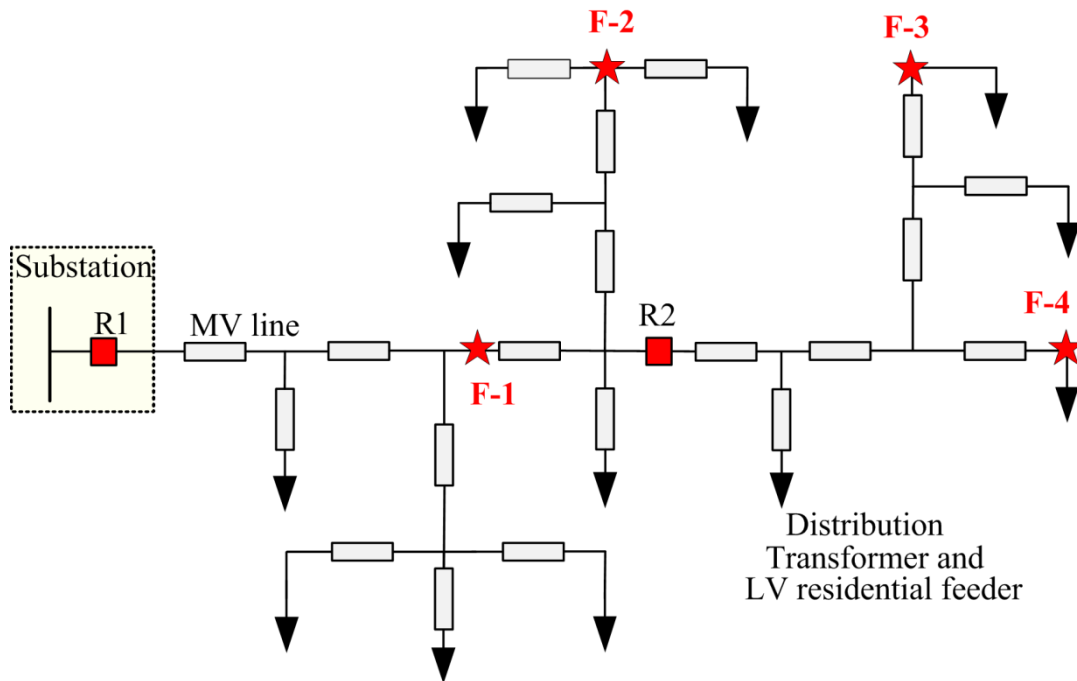
Figure 6.13. Schematic diagram of studied MV network in Figure 6.1.
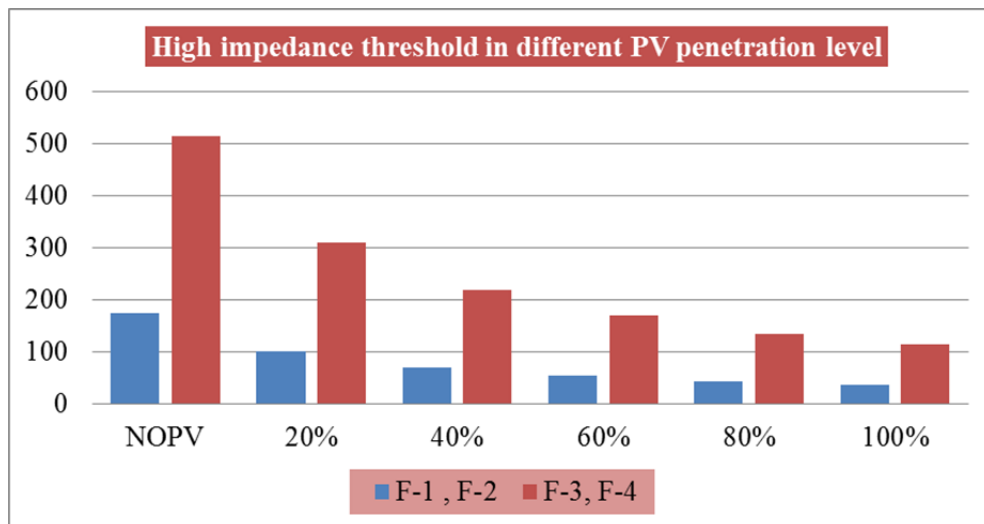
Figure 6.14. High impedance fault variation in different PV penetration level and fault locations.

124

Table 6.6 High impedance fault threshold for various PV penetration levels.

PV Penetration level	F-1, F-2	F-3, F-4
NOPV	175	515
20%	102	310
40%	70	220
60%	54	170
80%	44	135
100%	37	115

that as the PV penetration goes high, the high impedance fault margin reduces. For example, when fault occurs at F-4 and the PV penetration is 20%, faults with impedance higher than 515 (ohm) can be consider as high impedance fault. Because in these cases fault current becomes less that relay pickup current and protection system fails to trip. However, at the same position of fault when PV penetration reaches to 80% and 100% this threshold of high impedance fault gets to 135 and 115 (ohm) respectively. This trend is observed for all fault locations.

To analysis, the impact of loading of the network and penetration level ofPVs on the threshold of high impedance following tables have been provided. According to this tables which Table 6.7 belongs to relay 1(R1) and Table 6.8 belongs to relay R2. As it can be seen in specific loading rate as PV penetration level increases the impedance which is known as high impedance fault decreases. However in specific penetration level increasing loading rate leads to increase of high impedance fault threshold. This can be clearly seen in Figure 6.15 and Figure 6.16 which are for relays R1 and R2 respectively. As it is seen in loading rate of 25%, 82 ohm can be detected as high impedance fault while this value easily can be detected as a non high impedance fault by overcurrent relay. For another example, in100% of loading the threshold of high impedance fault can be a drop from 558 ohm to 123 ohm which makes significant difference in setting and successful operation of overcurrent relays. In fact with this variation of threshold impedance some of the faults that in NOPV mode can be easily detected by overcurrent protection, now will not be tracked. Hence, it is necessary to make another measure to successful detection of this type of faults at this level of loading and PV penetration level.

Table 6.7   High impedance fault threshold for different loading and PV penetration levels in relay R1.

High impedance fault edge (Ohm) for LG fault (Relay R1)				
Loading	25%	50%	75%	100%
NOPV	153	213	340	558
20%	131	169	237	321
40%	112	136	182	224
60%	100	120	151	179
80%	91	105	129	143
100%	82	94	112	123

Table 6.8   High impedance fault threshold for different loading and PV penetration levels in relay R2.

High impedance fault edge (Ohm) for LG fault (Relay R2)				
Loading	25%	50%	75%	100%
NOPV	54	74	111	205
20%	45	58	80	112
40%	38	46	57	78
60%	33	39	48	58
80%	29	33	40	46
100%	26	29	35	41

The results show that the settings of high impedance fault relays should be reset to managing to isolate the faulty part of the system in case of high impedance fault occurrence.

6.3.4 Impact of PV penetration on fault current of relays

The majority of references which are studied the impact of PVs on the system during the fault have not paid attention appropriately to the selection of correct and precise values for fault impedances. This parameter is crucial and shows its impact on the output of analysis (short circuit current) vividly. Hence, it should be simulated correctly to have a fair judgment about the PV penetration level impact on the protection system of the distribution network. In this research, a model of dynamic

arc for the fault is planned and implemented. Also, both of bolted fault and dynamic impedance fault have taken into account in analysis and simulations have been run for both. The following section pays attention to dynamic fault simulation and its characteristic.
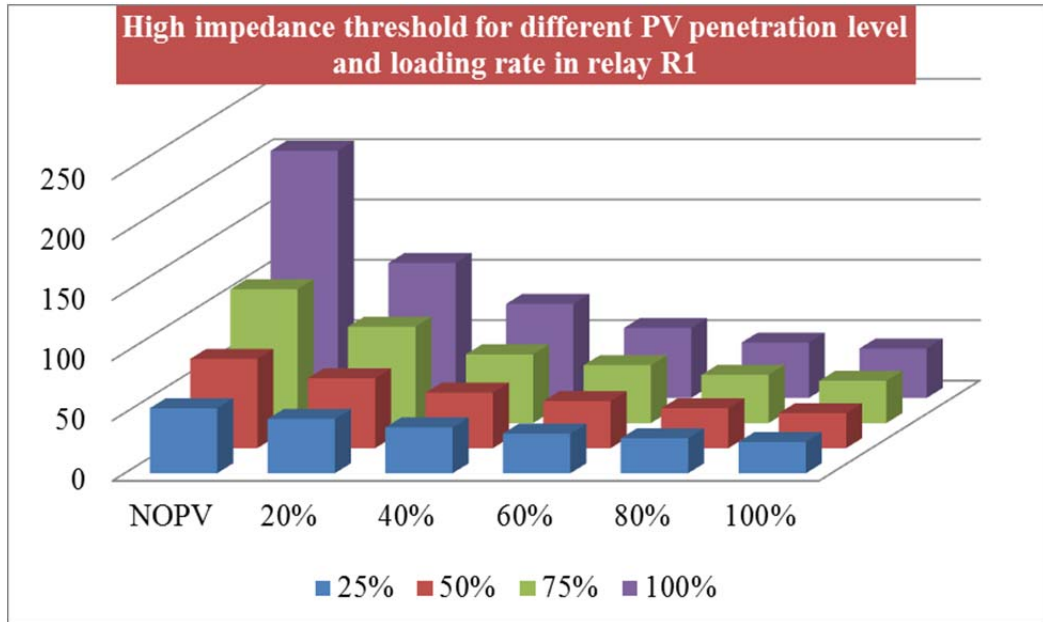
Figure 6.15. High impedance fault threshold (Ohm) for LG fault in different loading and PV penetration levels (Relay R1).
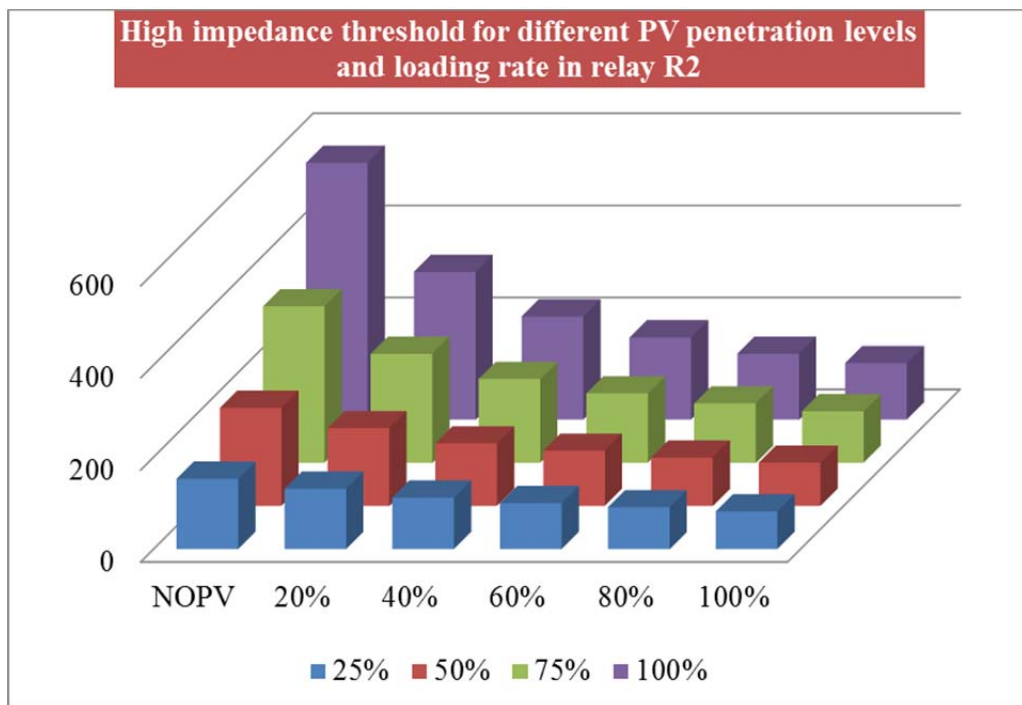
Figure 6.16. High impedance fault threshold (Ohm) for LG fault in different loading and PV penetration levels (Relay R2).

6.3.4.1. Dynamic arc fault

A precise model design for the fault is not easy as its nature is random. One option is choosing the model of resistance which varies with current. In this model, the arc is replaced with a time varying resistor or square wave voltage source which is synchronized with arc current [48].

This model is suitable for states that the fault level is high, i.e. it works well for cases that short circuit current is mainly supplied from utility side, and PVs do not have significant role on that. However, after the disconnection of source, the arc parameters are changed, and it is hard to determine the new parameters of this model. Thus, this model is not used in this study. There is another option to consider the both states of before and after the switch disconnection impact on simulated arc fault. This model is made based on the newly introduced model of the long fault arc in the air. The dynamic arc characteristic can be expressed as [48]

$$\frac{dg_P}{dt} = \frac{1}{T_P}(G_P - g_P) \tag{6.1}$$

T_p is the time constant and

G_p and g_p are the stationary and instantaneous arc conductance respectively.

$G_P = \frac{|i|}{V_P l_P}$ and $T_P = \frac{\alpha I_P}{l_P}$

where

I_P is the pick value of primary arc current

l_P is the primary arc length

i is the primary arc current

α is a constant

The secondary arc mainly is connected to the secondary arc current. Moreover, its length is affected by wind speed and primary arc current duration. However, the total secondary arc voltage is proportional to the arc length [48]. Low current secondary arc is written as:

$$\frac{dg_s}{dt} = \frac{1}{T_s}(G_s - g_s) \tag{6.2}$$

which

T_S is the secondary arc time constant

G_S is the stationary arc conductance

g_S is the instantaneous secondary arc conductance

Gs and T_S can be written as below;

$$G_S = \frac{|i|}{V_S \, l_S \, (t_r)} \tag{6.3}$$

$$T_S = \frac{\beta \, I_S^{1.4}}{l_S(t_r)} \tag{6.4}$$

where

i the secondary arc current

t_r time initiation of secondary arc

$l_s(t_r)$ the time varying arc length

I_S the steady state peak secondary arc current

β constant

Figure 6.17 shows the applied impedance as a dynamic impedance fault in this project. As it is seen the peak value of resistance dose not exceed 4 ohm.
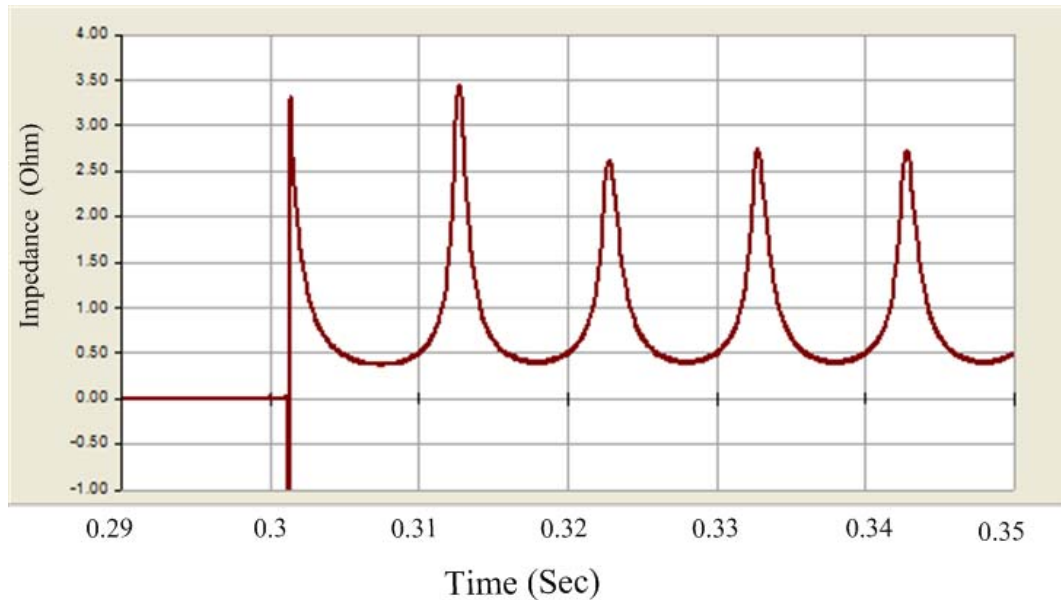
Figure 6.17. Applied dynamic impedance fault.

To analysis the impact of PV penetration in the presence of solid faults and dynamic arc fault, a three phase to ground fault is applied to different points of the network and the current sensed at the both primary and backup relays have been captured and tabulated in Table 6.9. It worth mentioning that these tests have been

129

carried out in the case of bolted fault (fault impedance equals to1m ohm) while Table 6.10 shows the results for same parameters and same conditions in the presence of dynamic fault impedance.

As it is shown in this tables the value of short circuit current is increasing in R1 in all of the faults (regardless of its location, either in downstream of both relays or between two relays) as the PV penetration goes high. However, the current passing from R2 is decreasing as PV penetration goes high from 20% to 100%. This is becausef the higher contribution of PVs in fault current and consequently changing the voltage profile along the feeder which results in less current absorbance from source. However, it remains untouched when a fault occurs between two relays. Looking at these numbers shows that the variation of short circuit current in relays in the presence of bolted faults in its worst case (which is F-3 in this case) does not exceed 30 A out of 1393A .(variation of fault current from NOPV mode to 100% Looking at the values of Table 6.10 shows that the trend of current decrease in R1 is similar to bolted fault results but more intense than it. And for R2 the trend is always increasing even when a fault occurs between the two relays. However, the highest percentage of current variation is seen again in F-3 where the fault current gets from1570 A in NOPV mode to 1494 A in 100% of PV penetration level. (4.7% variation) However, the variations of current for R2 when a fault occurs on between of two relays are not vital as in this situation the relay R1 is responsible for clearing the fault and disconnecting the source supply. This is a variation about 2.2% which is not considerable.

Table 6.9 Observed current by main and backup relays for different PV penetration levels during bolted fault.

Penetration level	F-1		F-2		F-3		F-4	
	R1	R2	R1	R2	R1	R2	R1	R2
NO PV	2159	1.8	1600	4	1393	1385	1393	1384
20%	2157	1.8	1595	4	1387	1388	1387	1388
40%	2155	1.8	1590	4	1381	1391	1381	1391
60%	2154	1.8	1585	4	1375	1394	1375	1393
80%	2152	1.8	1580	4	1369	1396	1369	1396
100%	2151	1.8	1575	4	1364	1399	1364	1399

Table 6.10 Observed current by main and backup relays for different PV penetration levels during dynamic fault impedance applied fault.

Penetration level	F-1		F-3		F-2		F-4	
	R1	R2	R1	R2	R1	R2	R1	R2
NO PV	2108	2.1	1423	1417	1570	4.2	1423	1417
20%	2095	15.8	1414	1420	1553	15.6	1410	1421
40%	2083	32.2	1404	1422	1537	31.7	1397	1424
60%	2073	48.3	1395	1424	1522	47.2	1384	1428
80%	2063	65.6	1386	1426	1508	64.1	1372	1431
100%	2054	82.4	1378	1428	1494	81.3	1360	1433

6.4 Impact of PV penetration on relays operation time

To investigate that how this variation in current of relays influence on relays operation time and their coordination it is required to pay attention to the time-current characteristic of relays. As it was mentioned in chapter 2, there are different time-current characteristics for overcurrent relays. One of the most common characteristics is the IEC inverse characteristic and here the calculation is carried out for this type of relays. The (6-5) shows this characteristic equation.

$$t = TMS \frac{0.14}{(I_r^{0.02} - 1)} \tag{6.5}$$

where

$$I_r = \frac{I_f}{I_p}$$

$$t_1 = TMS_1 \frac{0.14}{\left(\left(\frac{I_f}{I_p}\right)^{0.02} - 1\right)} \tag{6.6}$$

$$t_2 = TMS_2 \frac{0.14}{\left(\left(\frac{I_f}{I_p}\right)^{0.02} - 1\right)} \tag{6.7}$$

where

$$I_f = I_{f_1} = I_{f_2}$$

$$\Delta t = t_2 - t_1 = 0.14 \left(\frac{TMS_2}{\left(\left(\frac{I_f}{I_p} \right)^{0.02} - 1 \right)} - \frac{TMS_1}{\left(\left(\frac{I_f}{I_p} \right)^{0.02} - 1 \right)} \right)$$

$$= 0.14 \left(\frac{TMS_2 - TMS_1}{\left(\frac{I_f}{I_p} \right)^{0.02} - 1} \right) = 0.14 \frac{(\Delta TMS)}{(R^{0.02} - 1)} \qquad (6.8)$$

where

$$I_f = I_{f_1} = I_{f_2}$$

$$\Delta t = t_2 - t_1 = 0.14 \left(\frac{TMS_2}{\left(\left(\frac{I_f}{I_p} \right)^{0.02} - 1 \right)} - \frac{TMS_1}{\left(\left(\frac{I_f}{I_p} \right)^{0.02} - 1 \right)} \right)$$

$$= 0.14 \left(\frac{TMS_2 - TMS_1}{\left(\frac{I_f}{I_p} \right)^{0.02} - 1} \right) = 0.14 \frac{(\Delta TMS)}{(R^{0.02} - 1)} \qquad (6.9)$$

The equation (6.8) is showing the time difference for relay operation in the radial distribution system with NOPV. For PV dominated distribution network as a result of PV contribution in fault current and observing different currents by relays even in the case that fault happens at the downstream of the relays, the values of I_{f1} and I_{f2} will be different. Hence the relationships between the operations times of main and backup relays can be expressed as below.

$$t_1{}^{new} = TMS_1 \frac{0.14}{((\frac{I_{f_1}{}^{new}}{I_p})^{0.02} - 1)} \tag{6.10}$$

$$t_2{}^{new} = TMS_2 \frac{0.14}{((\frac{I_{f_2}{}^{new}}{I_p})^{0.02} - 1)} \tag{6.11}$$

$$R = \frac{I_{f_1}{}^{new}}{I_p} \tag{6.12}$$

$$I_{f_2}{}^{new} = k.I_{f_1}{}^{new} \tag{6.13}$$

$$\Delta t^{new} = t_2{}^{new} - t_1{}^{new}$$

$$= 0.14 \left(\frac{TMS_2}{\left(\left(\frac{I_{f_2}{}^{new}}{I_p}\right)^{0.02} - 1\right)} - \frac{TMS_1}{\left(\left(\frac{I_{f_1}{}^{new}}{I_p}\right)^{0.02} - 1\right)} \right) \tag{6.14}$$

$$= 0.14 \left(\frac{TMS_2}{((K)^{0.02}(.R)^{0.02} - 1)} - \frac{TMS_1}{((R)^{0.02} - 1)} \right)$$

Distributed systems are usually protected with switch fuses in LV side of the transformer. However, the overcurrent (OC) relays are the main protective devices used in MV distribution level to protect the system. In the studied network, there are two OC relays located on beginning and middle of the feeder. In the case of fault occurrence at the downstream of both relays, main and backup relays will see same current in NOPV mode, however, presence of PVs in the network will change the short circuit calculations and sensed current in first and second relays will be different even in case that fault occurs at downstream of both relays. If the current of the relay is reduced as a result of PV penetration increase, the operation time difference of that relay and its backup relay will be reduced, and it may lead to miscoordination of them if this effect becomes intense. However, the increase of relay current as a result of PV penetration increase can improve the coordination interval time.

Also, there is a possibility of faults occurrence at the middle of the feeder. In this

case, in NO-PV mode the relay on downstream of fault will not experience fault current but slight. However, even this slight current will be affected by PV penetration level.

As it can be seen the variation of the time difference in a new state (PV dominated network) depends on R and k which is the ratio of I_{f2} to I_{f1}. Depending on the fault location the ratio of I_{f1} to I_{f2} can become greater, equal or less than the unit. So it is evident that the values of the time difference, in this case, will be different from NOPV case. This difference results in miscoordination between these two protective devices, and it can be shown schematically in Figure 6.18. As it is seen the coordination interval time (*CTI*) may be disrupted by variation of relays operation time difference (Δt).
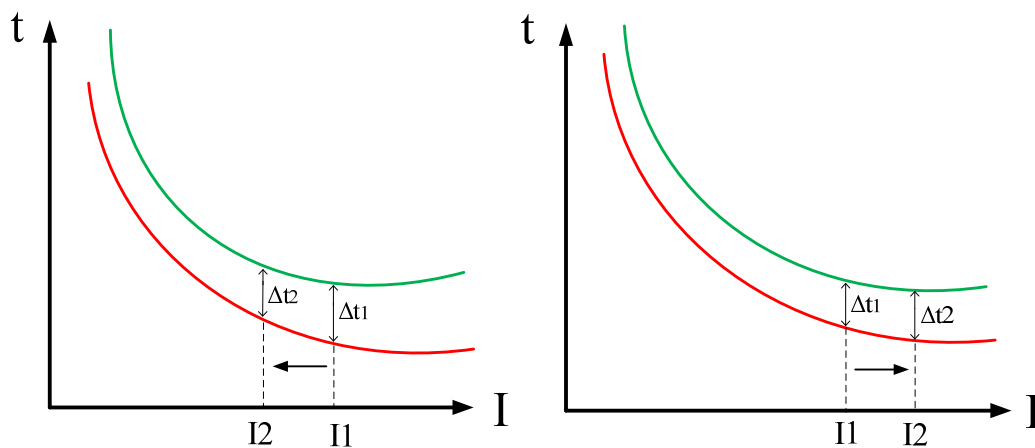
Figure 6.18. Relays operation time difference variation on Time - Current characteristic of OC relays.

In different PV penetration levels, to obtain the operation time for relays, the equation (6.7) with proper TMS and I_P is utilised.

Depending on fault location the ratio of main and backup relays detected current will vary and accordingly R and K will be changed at above equation. Hence the new time difference will be achieved. Table 6.11 presents the variation of the time difference in main and backup relays operation time as PV penetration level changes from zero to 100%. For faults F-1 and F-2 which occur between two relays, the second relay will not operate and only the operation time of relay (R1) is considered as a criterion of penetration level impact on the protective system operation time.

A new parameter is defined here to make the concept clearer. The total time difference (TTV) which is defined as a difference of relays operation time difference in NOPV mode and relays operation time difference in 100% of penetration level for faults on downstream of both relays. For faults on between two relays the TTM is defined as difference of first relays (R1) operation time in NOPV and 100% penetration level of PV.

$$TTV = \Delta t^{100\%} - \Delta t^{0\%} \qquad \text{for faults on downstream of bout relays}$$

$$TTV = t_1{}^{100\%} - t_1{}^{0\%} \qquad \text{for faults on downstream of bout relays}$$

The values for the time difference in the table has been calculated based on TMS1=0.05 and TMS2=0.2.

Table 6.11 Main and backup relays operation time difference for different penetration levels at various fault locations.

Penetration level	Δt (when fault occurs at)			
	F-1	F-2	F-3	F-4
NO PV	0.118	0.132	0.415	0.415
20%	0.118	0.133	0.414	0.414
40%	0.119	0.133	0.412	0.413
60%	0.119	0.134	0.411	0.412
80%	0.119	0.134	0.410	0.412
100%	0.119	0.135	0.410	0.411
TTV(s)	0.001	0.003	0.005	0.004

If the values of TTM are considered, it is seen that the increasing penetration level of PVs in the presence of dynamic impedance fault varies slightly and it is negligible in this range of time for relays operation. As the values of TTV show in Table, in the worst case, the Δt does not exceed 5ms, which is a quarter of a cycle.

The impact of high percentage of PV installation on MV and LV networks are different and consequently the effect of them on protection system of these two networks will be different. Reminding the conclusion drawn from chapter four about

LV networks, the results of LV distribution network have shown that current protection systems will be vulnerable if the earthing system of houses is not suitable enough. And in the rest of cases it will work well. In MV system study the result have demonstrated that there is a need to install high impedance relays in PV dominated networks to prevent unsuccessful operations of relays in case of the faults with relatively higher impedance but still much less than fault impedances that was required installation of high impedance relays in normal distribution networks.

6.5 Summary

This chapter focused on the impact of PV penetration on overcurrent relays operation in MV networks. It is demonstrated that the variation of load current at relay connection point as a result of PV penetration and different loading cannot make a big issue relay pickup process if the relay's pickup current has been set based on NOPV and 100% of loading condition.

On the other hand, the analysis of the impact of high PV penetration on relays operation during the fault revealed that the relay coordination in the presence of bolted faults is not affected considerably from high penetration. To make the results more precise, the dynamic impedance arc faults simulation was applied in fault cases. The comparison of results between bolted fault and dynamic impedance fault showed a slight difference in operation time of relays variation.

The result of an investigation on PV penetration impact on high impedance fault demonstrated that PV penetration level changes the threshold of high impedance fault detection significantly and as the PV penetration level increases the threshold of high impedance fault goes down. Consequently, this may lead to improper operation of high impedance relays in the distribution system. So the change in high set relays settings or their methods of detections should be revised based on these findings to improve the favorable operation rate of relays.

The next chapter summarizes the main findings of this research and proposes future research avenues.

Chapter 7. Conclusions and Recommendations

In this chapter, the general findings of the thesis and recommendations for future research are presented.

7.1 Conclusions

The general findings of the thesis are:

(1) To have a better understanding of PVs effect on a network having knowledge about the sensitivity of important factors of network such as voltage profile and feeder current is necessary. Sensitivity analysis showed that in LV distribution feeders one PV connection decreases the transformer current or may not change it if it is located on downstream of fault. PV installation point also varies the voltage profile in different ways depending on the location of its connection point and fault point. PV rating also have an effect on voltage and current of the feeder depending on the fault type, fault location and PV connection point. The behavior of LG and LLG faults in the presence of PV are similar. However, the LL fault will have somehow different impact.

(2) Stochastic analysis carried out using Monte Carlo simulation technique demonstrated the impact of protective factors such as SCF level, transformer current, and voltages of the nodes along the LVF. The results of the stochastic analysis proved that the PV ratings and PPLs do not sufficiently change the expected average current at the transformer secondary and EAV of the nodes along the LVF. Moreover, it is seen that the SCF location and fault impedance are the most dominant factors compared to other factors such as PV output, PV location, and their distribution along the feeder.

(3) Based on the outcomes of the MCA, two criteria were defined to evaluate the impact of the PV rating and PPL on the probability of the successful detection of the SCF by the switch-fuse at the transformer secondary and the disconnection of the PVs. These criteria show that to have the desired accuracy of successful detection of a fault by protective devices and also to have a specific rate of success in PVs disconnection for different types of faults, the PPL should be limited in specific range and should not violate that range.

(4) Study on disconnection sequence of PVs and effects of some important parameters such as PV rating, PV connection location, fault impedance and location on disconnection time and sequence of PVs has been also studied in detail. The study also pointed out the situations for which the current protection system is not sufficient. These situations are more likely to be faced in NEG systems or when the fault impedance is high in MEN systems. Thus, only utilizing the under/over voltage protection function will not guarantee the successful disconnection of PVs in such situations. In such situations, better protection system need to be designed.

(5) The impact of load current is also studied on the setting of the pick up current of the overcurrent relay for the MV primary side protection as a function of the penetration level of PVs. Also the effect of load demand together with PPL in the network on pickup current of relays is investigated. The reduction of high impedance fault threshold and consequently being unable to detect the more numbers of faults as a result of increase on PPL is another finding of this thesis. To solve this issue the necessity of installation of high set relays in highly PV penetrated feeders or to apply changes in their settings is strongly recommended. To get more accurate results on fault analysis in MV network, the dynamic impedance fault is utilized instead of bolted fault and the results are presented to see that the discrepancy in relays operation time will not be considerable despite small difference between them.

7.2 Thesis contribution to the knowledge

In this thesis the comprehensive analysis was carried out to illustrate the impact of high PV penetration level on protective devices in LV distribution network. The results revealed that increasing PV penetration level will not make serious problem for protective system of distribution network in LV level. However, the rate of the successful operation of protective devices such as switch fuse and under/over voltage disconnectors of PVs, varies with the PPL. So, to have a better operation results from protective system of distribution networks, choosing a specific interval for PPL depending on fault type can be useful.

Also this thesis illustrated that the disconnection sequence of PVs from the network during the different types of faults depends to many factors which impedance of fault and earthing method of network are the most important of them. In addition, the findings of this section show that unsuccessful disconnection of PVs during the faults are more likely to occur in NEG systems than MEN systems.

Finally the thesis focused on finding the problems in protection of the MV part of the distribution network in the presence of high percentage of PVs. The outcomes of the thesis in this part showed that the PV penetration level only disturb the protection system and their coordination when the high impedance fault occurs. And, for protective system even in the case of dynamic impedance faults, the higher PPL will not make a serious issue. The only impact of high PPL is reflected on high impedance fault detection which the high impedance fault threshold is decreased and overcurrent relays are not able to detect this type of faults ,which they was able before than increase of PPL to large values,. So using the high impedance relays is recommended for highly penetrated PV distribution network by this thesis.

7.3 Recommendations for future research

The scopes for future research are given below:

7.3.1 Analysis on none radial structure of distribution systems

In this research, only the distribution network with radial and branched radial structure was studied. However, other structures of distribution networks such as the

loop type distribution should be studied as well. Similar studies and investigation can be carried out on them to find out whether the PV penetration level or rating effect on different structures and topologies of the distribution networks are similar or not? This can be a topic for future research. The impact of unbalanced distribution of PVs and unbalanced loads should also be studied.

7.3.2 PVs anti islanding systems other than voltage based one

In this research, the concept of disconnection of PVs during the fault was studied primarily based on the effect of the under/over voltage protection of PVs were investigated. However, other technologies of anti-islanding which are used for newly introduced PVs such as overcurrent, overload, frequency variation detection, reverse current, over temperature, and deep discharge protection were not considered in this research. So consideration given to any other function of protection used in PVs for the similar analysis can be a topic for future research.

7.3.3 New high impedance detection technology

As it is mentioned in conclusion, the high impedance fault threshold for relays is changed when the PV penetration level varies and it becomes critical when the penetration level of PVs increases significantly. This was one of the important findings of this thesis and reporting such a potential problem and hazard in the case of high PV penetration levels in distribution networks. However, the investigation on other methods of high impedance fault detection and to propose the new methods for that which may lead to better detction of that type of faults even in the presence of large percentage of PVs can be a topic for a future research.

7.3.4 Protection problems of highly PV penetrated networks in the presence of DSTATCOM

In this research, it was assumed that there is no voltage compensating device for improving the voltage profile or voltage regulation in the network. However some of utilities are using DSTATCOM to get a better voltage regulation on distribution feeders. Using this component in the distribution network may raise other issues to the protection system of the distribution network and the coordination of protective devices might be influenced. So investigation on impact of DSTATCOM

on protection systems of highly penetrated PV embedded distribution networks is a research gap. There is no such study in the literature that this author has come across on this topic. Hence, this topic is a very good case which needs to be investigated and can be another topic for future research.

References

[1]   Australian Energy statistics - Energy Update, 2011.

http://data.daff.gov.au/data/warehouse/pe_abares99010610/EnergyUpdate_2011_REPORT.pdf

[2]   L. Romanach, Z. Contreras, and P. Ashworth, "Australian householders' interest in the distributed energy market –National survey results", CSIRO report prepared for the Australian Photovoltaic Association, 2013.

http://www.csiro.au/Organisation-Structure/Flagships/Energy-Flagship/Australian-householders-interest-in-the-distributed-energy-market.aspx

[3]   H. Cheung, A. Hamlyn, L. Wang, C. Yang and R. Cheung, "Investigations of impacts of distributed generations on feeder protections," 2009 IEEE Power & Energy Society General Meeting, Calgary, AB, 2009, pp. 1-7.

[4]   R. Benato, R. Caldon and S. Corsi, 'Protection requirements in distribution systems with high penetration of DG and possibility of intentional islanding," CIRED 2005. 18th International Conference and Exhibition on Electricity Distribution, Turin, Italy, 2005, pp. 1-4.

[5]   S. Tian, Y. Liu and G. Mei, "New theory of directional current protection for the distribution network containing DG based on fault component," 2011 International Conference on Advanced Power System Automation and Protection (APAP), Beijing, 2011, pp. 558-563.

[6]   V. Calderaro, V. Galdi, A. Piccolo and P. Siano, "DG and protection systems in distribution network: Failure monitoring system based on petri nets," Bulk Power System Dynamics and Control - VII. Revitalizing Operational Reliability, IREP Symposium, Charleston, SC, 2007, pp. 1-7.

[7]   M. M. Mirjalili, A. R. Sedighi and M. R. Haghifam, "Impact of DG location on protection coordination in distribution systems," Proceedings of 17th Conference on Electrical Power Distribution Networks (EPDC), 2012, Tehran, pp. 1-6.

143

[8]   J. Sadeh, M. Bashir and E. Kamyab, "Effect of distributed generation capacity on the coordination of protection system of distribution network," Transmission and Distribution Conference and Exposition: Latin America (T&D-LA), 2010 IEEE/PES, Sao Paulo, 2010, pp. 110-115.

[9]   G. Mokhtari, G. Nourbakhsh, F. Zare, A. Ghosh, "Improving the penetration level of PVs using DC link for residential buildings" , Journal of Energy and Buildings, 2013. pp 80-87.

[10] M. Ebad, W.M. Grady, "An approach for assessing high-penetration PV impact on distribution feeders", Electric Power Systems Research, 2016, pp347–354.

[11] M. P. Nthontho, S. P. Chowdhury, S. Winberg and S. Chowdhury, "Protection of domestic solar photovoltaic based microgrid," Developments in Power Systems Protection, 2012. DPSP 2012. 11th International Conference on, Birmingham, UK, 2012, pp. 1-6.

[12] W. L. Hsieh, C. H. Lin, C. S. Chen and et al, "Optimal penetration level of PV generation for distribution system load transfer," Next-Generation Electronics (ISNE), 2013 IEEE International Symposium on, Kaohsiung, 2013, pp. 490-493.

[13] The critical decade: Australia's future –solar energy, 2013.
http://www.climatecouncil.org.au/uploads/497bcd1f058be45028e3df9d020ed561.pdf

[14] M.J.E. Alam, K.M. Muttaqi, and D. Sutanto, "An approach for online assessment of rooftop solar PV impacts on low-voltage distribution networks," IEEE Trans. Sustainable Energy, vol.5, Issue.2, pp.663-672, 2014.

[15] F. Shahnia, R. Majumder, A. Ghosh, et al., "Voltage imbalance analysis in residential low voltage distribution networks with rooftop PVs," Electric Power Systems Research, vol.81, Issue.9, pp.1805-1814, 2011.

[16] F. Shahnia, A. Ghosh, G. Ledwich, and F. Zare, "Voltage unbalance improvement in low voltage residential feeders with rooftop PVs using custom power devices," International Journal of Electrical Power & Energy Systems, vol.55, pp.362-377, Feb. 2014.

[17] G. Mokhtari, G. Nourbakhsh, F. Zare, and A. Ghosh, "Overvoltage prevention in LV smart grid using customer resources coordination," Energy and Buildings, Vol.61, pp.387-395, June 2013.

[18] B. Noone, "PV integration on Australian distribution networks: Literature review," The Australian PV Association, 2013.

[19] V. Calderaro, S. Corsi, V. Galdi, and A. Piccolo, "Optimal setting of the protection systems in distribution networks in presence of distributed generation," 40th Int. Universities Power Engineering Conf., Sept. 2005.

[20] A. Alkuhayli, S. Raghavan, and B.H. Chowdhury, "Reliability evaluation of distribution systems containing renewable distributed generations," North American Power Symposium (NAPS), pp.1-6, 2012.

[21] P.K. Ray, S.R. Mohanty, N. Kishor, and J. Catalao, "Optimal feature and decision tree based classification of power quality disturbances in distributed generation systems," IEEE Trans. Sustainable Energy, vol.5, Issue.1, pp.200-208, 2014.

[22] K. Maki, S. Repo, and P. Jarventausta, "Protection planning development for DG installations," 20th Int. Conf. on Electricity Distribution, 2009.

[23] Guide to conducting distribution impact studies for distributed resource interconnection, IEEE Standard. 1547.7, 2012.

[24] R.A. Walling, R. Saint, R.C. Dugan, et. al, "Summary of distributed resources impact on power delivery systems," IEEE Trans. Power Delivery, Vol.23, Issue.3, pp.1636-1644, July 2008.

[25] B. Subhashish, T. Saha, and M.J. Hossein, "Fault current contribution from photovoltaic systems in residential power networks," 23rd Australian University Power Engineering Conf. (AUPEC), 2013.

[26] K. Kauheniemi and L. Kumpulainen, "Impact of distributed generation on the protection of distribution networks", 8th IEE Int. Conf. on Developments in Power System Protection, Vol. 1, pp. 315–318, April 2004.

[27] M. Patsalides, G.E. Georghiou, A. Stavrou and V. Efthimiou, "Assessing the power quality behavior of high photovoltaic (PV) penetration levels inside the distribution network", 3rd IEEE International Symposium on Power Electronics for Distributed Generation Systems," (PEDG), pp. 709–716, 2012.

[28] W. Peng, S. Haddad and Y. Baghzouz, "Improving power quality in distribution feeders with high PV penetration through inverter controls," CIRED Workshop on Integration of Renewables into the Distribution Grid. 2012.

[29] M.A. Eltawil and Z. Zhao, "Grid-connected photovoltaic power systems: Technical and potential problems-A review," Renewable & Sustainable Energy Reviews, Vol. 14, pp.112–129, 2010.

[30] N. Jabalameli, M. Masoum, T. Mehr and F. Shahnia, "Impact of battery rating on

performance of rooftop PV supporting household loads, regulating PCC voltage and providing constant output power to grid," 23rd Australasian Universities Power Engineering Conference (AUPEC), pp.1-6, Oct 2013.

[31] N. Jabalameli, N. Deilami, S. Masoum and F. Shahnia ,"Rooftop PV with battery storage for constant output power production considering load characteristics," 8th International Conference on Electrical and Electronics Engineering. (ELECO), Turkey, Nov. 2013.

[32] M.E. Baran, H. Hooshyar, H. Shen, et al., "Impact of high penetration residential PV systems on distribution systems", IEEE Power and Energy Society General Meeting, July 2011.

[33] H. Hooshyar, M. Baran, and L. Vanfretti, "Coordination assessment of overcurrent relays in distribution feeders with high penetration of PV systems," IEEE PowerTech. Conference, pp.1-6, 2013, France.

[34] H.H. Yengejeh, F. Shahnia and S. Islam, "Contributions of single-phase rooftop PVs on short circuits faults in residential feeders," 24th Australasian Universities Power Engineering Conference (AUPEC), Australia, Oct 2014.

[35] A. Bruce, S. Heslop, I. MacGill, M. Watt," Magnetic Island and Townsville Solar City: A Case Study of Increasing PV Penetration in Electricity Networks", a report by the University of New South Wales for the Australian PV Association. 2013.

[36] H. Hooshyar and M.E. Baran, "Fault analysis on distribution feeders with high penetration of PV systems" IEEE Trans. on Power Systems", Vol. 28, Issue 3, pp. 2890-2896, 2013.

[37] T.G. Alvin, I.Z. Abidin, H. Hashim and A. Zainul Abidin, "Phase comparison protection for distribution networks with high PV penetration," IEEE PES Innovative Smart Grid Technologies-Asia Conference (ISGT Asia), pp. 216-221, 2014.

[38] H.A. Abyaneh, M. Taleshian, "Relays and Protection", Amirkabir Publication, third publication, 2005.

[39] Matin Meshkin, "Coordination of overcurrent relays with distance relays in interconnected networks", MSC Thesis, Amirkabir university of Technology, 2002.

[40] Reza. Mohammadi Chabanloo,"Optimal setting and protection coordination of distribution network",Msc Thesis, Amirkabir Universit of Technology,2007.

[41] "Protective Relaying Application Guide", GEC Measurement, 1986.

[42] Antonio s. Braga and Joao Tome Saraiva ,"Coordination of Overcurrent Directional Relays in Meshed Networks Using The Simplex Method", IEEE Computer Applications in Power, July 1996.

[43] V. Garcia, J.C. Cebrian and N. Kagan, "Evaluation of probability functions related to short circuit random variables using power quality meters," IEEE/PES Transmission & Distribution Conf. Latin America, 2010.

[44] Energex/Ergon Energy connection standard on Small Scale Parallel Inverter Energy Systems up to 30 kVA, 2014.
https://www.ergon.com.au/__data/assets/pdf_file/0005/198698/STNW1170ver2-Connection-Standard-for-IES-up-to-30kVA.pdf

[45] Australian Standard on Grid Connection of Energy Systems via Inverters, AS 4777, Draft version, 2013.

[46] Photovoltaic system protection application guide, 2012.
http://www1.cooperbussmann.com/pdf/1b416a65-f5ac-4730-ab77-9e2faa147945.pdf

[47] J.G. Grainger, and W.D. Stevenson Jr. Power System Analysis, McGraw-Hill, 1994.

[48] M. Dewadasa, "Protection of Distributed Generation Interfaced Networks," PhD Thesis, Queensland University of Technology, July 2010.

[49] Perth solar city annual report, 2011.
http://www.westernpower.com.au/documents/psc_-_2012_annual_report_-_final_for_distribution_(lo-res_18.pdf

[50] F. Shahnia, A. Ghosh, G. Ledwich, and F. Zare, "Predicting voltage unbalance impacts of plug-in electric vehicles penetration in residential low voltage distribution networks," Electric Power Components and Systems, vol.41, Issue.16, pp.1594-1616, 2013.

[51] C. Robert and G. Casella, Monte Carlo Statistical Methods, Springer, 2004.

[52] Average annual and monthly sunshine duration, Bureau of Metrology,
http://www.bom.gov.au/jsp/ncc/climate_averages/sunshine-hours/index.jsp

[53] H.H. Yengejeh, F. Shahnia, and S. Islam, "Disconnection time and sequence of rooftop PVs under short-circuit faults in low voltage networks," North American Power Symposium (NAPS), pp. 1-6, Charlotte, USA, 2015.

[54] N. Nikmehr, and S. Najafi-Ravadanegh, "Optimal power dispatch of multi-

microgrids at future smart distribution grids," IEEE Trans. Smart Grid, vol.6, no.4, pp.1648-1657, 2015.

[55]   IEEE Recommended Practice for Utility Interface of Photovoltaic (PV) Systems, IEEE Standard 929-2000.

[56]   Earthing of the distribution network, Technical Standard TS 109, SA Power Networks, March 2014.

[57]   D. Dong, Z. Qi and Y.H. Yang, "Non-effectively grounded system line selection device based on ARM," China Int. Conf. on Electricity Distribution (CICED), pp. 1-6, Dec. 2008.

[58]   Western Australian Distribution Connections Manual, WesternPower, 2015.
http://www.westernpower.com.au/documents/WA_Distribution_Connections_Manual.pdf

[59]   A. Hoke, R. Butler, J. Hambrick and B. Kroposki, "Steady-State Analysis of Maximum Photovoltaic Penetration Levels on Typical Distribution Feeders," IEEE Transactions on Sustainable Energy, Vol. 4, No.2, pp 350-357, April 2013.

[60]   T.A. Short, *Electric power distribution handbook*, CRC Press, 2004.

[61]   Distribution construction standards handbook-Part 6, WesternPower, 2007.
http://www.westernpower.com.au/documents/low-voltage-overhead-distribution-construction-standards-han.PDF

[62]   IEEE Recommended Practice for Utility Interface of Photovoltaic (PV) Systems, IEEE Std 929-2000.

[63]   Photovoltaic system protection application guide, 2012.
http://www1.cooperbussmann.com/pdf/1b416a65-f5ac-4730-ab77-9e2faa147945.pdf

[64]   http://www.solarchoice.net.au/blog/residential-solar-pv-system-prices-may-2015

[65]   Clenergy product catalogue,
http://www.supplypartners.com.au/media/pdf/Clenergy%20Product%20Catalogue.pdf

[66]   ABB solar inverters catalogue,
http://new.abb.com/docs/librariesprovider22/technical-documentation/solar-inverter-pvs300-flyer.pdf?sfvrsn=2

[67]   Residential Design After Diversity Maximum Demand (DADMD) calculation, Western Power.
http://www.westernpower.com.au/land-developers-designers-residential-dadmd-calculator.html

[68] Australian Standard on Grid Connection of Energy Systems via Inverters, AS 4777, Draft version, 2013.

[69] Clipsal Solar Product Overview Catalogue, 2013.
http://updates.clipsal.com/ClipsalOnline/Files/Brochures/I0000114.pdf

[70] W. Bower and M. Ropp, "Evaluation of islanding detection methods for utility-interactive inverters in photovoltaic systems," Technical report, Sandia National Laboratories, 2002.

[71] N. Hoang and A. Yokoyamaa, "Influence of penetration levels and fault ride through characteristics of photovoltaic generation on voltage stability," Journal of International Council on Electrical Engineering, pp. 283-289, Sep. 2014.

[72] C.Y. Tang, Y.T. Chen and Y.M. Chen, "PV power system with multi-mode operation and low-voltage ride-through capability," To be published in *IEEE Trans. on Industrial Electronics*, DOI 10.1109/TIE.2015.2449777, 2015.

[73] Olex aerial conductors catalogue, 2012.
http://www.olex.com.au/Australasia/2012/OLC12641_AerialCat.pdf

Publications arising from the thesis

Journal papers (Published)

(1) **H. Hosseinian Yengejeh**, F. Shahnia, S. Islam," Disconnection of Single-Phase Rooftop PVs after Short-Circuit Faults in Residential Feeders", *Australian Journal of Electrical and Electronic Engineering*, Vol. 13, Issue 2. Pages 151-165, 2016. http://dx.doi.org/10.1080/1448837X.2016.1221637

Journal papers (Under Review/Revision)

(2) **H. Hosseinian Yengejeh,** F. Shahnia, S. Islam,"Sensitivity and Stochastic Analysis of the Impact of Randomly Distributed Rooftop PV Systems on Unsymmetrical Short-Circuit Faults of Low Voltage Electric Systems", Electric Power Component and Systems Journal. UEMP-2016-0106, 2016.

(3) **H. Hosseinian Yengejeh**, F. Shahnia, S. Islam, "Impact on High Impedance fault Detection in Rooftop Photovoltaic Dominated Distribution Networks," *IEEE Transaction on Sustainable Energy*.

Conference papers (Published)

(4) **H. Hosseinian Yengejeh**, F. Shahnia, S. Islam,"Disconnection Time and Sequence of Rooftop PVs under Short-circuit Faults in Low Voltage Networks", *North American Power Symposium (NAPS 2015),* Charlotte, USA, Oct 2015.

(5) **H. Hosseinian Yengejeh**, F. Shahnia, S. Islam,"Contributions of Single-Phase Rooftop PVs on Short Circuits Faults in Residential Feeders", *Australian Power Engineering Conference (AUPEC 2014),* Perth, Australia, September 2014.

(6) F. Shahnia, M. Moghbel, **H. Hosseinian Yengejeh**,"Improving the learning experience of power system protection students using computer-based simulations and practical experiments", *Australasian Universities Power Engineering Conference (AUPEC 2014)*, Perth, Australia 2014.